The Osteolytic Potential of Polyethylene Wear Debris in Periprosthetic Tissues Surrounding Total Joint Replacements

A dissertation

Submitted to the Faculty

of

Drexel University

by

Ryan Michael Baxter

In partial fulfillment of the

Requirements for the degree

of

Doctor of Philosophy

August 2011

Dedication

This dissertation is dedicated to my loving, impatient, demanding and beautiful wife.

Acknowledgements

I would like to thank and acknowledge my academic advisor, Dr. Steven Kurtz, who provided me with countless opportunities to pursue clinically and societally relevant studies related to orthopedics, and who offered valuable mentorship and guidance throughout the duration of my graduate work.

I would also like to thank my advisor, Dr. Marla Steinbeck, for imparting her many years of acquired knowledge in the field of biology, and for sharing her unfailing dedication to science and learning.

I would like to acknowledge my committee members, Dr. Fred Allen, Dr. Sriram Balasubramanian, Dr. Todd Doehring, and Dr. Theresa Freeman, for their many intellectual contributions and for providing the tools to perform innovative investigations.

Special thanks to the participating physicians, residents and clinical coordinators whose collaborations with the Implant Research Center were instrumental in procuring the implants and tissue samples necessary to perform this work.

Special thanks to Dr. Judd Day for encouraging me to put down the pizza and pick up the implants.

Finally, I would like to acknowledge my fellow graduate students, friends, family and especially my parents for their endless support and patience, especially when I didn't ask for it.

"*Roads*? *Where we're going, we don't need roads*."
--Dr. Emmett Brown

Table of Contents

List of Tables

List of Figures

List of Equations

Abstract

The Osteolytic Potential of Polyethylene Wear Debris in Periprosthetic Tissues Surrounding Total Joint Replacements

Ryan Michael Baxter

Implant component wear and the associated immune reactions to wear debris are among the most important factors in determining the longevity of total joint replacements. Inflammation-mediated bone loss and osteolysis were initially attributed to "cement disease," resulting from the fragmentation of acrylic cement used for fixation of the bone-implant interface. However, the observation of radiographic bone loss around uncemented components shifted the attention from bone cement to the role of ultra-high molecular weight polyethylene (hereafter, polyethylene) wear debris in promoting osteolysis. Clinical concern regarding osteolysis provided the impetus for the development of wear-resistant bearing surface technologies in the 1990s. Since that time, the advent of highly crosslinked and thermally treated polyethylene (HXLPE) components has shown marked reductions in implant wear and radiographic osteolysis at mid-term follow-up. However, after slightly more than a decade of service for HXLPE components, the understanding of particle characteristics *in vivo* and the associated immune responses in peri-implant tissues is limited to a few case studies. To address unanswered questions related to particle-mediated periprosthetic inflammation, the current dissertation outlines several studies that have evaluated the wear particle characteristics and the resulting biological responses in tissue samples obtained during revision surgery. This research addressed the following principal research

questions: (1) What is the comparative efficiency of established tissue digestion methods for polyethylene wear particle extraction? (2) What morphological changes and immune cells are present in tissues obtained at early revision surgery of loosened highly crosslinked polyethylene (HXLPE) components in the absence of radiographic osteolysis? (3) How do modes of implant wear affect the biological activity of polyethylene wear debris generated *in vivo*? (4) Can the reduced incidence of osteolysis around HXLPE components be attributed to a decrease in the biological activity of polyethylene wear debris generated *in vivo*? Ultimately, this dissertation lends itself to a greater understanding of the significance of polyethylene wear debris *in vivo* in the context of the revision surgery.

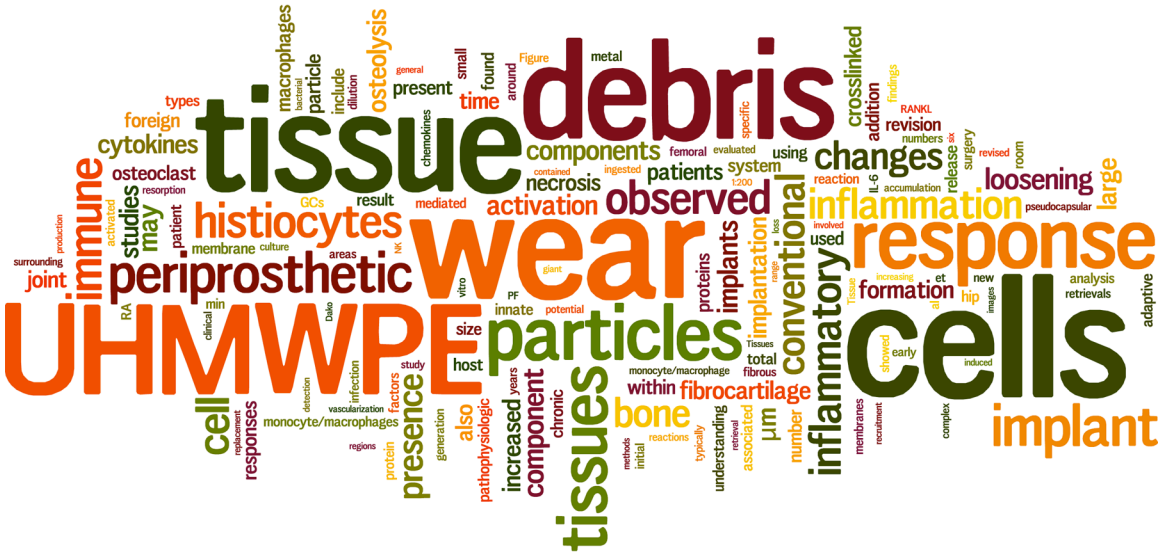
UHMWPE
wear
debris
tissue
cells
particles
tissues
response
inflammation
periprosthetic
implant
bone
fibrocartilage
inflammatory
conventional
observed
activation
histiocytes
components
changes
osteolysis
immune
presence
cell
implantation
implants
formation
loosening
crosslinked
revision
cytokines
foreign
macrophages
particle
osteoclast
necrosis
patients
system
joint
proteins
monocyte/macrophages
responses
pathophysiologic
increased
component
chronic
within
total
fibrous
used
number
understanding
associated
membranes
complex
adaptive
analysis
retrievals
pseudocapsular
large
surgery
revised
room
release
RANKL
numbers
addition
findings
specific
metal
Figure
small
found
around
time
present
general
include
dilution
bacterial
types
chemokines
result
mediated
GCs
resorption
activated
studies
may
patient
membrane
culture
areas
surrounding
production
RA
clinical
min
Dako
NK
vitro
PF
giant
innate
potential
size
host
study
infection
detection
vascularization
factors
protein
regions
generation
also
years
reactions
typically
methods
initial
retrieval
recruitment
μm
Tissues
monocyte/macrophage
showed
early
induced
increasing
et
al
new
hip
images
contained
ingested
1:200
IL-6
accumulation
evaluated
femoral
using
reaction
involved
loss
range
Dako

wordle.net

Executive Summary

For total joint replacements, osteolysis, the loss of bone loss at the bone-implant interface, and aseptic implant loosening have been identified as the prevalent reasons for revision surgery. However, for highly crosslinked polyethylene THA components as well as mobile-bearing TDRs, the clinical observation of osteolysis is rare. The current dissertation work provides an introduction to important concepts in total joint replacement, which are followed by five chapters that address unknown issues related to polyethylene wear debris in the hip and, briefly, in the spine. The work performed in these chapters addresses the following questions:

(1) What is the comparative efficiency of established tissue digestion methods for polyethylene wear particle extraction?

- Less than 1% of the initial one-gram porcine and human hip tissue samples remained after 24-hour digestion in 5*M* sodium hydroxide (NaOH), 5*M* and 15*M* potassium hydroxide (KOH) or 15.8M nitric acid (HNO_3) ($p < 0.05$).

- For formalin-fixed porcine hip tissues, less than 1% of the initial one-gram tissue weight remained after 24-hour digestion in 15.8*M* (HNO_3) ($p < 0.05$).

- Scanning electron microscopy was used to confirm the compatibility of 5*M* NaOH, 5*M* KOH or 15.8*M* solutions with both GUR415 polyethylene powder and Ceridust 3715 HDPE particles.

(2) What morphological changes and immune cells are present in tissues obtained at early revision surgery of loosened highly crosslinked polyethylene (HXLPE) components in the absence of radiographic osteolysis?

- Tissues were collected during revision surgery of gamma air-sterilized polyethylene (n = 9) and highly crosslinked polyethylene (HXLPE) implant components (n = 9) used in total hip replacement (THR).

- For tissues from the gamma air-sterilized polyethylene cohort, the presence of predominantly histiocytes, giant cells and focal regions of necrosis were associated with polyethylene wear debris.

- For the gamma air-sterilized polyethylene cohort, correlations were observed between wear debris and the magnitude of individual patient macrophage (ρ = 0.70) and T cell responses (ρ = 0.71), and separately between the overall number of macrophages and T cells in revision tissues (ρ = 0.77).

- For the HXLPE cohort, the presence of inflammation and associated wear debris were limited to tissues from patients revised >2 years after implantation; whereas, significant amounts of fibrocartilage/bone, were observed at earlier implantation times.

- For the HXLPE cohort, correlations were observed between wear debris and the magnitude of individual patient macrophage responses (ρ = 0.57), and separately between the overall number of macrophages and T cells in revision tissues (ρ = 0.68).

(3) How do modes of implant wear affect the biological activity of polyethylene wear debris generated in vivo?

- Tissues were collected during revision surgery of mobile-bearing total disc replacement (TDR) components with intermittent (mild; n = 4) or chronic (severe; n = 6) rim impingement, as well as one TDR revised for osteolysis.

- Overall, mean values of particle size, shape and number were not significantly different between intermittent and chronic impingement groups.

- Separation of particles into size ranges with high (<0.1-1 μm), intermediate (1-10 μm) and low (>10 μm) biological relevance revealed an increased mean particle size in the >10 μm range (p = 0.03) and an increased mean particle number in the 1-10 μm size range (p = 0.03) for the chronic impingement group.

- Analysis of the polyethylene particle volume distribution revealed significantly higher volume percentages in the <0.1-1 μm and 1-10 μm size ranges from TDRs with intermittent impingement (p = 0.04 and p = 0.03, respectively). Based on the increased biological relevance of these two size ranges, the specific biological activity (SBA) per unit volume was increased for the intermittent impingement group (p < 0.01).

- For the chronic impingement group, the increased number of particles in the 1-10 μm range, and larger particles in the >10 μm size range contributed to an increase in the total particle volume (mm^3)/gram of tissue ($p = 0.01$).

- When SBA was normalized by total particle volume (mm^3)/gram of tissue, functional biological activity (FBA) of particles from the chronic impingement group was significantly increased ($p = 0.01$).

- When considering all TDRs regardless of impingement group, the extent of linear rim penetration was positively correlated with both increasing particle size ($\rho = 0.68$) and number ($\rho = 0.72$). Linear rim penetration was also positively correlated with increasing values of FBA ($\rho = 0.75$).

- For the single TDR revised for osteolysis, equal percentages of rim and dome penetration likely contributed to the increase in both SBA and FBA.

(4) Can the reduced incidence of osteolysis around HXLPE components be attributed to a decrease in the biological activity of polyethylene wear debris generated *in vivo*?

- Tissues were collected during revision THR surgery of gamma inert-sterilized polyethylene (CPE; n = 4), as well as annealed (n = 5) and remelted highly crosslinked polyethylene (n = 5) implant components.

- Comparison of all three distributions revealed an increased particle size for the CPE cohort compared to the remelted and annealed HXLPE cohort tissues ($p < 0.001$).

- For all three cohorts, particles were predominantly granular or ellipsoidal, and the percentage of fibrils represented less than 10% of the total debris. However, particles in the CPE cohort possessed increased values of aspect ratio and decreased values of both roundness and form factor compared to the HXLPE cohorts ($p < 0.001$).

- Overall, the mean number of particles in the CPE cohort was higher than both annealed and remelted HXLPE cohorts ($p = 0.005$); however, submicron particles represented ~95% of the total debris in both HXLPE cohorts, which was significantly higher than the 90% in CPE cohort tissues ($p = 0.016$).

- Analysis of the polyethylene particle volume distribution did not reveal significant differences in the percentage of particle volume in <0.1-1 μm, 1-

10 μm or >10 μm size ranges. Similarly, the specific biological activity (SBA) per unit volume was not significantly different between CPE and/or HXLPE cohorts.

- For the CPE cohort, the increased particle size and particle number/gram of tissue contributed to a significant increase in total particle volume (mm^3)/gram compared to both HXLPE cohorts ($p = 0.006$).

- When SBA was normalized by the total particle volume (mm^3)/gram of tissue, functional biological activity (FBA) of particles from the CPE cohort was significantly higher than both HXLPE cohorts ($p = 0.014$).

- Statistically significant correlations between levels of tumor necrosis factor (TNF)-α, clinical variables or particle characteristics were not observed. However, in tissues revised after the longest implantation time, the levels of TNF-α were the lowest, which may represent a lesser involvement of TNF-α in end-stage osteolysis or the effect of tissue necrosis.

Overall, for periprosthetic and pseudocapsular tissues that were currently available, the work presented in this dissertation lends itself to a greater understanding of the significance of polyethylene wear debris *in vivo* in the context of the reasons for revision.

Introduction

Total joint replacement (TJR) surgery is intended to treat painful, end-stage joint disease, including osteoarthritis, rheumatoid arthritis and fractures, using a low-friction, load-bearing motion-preserving implant system. The successful clinical outcome of an initial, or primary, TJR surgery is contingent upon many factors, which include clinical factors such as surgical placement [1]; patient-specific factors such as genetics [2-5]; implant factors such as design; and a complex, dynamic process involving the host-response to the biomaterial components articulating in the surgically-altered joint [6-8]. Before studying joint arthroplasty, it is helpful to briefly review the history of total joint replacements, as well as the factors that drive the evolution of prevailing scientific theories about wear particle-mediated bone loss.

Now six decades after the pioneering work in total hip arthroplasty (THA) by Sir John Charnley, there have been many paradigm shifts in the understanding of the clinical performance of orthopedic devices. Charnley is credited with the first implementation of a low friction joint arthroplasty fixed to the bone using acrylic cement. After a series of catastrophic failures using hip replacements fabricated from polytetrafluoroethylene (PTFE), Charnley introduced polyethylene as a bearing material for use in the acetabulum [9]. After the introduction of polyethylene as a bearing material in 1962, another major shift occurring in the formative years of total joint replacement was modularity. This introduction of metal-backed polyethylene acetabular component designs in the 1980s was

intended to allow for revision of the polyethylene liner without disrupting an otherwise intact cement mantle [10]. The metal backing was also thought to better distribute the stresses of the bearing surface to the underlying bone [11]. The modular, metal-backed acetabular component represented the first full-scale implementation of the designs that are akin to THA components currently in widespread clinical use in the United States.

Based on the seminal work of Willert et al. in the early 1970s, the formation of granulation tissue, including macrophages and foreign-body giant cells in tissues from revision surgery of cemented THAs was attributed to the fragmentation of acrylic cement [12, 13]. Subsequently, the term “cement disease” was categorized as the coupling of cement-induced biological reactions with the observation of radiographic bone loss [14, 15]. Ultimately, as cementless total joint replacements became a more common practice, studies showing revision surgery due to osteolysis represented a crucial role for polyethylene wear debris in the biological response [16-20]. In both cases (cemented or uncemented) this loss of bone at the fixation interface resulted in the development of a loose implant requiring revision surgery. Ultimately, these early retrieval studies represented a major impetus for the development of wear-resistant polyethylene bearing surface technologies [21].

In the current dissertation, a summary of the literature on polyethylene wear particles and the corresponding biological responses to wear debris is provided. Through this overview of the literature, various unknown aspects of wear particle analysis are explored. Specifically, the current dissertation addresses the following

questions: (1) What is the comparative efficiency of established tissue digestion methods for polyethylene wear particle extraction? (2) What morphological changes and immune cells are present in tissues obtained at early revision surgery of loosened highly crosslinked polyethylene (HXLPE) components in the absence of radiographic osteolysis? (3) How do modes of implant wear affect the biological activity of polyethylene wear debris generated *in vivo*? (4) Can the reduced incidence of osteolysis around HXLPE components be attributed to a decrease in the biological activity of polyethylene wear debris generated *in vivo*?

Wear Particle Generation

Regardless of joint type or bearing surface materials, it is understood that the generation of wear debris occurs during each loading cyclic of a patient's daily activities [22]. Through the study of tribology, multiple factors are known to contribute to the wear of total joint replacement components. For polyethylene, wear has been attributed to variables that include surface roughness, implant conformity, the level of polymer crosslinking, the complexity of the wear path (combination of distance and direction), and the applied load [1, 22-26]. Although certain factors have a more constant effect on the wear performance, others such as the surface roughness, are variable throughout the duration of implantation [27]. In wear simulators and in the human body, protein fluid films help to mitigate the friction due to the roughness of a bearing surface. When the average fluid film thickness falls below the average surface roughness, the implant surface becomes a dominant factor of the load supporting system leading to fatigue of the material.

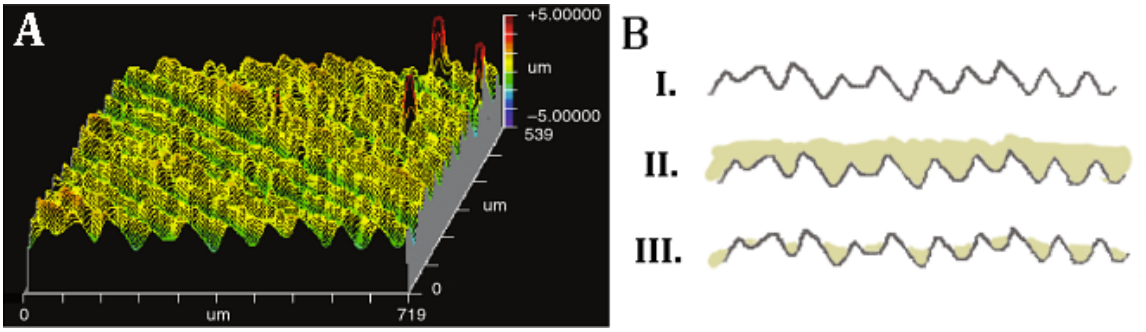

(A) White Light Interferometry showing deconvoluted machine marks of a never-implanted GUR 1050 polyethylene component used in THA, originally published by Kurtz et al., (2002)[28]. (B) Modified profile of (I) machine marks from A, (II) machine marks in the presence of excessive surface lubricant or (III) in the presence of sub-optimal surface lubricant resulting in the potential for accumulation of surface strains.

The formation of distinct particles is the result of strain accumulation in the surface layer resulting in nodular and/or fibrillar extensions along the predominant direction of the shear force [29]. When shear forces occur in an increasingly multidirectional loading environment, these extensions can then rupture to become what is classically known as a wear particle [29]. Particle generation resulting from the interaction of primary and/or secondary bearing surfaces can occur by several distinct wear modes [22]. Mode 1 wear occurs with the articulation of two bearing surfaces as intended by the design. Mode 2 is represented by the articulation of a bearing and a non-bearing surface, which may occur during the partial or complete dislocation of the femoral head from within the acetabular liner. Mode 3 occurs when abrasive third-body particles become entrapped between two articulating surfaces. Typically, in the context of polyethylene bearings, third-body particles possess a hardness that exceeds that of the polymer; whereas, polyethylene particles themselves can adhere to the bearing surface instead of acting as an

accelerant of the wear process. Finally, Mode 4 is the result of unintended articulation between two non-bearing surfaces [22].

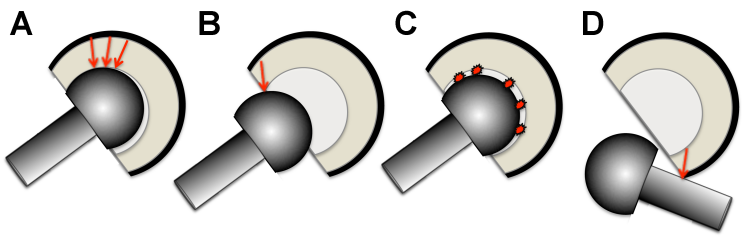

Schematic showing modes of wear on a representative acetabular liner and femoral head. (A) Mode 1, (B) Mode 2, (C) Mode 3, (D) Mode 4.

Impingement, which is typically ascribed to wear Mode 4, has been a recurrent source of concern in total hip and knee joint replacement, and has recently been acknowledged in the context of total disc replacements used in the lumbar spine. Ultimately, these modes of wear, individually or in combination, produce a variety of changes to the surface morphology of polyethylene components, which have been classified as burnishing, abrasion, scratches, plastic deformation, cracking, pitting, delamination, and the presence of embedded debris [30]. To date, neither *in vitro* wear simulation studies nor *in vivo* retrieval analyses have determined the effect(s) of implant wear modes on the characteristics and biological activity of polyethylene wear debris.

Advancements in Polyethylene Bearing Technology

For the polyethylenes originally used in THA, sterilization in air and storage in an air-permeable membrane resulted in exposure to atmospheric oxygen prior to implantation in the body. Much as the generation of wear debris is unavoidable

during the articulation of two bearing surfaces, the process of oxidation is similarly unavoidable after the exposure of polyethylene to oxygen. Generally, polyethylene is a chain of hydrogen and carbon bonds, which are bound covalently to form a chain. The length of the chain and the interaction between chains affect the strength and performance of materials *in vivo* [9]. For polyethylenes used in total joint replacement, Costa et al. (1998) demonstrated that the reaction of oxygen with macroradicals in the polymer induced the scission of polyethylene chains and the production of free radicals [31, 32]. Since the early acknowledgement of oxidation, others have also shown these reactions to occur both on the shelf and *in vivo* [31, 33, 34]. Currently, it is well-understood that oxidation and its secondary effects result in implant degradation, embrittlement, fatigue and accelerated wear occurring after a reduction in the mechanical properties of the material [9, 35]. To reduce oxidation, wear and wear-debris induced inflammatory reactions leading to osteolysis, these observations led to improved manufacturing standards, the sterilization of polyethylene in an inert environment (such as argon or nitrogen) and the development of a air-impermeable packaging [9]. To further improve implant wear resistance and decrease the incidence of osteolysis, highly crosslinked polyethylenes (HXLPE) were introduced as an alternative to conventional, gamma inert-sterilized polyethylene (CPE)[9, 36-38]. This first generation of HXLPE components was created by an initial phase of gamma-irradiation in an inert environment followed by an remelting or annealing phase performed above or below the crystalline transition temperature, respectively [9, 35, 39]. To date, both approaches have yielded improved clinical outcomes with regard to the reduction of

osteolysis at early-term (≤5 year) [40-45] and mid-term (5-10 year) follow-up [46-51]. However, the manufacture of annealed polyethylene results in the formation of residual free radicals with the potential to cause oxidation and component destabilization *in vivo* [31, 52-54]; whereas remelted polyethylene eliminates the entrapment of free radicals within the polymer but does so at the expense of reduced mechanical properties [55-58]. Each of these changes occurred over a period of years or even decades, requiring the accumulation of data to support the improvements compared to the previous generation of implants. Importantly, despite good early and mid-term results, the clinical performance of HXLPE bearings *in vivo* remains unproven after long-term implantation. Now slightly more than a decade after the first generation of HXLPE liners, additional measures have been employed to stabilize polyethylene implant components. These efforts include sequential irradiation and annealing to iteratively remove free radicals and the addition of antioxidants such as vitamin E [35, 59-61]; however, the understanding of the clinical impact of these newest approaches is limited to implantation times of less than five years [62].

Aseptic Loosening

Despite the improvements in the wear resistance of first-generation highly crosslinked polyethylene (HXLPE) used in THA, it is noteworthy that aseptic loosening remains the foremost reason for revision surgery [63, 64]. However, this loosening has been observed in the absence of a correlation with component wear and associated osteolysis. Terminology for loosening and osteolysis are often

considered interchangeably; however, the development of loosening is a complex process involving multiple etiologies [6, 65]. The distinctions between reasons leading to loosening are often not made at the time of revision surgery due to the difficulty in detecting small radiographic changes at early time points, and the potential involvement of poor initial fixation, stress shielding [66, 67], hydraulic fluid pressure [68] and/or endotoxin [69-73]. Nevertheless, the complexity of interactions at the bone-implant interface does not invalidate the need to understand mechanisms by which wear particles can affect the performance of total joint replacements. Importantly, for first-generation HXLPE liners, it remains unknown whether the decreased incidence of osteolysis can be attributed to a reduction in the biological activity of polyethylene wear particles generated *in vivo*.

Mechanisms of Wear Particle-Induced Inflammation

Studies investigating the biological response to wear debris have been performed with the specific goal of understanding the biological pathways, early clinical diagnostics and/or potential therapeutic interventions to wear particle induced-osteolysis. Based on clinical experience with and prior histological studies of tissues from revised gamma air-sterilized polyethylene components, the biological response to wear debris primarily involves macrophages [6, 12, 74]. Macrophages and other antigen-presenting cells ingest particles with the intent to degrade the foreign material [75]. For macrophages, the ingestion of foreign material begins within a phagosomal compartment, which fuses with internal lysosomal compartments containing digestive enzymes and peroxides [76-78].

Although this process temporarily sequesters wear particles, the digestive action of these enzymes and reactive oxygen species does not effectively degrade polyethylene wear debris. Ultimately, as particles continue to accumulate, the process of frustrated phagocytosis results in disruption of the phagolysosomal membrane, releasing both the toxic chemicals and the intact polyethylene wear debris into the local tissue environment [79]. Thus, the initiation of a cellular response to wear debris results in chronic inflammation that continues unabated unless the implant and affected tissues are removed during revision surgery [80].

Macrophages and other cells that have become activated by particle ingestion produce a multitude of cytokines, which include but are not limited to interleukin (IL)-1α, IL-1β, IL-6, IL-8, IL-11, IL-17 and tumor necrosis factor (TNF)-α [81-85]. Each of these cytokines plays a distinct role in the process leading to bone resorption, which is further modulated by the recruitment of additional innate and adaptive immune cells to the site of inflammation. The aforementioned cytokines, IL-1α and IL-1β, are also involved in promoting bone resorption by increasing the production of prostaglandins, collagenases and matrix metalloproteinases (MMPs) [86, 87], and have been shown to act synergistically with TNF-α to promote the maturation of osteoclast precursors [82, 88]. Separately, the activity of anti-inflammatory cytokines, such as transforming growth factor-beta (TGF-β), can dampen the inflammatory response or increase the relative rate of bone formation [88]. Importantly, bone remodeling that occurs naturally in the skeletal system involves both osteoclasts (bone resorbing cells) and osteoblasts (bone producing

cells). Wear particle-induced osteolysis is not a systemic disease but rather a prolonged, localized, deregulation of the balance between the actions of these two cell types [89]. One of the major regulatory mechanisms of bone homeostasis is the receptor activated NF-κB/RANK ligand/osteoprotegerin (RANK/RANKL/OPG) system. Specifically, OPG represents a soluble decoy receptor for RANK that blocks osteoclast formation by inhibiting binding of RANKL to RANK, thereby preventing excessive levels of bone resorption. Importantly, even a relative decrease in OPG can result in a greater potential for RANK and RANKL to promote the differentiation of osteoclast precursor cells into osteoclasts [90, 91]. Increased osteoclastogenesis has also been observed *in vitro* due to a separate synergistic effect of RANKL and TNF-α [92].

Following the ingestion of cellular debris by phagocytic cells, the presence of an antigen-specific major histocompatibility complex (MHC) along with T cells containing a co-stimulatory molecule enables the development of an adaptive immune response [77]. In the context of polyethylene wear debris, the immune response is classically considered to be non-specific (i.e. - involving components of the innate immune system). Thus, the role of T cells and the adaptive immune system in aseptic loosening remains controversial. In an osteolysis model of T cell-deficient rats, macrophage recruitment was maintained in response to HDPE particles compared to healthy controls [93]. In addition, an immunohistochemical study showing a lack of lymphokines (lymphocyte-derived cytokines) suggests that T cells are not activated in periprosthetic tissues, and thus do not play a role in

modulating the macrophage response to wear debris [94]. Nevertheless, recent tissue studies revealing significantly elevated levels of potent lymphocyte chemoattractants, interferon-γ-inducible protein of 10 kDa (IP-10) and monokine induced by interferon-γ (MIG), represent a chemotactic mechanism for T cell recruitment and support their potential role in wear particle-induced loosening pathways [91, 95]. Additional details on the types of T cells are provided in Chapter 3.

In Vitro and Animal Models

Overall, due to the redundancy of signaling pathways and the complex dynamic nature of the inflammatory response, no single therapeutic intervention has been shown to effectively treat aseptic loosening occurring as a result of wear particle-induced inflammation in humans [96]. However, because *in vitro* studies have fewer confounding variables, they offer an ideal method of separately evaluating the effects of particle-cell interactions. In these models, particles are exposed to a subset of cells capable of producing a representative, albeit limited, set of inflammatory cytokine responses [97]. In an evaluation of culture medium from rabbit synovial cells exposed to polyethylene wear debris, Kim et al., (1996) demonstrated the production of soluble factors involved in osteoclastogenesis [98]. Others simultaneously began to identify the effects of varying polyethylene wear particle size [99-101], dose/surface area ratio [99, 101] and polymer chemistry [102] on the cellular response of macrophage cell lines *in vitro*. Ultimately, the addition of controlled wear particle sizes and quantities led to the establishment of

predictive *in vitro* models, which allowed for pre-clinical assessments of the immunogenic potential of wear debris [103-106]. Currently of critical interest in these studies is the comparative assessment of the cellular response to clinically-relevant particles from conventional gamma inert-sterilized and HXLPE bearings [103, 104, 107, 108]. In the recent study by Illgen et al., (2008), HXLPE and CPE wear debris isolated from hip simulators were added to macrophages *in vitro* to measure the relative expression of cytokines [104] At the highest particle concentration based on surface area ratio, and acknowledging a contribution of endotoxin, macrophage expression of TNF-α was increased by 50% in response to HXLPE wear debris (mean size, 0.111 μm) compared to CPE wear debris (mean size, 0.196 μm). However, apart from these preliminary *in vitro* results, the comparison of the inflammatory potential has not been evaluated for CPE versus HXLPE wear debris *in* v*ivo*.

The use of animal models also represents a controlled environment to evaluate the biological response to polyethylene wear debris. Non-implant animal models involving the addition of particles in a non-physiologic location have been used to show the effects of varying particle characteristics [109-111]. In larger animal models, increased costs prevent the routine use of animals with physiologically-relevant loads compared to those experienced by implants and surrounding bones in humans [113]. Alternatively, small animal models, such as mice and rats, are advantageous due to the relatively low expense [51, 112]. However, the major advantage offered by animal studies is the ability to use

genetically-modified subjects (transgenic or knockout) to investigate specific osteoclastogenic pathways or factors believed to play a role in osteolysis and/or aseptic loosening [114-118]. In early studies of rabbit tibia, a foreign body inflammatory response as well as the suppression of bone formation was observed in response to polyethylene wear debris [119-121]. Subsequently, a series of studies performed on murine (mouse) air pouches also identified the potential importance of wear particle morphology, showing increased gene expression of RANK, RANKL, IL-1 and TNF-α in response to elongated particles versus globular particles [122, 123]. In addition, as demonstrated in the RANK knockout (RANK -/-) study by Ren et al., (2006), wear particle-induced inflammation in mice was shown to occur separately from the development of bone resorption [114]. In the past five years, animal studies have become increasingly complex, involving continuous infusion of particles [124, 125], the use of biologically relevant particles obtained from wear simulators [124], non-invasive volumetric outcomes measures of osteolysis in live animals using micro-computed tomography [116, 117], and the establishment of reproducible, quantitative criteria to screen therapeutic agents for their potential to prevent aseptic loosening [126]. As with rapid changes in bearing surface technology, an improved understanding of biological responses and superior technologies to characterize them will likely yield more clinically relevant outcomes over the next decade.

Human Tissue Studies

Although it represents the highest level of complexity, the most relevant method of the evaluating the effects of wear debris in humans requires the study of human tissues. Tissue samples can be collected from loosened TJRs during revision surgery or as part of an approved post-mortem follow-up [127, 128]. In a limited number of studies, the involvement of polyethylene wear debris in the development of osteolysis is refuted [129, 130]. Despite these infrequent contradictions, tissue studies have routinely acknowledged a crucial role of polyethylene wear debris as a primary driving force in biological responses resulting in the loss of bone at the fixation interface [7, 15, 21, 131, 132]. A more controversial aspect within tissue studies is the identification of a number threshold ($>10^9$/gram) associated with regions of radiographic osteolysis [133]. Opponents of this threshold have argued that definition of a number threshold is only representative of the clinical experience with gamma air-sterilized or gamma inert-sterilized polyethylene liners. Rather, in an adapted theory, it is proposed that the onset of osteolysis is dictated by a dose-response curve, which involves the dynamic balance of particle accumulation and particle migration [134]. In the event of a damaged lymphatic drainage mechanism, particle migration would be negatively affected, resulting in a more rapid accumulation of wear debris in the periprosthetic tissue and at the bone-implant interface [135]. In addition to the efficiency of lymphatic clearance, the potential for particle migration is also dependent on particle size and the anatomical variability in the morphology of the tissue surrounding the joint [136]. For first-generation HXLPE liners, the migration of and inflammatory response to wear

debris in periprosthetic tissues represents a major unknown aspect in the understanding of early and mid-term implant loosening.

Also among the currently underappreciated aspects of particle analysis is the relationship between particle number and penetration of the implant surface. Penetration is a term used to describe the combination of creep and wear. The former, occurring during the first 6-12 months after implantation [137], is categorized as a change in the surface dimension without an associated loss of material volume (i.e. – changes entirely occurring due to creep would not result in the generation of particles). After the implant has reached the maximum limit of creep, additional changes in implant dimension are attributed to the loss of material. Prior to the introduction of HXLPE, a review of clinical data from THR studies revealed a decreased incidence of osteolysis for femoral head penetration rates <0.1 mm/year [138]. Ultimately, based on their survey of the literature, Dumbleton et al., (2002) identified a critical threshold for the penetration rate of acetabular liners (0.05 mm/year), below which the clinical presentation of osteolysis would not be observed. However, opponents have argued that standardized assessments of penetration rate are confounded by differences in acetabular liner diameter, and are unproven for longer implantation times [139, 140]. Further discrepancies arise when considering the lack of correlations between gravimetric wear rate and the rate of polyethylene particle generation *in vitro* [141]. This controversy was also echoed in a recent computational study by Gallo et al., (2010) [140]. Using an algorithm to calculate the total number of polyethylene particles for a fixed volume

of component wear, they showed 4 and 5 orders of magnitude differences in the number of particles as a function of the width of the distribution and the size of the wear debris, respectively. Overall, these observations are extremely relevant to newer HXLPE acetabular liners [104, 141-143], and support the need for detailed characterizations of wear debris generated *in vivo*.

The overall objective of the current dissertation work is to address unknown aspects of the inflammatory responses, particle characteristics and osteolytic potential associated with polyethylene wear debris generated *in vivo*. Specifically, the following chapters address the following unanswered questions: (1) What is the comparative efficiency of established tissue digestion methods for polyethylene wear particle extraction? (2) What morphological changes and immune cells are present in tissues obtained at early revision surgery of loosened HXLPE components in the absence of radiographic osteolysis? (3) How do modes of implant wear affect the biological activity of polyethylene wear debris generated *in vivo*? (4) Can the reduced incidence of osteolysis around first-generation HXLPE components be attributed to a decrease in the biological activity of polyethylene wear debris generated *in vivo*?

To address these questions, Chapter 1 begins with an introduction of wear particle analysis, and provides a comparison of existing tissue digestion methods for wear particle extraction. The work presented in Chapter 2 focuses on comparing the more well-known histomorphologic changes occurring in tissues from revised gamma air-sterilized implants to a cohort of tissues from revised gamma inert-

sterilized highly crosslinked polyethylene (HXLPE) implants. For the HXLPE cohort, this chapter includes the most comprehensive characterization of tissues revised for aseptic loosening, which was made possible by revision surgeries performed between 2-6 years after implantation. These data provide insight into the range of regional tissue responses associated with implant loosening prior to the development of radiographic osteolysis. In chapter 3, the initial analysis of tissues from gamma air-sterilized and HXLPE implant components is extended to evaluate the role of innate and adaptive immune cells in implant loosening. For both polyethylene cohorts, this chapter evaluates potential correlations between the magnitudes of immune cell responses to wear debris, and ultimately lends support to the potential involvement of T cells in aseptic loosening based on the effect of cellular recruitment. In chapter 4, the attention is focused on determining the relationship between wear debris and implant component damage. Initially, a characterization of wear debris from revised mobile-bearing total disc replacements was performed to determine particle size, shape and number. In addition, the experimental application of an *in vitro* model of biological activity is provided for polyethylene wear debris generated *in vivo*. In the current work, biological activity values are used to distinguish differences between multiple wear modes compared to mean values of particle size, shape or number alone. In addition, these analyses reveal significant correlations between the extent of regional component damage and the size, number and biological activity of wear debris from revised mobile-bearing TDR components. In the final chapter, detailed analyses of wear particle characteristics and biological activity (osteolytic potential) are provided for two

cohorts of HXLPE acetabular liners, which are compared to a gamma inert-sterilized THA control group. These data represent the first *in vivo* comparison of wear particles from revised conventional and HXLPE polyethylene acetabular liners used in THA, and show that the inflammatory potential of HXLPE wear debris is outweighed by significant improvements in implant wear resistance. In the final chapter, patient-specific levels of a potent pro-inflammatory cytokine are determined to evaluate potential correlations with wear particle characteristics and biological activity. Overall, these results lend themselves to a greater understanding of the significance of polyethylene wear debris *in vivo* in the context of reasons for revision.

References

1. Tsao, A.K., L.C. Jones, and D.G. Lewallen, *What patient and surgical factors contribute to implant wear and osteolysis in total joint arthroplasty?* J Am Acad Orthop Surg, 2008. 16 Suppl 1: p. S7-13.
2. Gallo, J., F. Mrazek, and M. Petrek, *Variation in cytokine genes can contribute to severity of acetabular osteolysis and risk for revision in patients with ABG 1 total hip arthroplasty: a genetic association study.* BMC Med Genet, 2009. 10: p. 109-19.
3. Malik, M.H., et al., *Genetic susceptibility to total hip arthroplasty failure--positive association with mannose-binding lectin.* Journal of Arthroplasty, 2007. 22(2): p. 265-70.
4. Malik, M.H., et al., *Genetic susceptibility to hip arthroplasty failure--association with the RANK/OPG pathway.* Int Orthop, 2006. 30(3): p. 177-81.
5. Malik, M.H.A., et al., *Genetic susceptibility to total hip arthroplasty failure: a preliminary study on the influence of matrix metalloproteinase 1, interleukin 6 polymorphisms and vitamin D receptor.* Annals of the Rheumatic Diseases, 2007. 66(8): p. 1116-20.
6. Goodman, S.B., *Does the immune system play a role in loosening and osteolysis of total joint replacements?* Journal of Long-Term Effects of Medical Implants, 1996. 6(2): p. 91-101.
7. Goodman, S.B., *Wear particles, periprosthetic osteolysis and the immune system.* Biomaterials, 2007. 28(34): p. 5044-8.

8. Revell, P.A., *The combined role of wear particles, macrophages and lymphocytes in the loosening of total joint prostheses.* J R Soc Interface, 2008. 5(28): p. 1263-78.
9. Kurtz, S.M., *The UHMWPE Biomaterials Handbook: Ultra-High Molecular Weight Polyethylene in Total Joint Replacement and Medical Devices*. 2nd Edition ed. 2009, Burlington, MA Academic Press.
10. *Turek's Orthopaedics: Principles and Their Application*. 6 ed, ed. S.L. Weinstein and J.A. Buckwalter. 2005, Philadelphia: Lippincott Williams & Wilkins. 773.
11. Bartel, D.L., T.M. Wright, and D. Edwards, *The effect of metal backing on stresses in polyethylene acetabular components.* Hip, 1983: p. 229-39.
12. Willert, H.G., *Reactions of the articular capsule to wear products of artificial joint prostheses.* Journal of Biomedical Materials Research, 1977. 11(2): p. 157-64.
13. Willert, H.G., J. Ludwig, and M. Semlitsch, *Reaction of bone to methacrylate after hip arthroplasty: a long-term gross, light microscopic, and scanning electron microscopic study.* Journal of Bone & Joint Surgery - American Volume, 1974. 56(7): p. 1368-82.
14. Johanson, N.A., et al., *The microscopic anatomy of the bone-cement interface in failed total hip arthroplasties.* Clin Orthop Relat Res, 1987(218): p. 123-35.
15. Goodman, S.B., *Wear particulate and osteolysis.* Orthop Clin North Am, 2005. 36(1): p. 41-8.
16. Morscher, E.W., *Cementless total hip arthroplasty.* Clin Orthop Relat Res, 1983(181): p. 76-91.
17. Morscher, E.W., W. Dick, and V. Kernen, *Cementless fixation of polyethylene acetabular component in total hip arthroplasty.* Arch Orthop Trauma Surg, 1982. 99(4): p. 223-30.
18. Maloney, W.J., et al., *Endosteal erosion in association with stable uncemented femoral components.* Journal of Bone & Joint Surgery - American Volume, 1990. 72(7): p. 1025-34.
19. Peters, P.C., Jr., et al., *Osteolysis after total knee arthroplasty without cement.* J Bone Joint Surg Am, 1992. 74(6): p. 864-76.
20. Jasty, M., et al., *Etiology of osteolysis around porous-coated cementless total hip arthroplasties.* Clin Orthop Relat Res, 1994(308): p. 111-26.
21. Willert, H.G., H. Bertram, and G.H. Buchhorn, *Osteolysis in alloarthroplasty of the hip. The role of ultra-high molecular weight polyethylene wear particles.* Clinical Orthopaedics & Related Research, 1990(258): p. 95-107.
22. McKellop, H.A., *The lexicon of polyethylene wear in artificial joints.* Biomaterials, 2007. 28(34): p. 5049-57.
23. Williams, P.A. and I.C. Clarke, *Understanding polyethylene wear mechanisms by modeling of debris size distributions.* Wear, 2009. 267(1-4): p. 646-652.
24. Fisher, J., *Wear of Ultra High Molecular Weight Polyethylene in Total Artificial Joints.* Current Orthopaedics, 1994. 8: p. 164-169.
25. Buford, A. and T. Goswami, *Review of wear mechanisms in hip implants: Paper I - General.* Materials and Design, 2004. 25: p. 385-93.

26. Shanbhag, A.S., et al., *Quantitative analysis of ultrahigh molecular weight polyethylene (UHMWPE) wear debris associated with total knee replacements.* J Biomed Mater Res, 2000. 53(1): p. 100-10.
27. Bhushan, B., *Modern Tribology Handbook*. Vol. 1. 2000: CRC Press LLC. 1690.
28. Kurtz, S.M., et al., *Deconvolution of surface topology for quantification of initial wear in highly cross-linked acetabular components for THA.* J Biomed Mater Res, 2002. 63(5): p. 492-500.
29. Wang, A., C. Stark, and J.H. Dumbleton, *Mechanistic and morphological origins of ultra-high molecular weight polyethylene wear debris in total joint replacement prostheses.[comment].* Proceedings of the Institution of Mechanical Engineers. Part H - Journal of Engineering in Medicine, 1996. 210(3): p. 141-55.
30. Hood, R.W., T.M. Wright, and A.H. Burstein, *Retrieval analysis of total knee prostheses: a method and its application to 48 total condylar prostheses.* J Biomed Mater Res, 1983. 17(5): p. 829-42.
31. Costa, L., et al., *In vivo UHMWPE biodegradation of retrieved prosthesis.* Biomaterials, 1998. 19(15): p. 1371-1385.
32. Costa, L., et al., *Oxidation in orthopaedic UHMWPE sterilized by gamma-radiation and ethylene oxide.* Biomaterials, 1998. 19(7-9): p. 659-668.
33. Kurtz, S.M., et al., *In vivo degradation of polyethylene liners after gamma sterilization in air.* J Bone Joint Surg Am, 2005. 87(4): p. 815-23.
34. Currier, B.H., et al., *Shelf life and in vivo duration. Impacts on performance of tibial bearings.* Clin Orthop Relat Res, 1997(342): p. 111-22.
35. Gomez-Barrena, E., F. Medel, and J.A. Puertolas, *Polyethylene oxidation in total hip arthroplasty: evolution and new advances.* Open Orthop J, 2009. 3: p. 115-20.
36. Harris, W.H. and O.K. Muratoglu, *A review of current cross-linked polyethylenes used in total joint arthroplasty.* Clinical Orthopaedics & Related Research, 2005(430): p. 46-52.
37. McKellop, H., et al., *Development of an extremely wear-resistant ultra high molecular weight polyethylene for total hip replacements.* J Orthop Res, 1999. 17(2): p. 157-67.
38. Muratoglu, O.K., et al., *A novel method of cross-linking ultra-high-molecular-weight polyethylene to improve wear, reduce oxidation, and retain mechanical properties. Recipient of the 1999 HAP Paul Award.* J Arthroplasty, 2001. 2001: p. 149-160.
39. Oral, E. and O.K. Muratoglu, *Radiation cross-linking in ultra-high molecular weight polyethylene for orthopaedic applications.* Nucl Instrum Methods Phys Res B, 2007. 265(1): p. 18-22.
40. Kurtz, S.M., et al., *Mechanical properties of retrieved highly cross-linked crossfire liners after short-term implantation.* J Arthroplasty, 2005. 20(7): p. 840-9.
41. Rajadhyaksha, A.D., et al., *Five-year comparative study of highly cross-linked (crossfire) and traditional polyethylene.* J Arthroplasty, 2009. 24(2): p. 161-7.

42. Digas, G., et al., *5-year experience of highly cross-linked polyethylene in cemented and uncemented sockets: two randomized studies using radiostereometric analysis.* Acta Orthopaedica, 2007. 78(6): p. 746-54.
43. D'Antonio, J.A., et al., *Five-year experience with Crossfire highly cross-linked polyethylene.* Clin Orthop Relat Res, 2005. 441: p. 143-50.
44. Olyslaegers, C., et al., *Wear in conventional and highly cross-linked polyethylene cups: a 5-year follow-up study.* Journal of Arthroplasty, 2008. 23(4): p. 489-94.
45. Geerdink, C.H., et al., *Crosslinked polyethylene compared to conventional polyethylene in total hip replacement: pre-clinical evaluation, in-vitro testing and prospective clinical follow-up study.* Acta Orthopaedica, 2006. 77(5): p. 719-25.
46. Engh, C.A., Jr., et al., *A randomized prospective evaluation of outcomes after total hip arthroplasty using cross-linked marathon and non-cross-linked Enduron polyethylene liners.* J Arthroplasty, 2006. 21(6 Suppl 2): p. 17-25.
47. Rohrl, S.M., et al., *Very low wear of non-remelted highly cross-linked polyethylene cups: an RSA study lasting up to 6 years.* Acta Orthopaedica, 2007. 78(6): p. 739-45.
48. Geerdink, C.H., et al., *Cross-linked compared with historical polyethylene in THA: an 8-year clinical study.* Clin Orthop Relat Res, 2009. 467(4): p. 979-84.
49. Kurtz, S.M., et al., *Mechanical properties, oxidation, and clinical performance of retrieved highly cross-linked Crossfire liners after intermediate-term implantation.* Journal of Arthroplasty, 2010. 25(4): p. 614-23 e1-2.
50. Kurtz, S.M., H.A. Gawel, and J. Patel, *History and Systematic Review of Wear and Osteolysis Outcomes for First-Generation Highly Crosslinked Polyethylene.* Clin Orthop Relat Res, 2011. Epub Mar 23.
51. Langlois, J. and M. Hamadouche, *New animal models of wear-particle osteolysis.* Int Orthop, 2011. 35(2): p. 245-51.
52. Kurtz, S.M., et al., *2006 Otto Aufranc Award Paper: significance of in vivo degradation for polyethylene in total hip arthroplasty.* Clin Orthop Relat Res, 2006. 453: p. 47-57.
53. Maitra, R., et al., *Immunogenecity of modified alkane polymers is mediated through TLR1/2 activation.* PLoS One, 2008. 3(6): p. e2438.
54. Ferroni, D. and V. Quaglini, *Thermal stabilization of highly crosslinked UHMWPE: a comparative study between annealed and remelted resins.* J Appl Biomater Biomech, 2010. 8(2): p. 82-8.
55. Pruitt, L.A., *Deformation, yielding, fracture and fatigue behavior of conventional and highly cross-linked ultra high molecular weight polyethylene.* Biomaterials, 2005. 26(8): p. 905-15.
56. Oral, E., A.S. Malhi, and O.K. Muratoglu, *Mechanisms of decrease in fatigue crack propagation resistance in irradiated and melted UHMWPE.* Biomaterials, 2006. 27(6): p. 917-25.
57. Tower, S.S., et al., *Rim cracking of the cross-linked longevity polyethylene acetabular liner after total hip arthroplasty.* J Bone Joint Surg Am, 2007. 89(10): p. 2212-7.

58. Furmanski, J., et al., *Clinical fracture of cross-linked UHMWPE acetabular liners.* Biomaterials, 2009. 30(29): p. 5572-82.
59. Morrison, M.L. and S. Jani, *Evaluation of sequentially crosslinked ultra-high molecular weight polyethylene.* J Biomed Mater Res B Appl Biomater, 2009. 90(1): p. 87-100.
60. Bracco, P. and E. Oral, *Vitamin E-stabilized UHMWPE for Total Joint Implants: A Review.* Clin Orthop Relat Res, 2010.
61. Oral, E. and O.K. Muratoglu, *Vitamin E diffused, highly crosslinked UHMWPE: a review.* Int Orthop, 2011. 35(2): p. 215-23.
62. Campbell, D.G., J.R. Field, and S.A. Callary, *Second-generation highly cross-linked X3 polyethylene wear: a preliminary radiostereometric analysis study.* Clin Orthop Relat Res, 2010. 468(10): p. 2704-9.
63. Kurtz, S.M., et al., *Reasons for Revision of First-Generation Highly Cross-Linked Polyethylenes.* Journal of Arthroplasty, 2010.
64. Clohisy, J.C., et al., *Reasons for revision hip surgery: a retrospective review.* Clinical Orthopaedics & Related Research, 2004(429): p. 188-92.
65. Sundfeldt, M., et al., *Aseptic loosening, not only a question of wear: a review of different theories.* Acta Orthop, 2006. 77(2): p. 177-97.
66. *Revision total knee arthroplasty*, ed. J.V. Bono and R.D. Scott. 2005: Springer Science + Business Media, Inc.
67. Bertani, A., et al., *Total hip arthroplasty in severe segmental femoral bone loss situations: use of a reconstruction modular stem design (JVC IX). Retrospective study of 23 cases.* Orthop Traumatol Surg Res, 2009. 95(7): p. 491-7.
68. Fahlgren, A., et al., *Fluid pressure and flow as a cause of bone resorption.* Acta Orthop, 2010. 81(4): p. 508-16.
69. Bi, Y., et al., *Adherent endotoxin on orthopedic wear particles stimulates cytokine production and osteoclast differentiation.* Journal of Bone & Mineral Research, 2001. 16(11): p. 2082-91.
70. Cho, D.R., et al., *The role of adsorbed endotoxin in particle-induced stimulation of cytokine release.* J Orthop Res, 2002. 20(4): p. 704-13.
71. Greenfield, E.M., et al., *Bacterial pathogen-associated molecular patterns stimulate biological activity of orthopaedic wear particles by activating cognate Toll-like receptors.* Journal of Biological Chemistry, 2010. 285(42): p. 32378-84.
72. Tatro, J., et al., *The Balance between Endotoxin Accumulation and Clearance During Particle-Induced Osteolysis in Murine Calvaria.* Journal of Orthopaedic Research, 2006. 24: p. 1-9.
73. Wilkins, R., M. Tucci, and H. Benghuzzi, *Evaluation of endotoxin binding to uhmwpe and inflammatory mediator production by macrophages.* Biomed Sci Instrum, 2008. 44: p. 459-64.
74. Mirra, J.M., et al., *The pathology of the joint tissues and its clinical relevance in prosthesis failure.* Clin Orthop, 1976. 117: p. 221-240.
75. Ingham, E. and J. Fisher, *Biological reactions to wear debris in total joint replacement.* Proc Inst Mech Eng [H], 2000. 214(1): p. 21-37.

76. Ingham, E. and J. Fisher, *The role of macrophages in osteolysis of total joint replacement.* Biomaterials, 2005. 26(11): p. 1271-86.
77. *Handbook of Human Immunology*, ed. M.R.G. O'Gorman and A.D. Donnenberg. 2008, Boca Raton: CRC Press.
78. Aderem, A. and D.M. Underhill, *Mechanisms of Phagocytosis in Macrophages.* Annu Rev Immunol, 1999. 17: p. 593-623.
79. Stea, S., et al., *Apoptosis in peri-implant tissue.* Biomaterials, 2000. 21: p. 1393-1398.
80. Abu-Amer, Y., I. Darwech, and J.C. Clohisy, *Aseptic loosening of total joint replacements: mechanisms underlying osteolysis and potential therapies.* Arthritis Res Ther, 2007. 9 Suppl 1: p. S6.
81. Xu, J.W., et al., *Interleukin-11 in aseptic loosening of total hip replacement.* Scand J Rheumatol, 1998. 27(5): p. 363-367.
82. Wei, S., et al., *IL-1 mediates TNF-induced osteoclastogenesis.* J Clin Invest, 2005. 115(2): p. 282-290.
83. al Saffar, N. and P.A. Revell, *Interleukin-1 production by activated macrophages surrounding loosened orthopaedic implants: a potential role in osteolysis.* British Journal of Rheumatology, 1994. 33(4): p. 309-16.
84. Bendre, M.S., et al., *Interleukin-8 stimulation of osteoclastogenesis and bone resorption is a mechanism for the increased osteolysis of metastatic bone disease.* Bone, 2003. 33(1): p. 28-37.
85. Miossec, P., *Interleukin-17 in rheumatoid arthritis: if T cells were to contribute to inflammation and destruction through synergy.* Arthritis & Rheumatism, 2003. 48(3): p. 594-601.
86. Gallo, J., et al., *Particle disease. A comprehensive theory of periprosthetic osteolysis: a review.* Biomedical Papers of the Medical Faculty of Palacky University in Olomouc, Czech Republic, 2002. 146(2): p. 21-8.
87. Tuan, R.S., et al., *What are the local and systemic biologic reactions and mediators to wear debris, and what host factors determine or modulate the biologic response to wear particles?* Journal of the American Academy of Orthopaedic Surgeons, 2008. 16 Suppl 1: p. S42-8.
88. Fiorito, S., L. Magrini, and C. Goalard, *Pro-inflammatory and anti-inflammatory circulating cytokines and periprosthetic osteolysis.* J Bone Joint Surg Br, 2003. 85: p. 1202-1206.
89. Dean, D.D., et al., *The effect of ultra-high molecular weight polyethylene wear debris on MG63 osteosarcoma cells in vitro.* J Bone Joint Surg Am, 1999. 81(4): p. 452-61.
90. Boyce, B.F. and L. Xing, *Functions of RANKL/RANK/OPG in bone modeling and remodeling.* Arch Biochem Biophys, 2008. 473(2): p. 139-46.
91. Wang, C.T., et al., *Over-expression of receptor activator of nuclear factor-kappaB ligand (RANKL), inflammatory cytokines, and chemokines in periprosthetic osteolysis of loosened total hip arthroplasty.* Biomaterials, 2010. 31(1): p. 77-82.

92. Holding, C.A., et al., *The correlation of RANK, RANKL and TNFalpha expression with bone loss volume and polyethylene wear debris around hip implants.* Biomaterials, 2006. 27(30): p. 5212-9.
93. Goodman, S., et al., *T-lymphocytes are not necessary for particulate polyethylene-induced macrophage recruitment. Histologic studies of the rat tibia.* Acta Orthop Scand, 1994. 65(2): p. 157-60.
94. Li, T.F., et al., *No lymphokines in T-cells around loosened hip prostheses.* Acta Orthop Scand, 2001. 72(3): p. 241-7.
95. Shanbhag, A.S., et al., *Assessing osteolysis with use of high-throughput protein chips.* Journal of Bone & Joint Surgery - American Volume, 2007. 89(5): p. 1081-9.
96. Goodman, S.B. and T. Ma, *Cellular chemotaxis induced by wear particles from joint replacements.* Biomaterials, 2010. 31(19): p. 5045-50.
97. *What experimental approaches (tissue retrieval, in vivo, in vitro, etc) have been used to investigate the biologic effects of particles?* Transaction of the 68th Meeting of the American Association of Orthopaedic Surgeons, 2001: p. 10.
98. Kim, K.J., et al., *Activation of osteoclast-mediated bone resorption by the supernatant from a rabbit synovial cell line in response to polyethylene particles.* J Biomed Mater Res, 1996. 32(1): p. 3-9.
99. Shanbhag, A.S., et al., *Effects of particles on fibroblast proliferation and bone resorption in vitro.* Clin Orthop Relat Res, 1997(342): p. 205-17.
100. Green, T.R., et al., *Polyethylene particles of a 'critical size' are necessary for the induction of cytokines by macrophages in vitro.* Biomaterials, 1998. 19(24): p. 2297-302.
101. Green, T.R., et al., *Effect of size and dose on bone resorption activity of macrophages by in vitro clinically relevant ultra high molecular weight polyethylene particles.* J Biomed Mater Res, 2000. 53(5): p. 490-7.
102. Boynton, E., et al., *The Effect of polyethylene particle chemistry on human monocyte-macrophage function in vitro.* Journal of Biomedical Materials Research, 2000. 52: p. 7.
103. Fisher, J., et al., *A novel method for the prediction of functional biological activity of polyethylene wear debris.* Proceedings of the Institution of Mechanical Engineers. Part H - Journal of Engineering in Medicine, 2001. 215(2): p. 127-32.
104. Illgen, R.L., 2nd, et al., *Highly crosslinked vs conventional polyethylene particles--an in vitro comparison of biologic activities.* Journal of Arthroplasty, 2008. 23(5): p. 721-31.
105. Matthews, J.B., et al., *Evaluation of the Response of Primary Human Peripheral Blood Mononuclear Phagocytes to Challenge with In Vitro Generated Clinically Relevant UHMWPE Particles of Known Size and Dose.* J Biomed Mater Res 2000. 52: p. 296-307.
106. Matthews, J.B., et al., *Comparison of the response of primary human peripheral blood mononuclear phagocytes from di!erent donors to challenge with model polyethylene particles of known size and dose.* Biomaterials, 2000. 21: p. 2033-2044.

107. Sethi, R.K., et al., *Macrophage response to cross-linked and conventional UHMWPE.* Biomaterials, 2003. 24(15): p. 2561-73.
108. Ingram, J., et al., *Comparison of the biological activity of grade GUR 1120 and GUR 415HP UHMWPE wear debris.* Biomed Mater Eng, 2002. 12(2): p. 177-88.
109. Goodman, S., *The effects of micromotion and particulate materials on tissue differentiation.* Acta Orthop Scand Suppl, 1994. 258: p. 1-43.
110. Goodman, S., et al., *Local infusion of FGF-2 enhances bone ingrowth in rabbit chambers in the presence of polyethylene particles.* Journal of Biomedical Materials Research, 2003. 65A: p. 8.
111. Trindade, M., et al., *Proinflammatory mediator release in response to particle challenge: studies using the bone harvest chamber.* J Biomed Mater Res, 1999. 48: p. 434-439.
112. Ren, P., et al., *Surveillance of systemic trafficking of marophages induced by UMWPE particle in nude mice by noninvasive imaging.* j Biomed Mater Res 2010. 94(3): p. 706-711.
113. Shanbhag, A.S., C.T. Hasselman, and H.E. Rubash, *The John Charnley Award. Inhibition of wear debris mediated osteolysis in a canine total hip arthroplasty model.* Clinical Orthopaedics & Related Research, 1997(344): p. 33-43.
114. Ren, W., et al., *Implant wear induces inflammation, but not osteoclastic bone resorption, in RANK(-/-) mice.* Journal of Orthopaedic Research, 2006. 24(8): p. 1575-86.
115. Taki, N., et al., *Comparison of the roles of IL-1, IL-6, and TNFalpha in cell culture and murine models of aseptic loosening.* Bone, 2007. 40(5): p. 1276-83.
116. Wedemeyer, C., et al., *Polyethylene particle-induced bone resorption in substance P-deficient mice.* Calcified Tissue International, 2007. 80(4): p. 268-74.
117. Tsutsumi, R., et al., *PGE2 Signaling Through the EP4 Receptor on Fibroblasts Upregulates RANKL and Stimulates Osteolysis.* Journal of Bone and Mineral Research, 2009. 24(10): p. 1753-1762.
118. Merkel, K.D., et al., *Tumor necrosis factor-alpha mediates orthopedic implant osteolysis.* American Journal of Pathology, 1999. 154(1): p. 203-10.
119. Goodman, S., et al., *Polyethylene and titanium alloy particles reduce bone formation. Dose-dependence in bone harvest chamber experiments in rabbits.* Acta Orthop Scand, 1996. 67(6): p. 599-605.
120. Goodman, S.B., et al., *Histomorphological reaction of bone to different concentrations of phagocytosable particles of high-density polyethylene and Ti-6Al-4V alloy in vivo.* Biomaterials, 1996. 17(20): p. 1943-7.
121. Sacomen, D., et al., *Effects of polyethylene particles on tissue surrounding knee arthroplasties in rabbits.* J Biomed Mater Res, 1998. 43(2): p. 123-30.
122. Ren, W., et al., *Distinct gene expression of receptor activator of nuclear factor-kappaB and rank ligand in the inflammatory response to variant morphologies of UHMWPE particles.* Biomaterials, 2003. 24(26): p. 4819-26.
123. Yang, S., et al., *Diverse cellular and apoptotic responses to variant shapes of UHMWPE particles in a murine model of inflammation.* Biomaterials, 2002. 23: p. 3535-3543.

124. Ma, T., et al., *An in vivo murine model of continuous intramedullary infusion of polyethylene particles.* Biomaterials, 2008. 29(27): p. 3738-42.
125. Ortiz, S.G., et al., *Validation and quantification of an in vitro model of continuous infusion of submicron-sized particles.* Journal of Biomedical Materials Research, 2008. Part B, Applied Biomaterials. 84(2): p. 328-33.
126. Schwarz, E.M., et al., *Quantitative small-animal surrogate to evaluate drug efficacy in preventing wear debris-induced osteolysis.* Journal of Orthopaedic Research, 2000. 18(6): p. 849-55.
127. Urban, R.M., et al., *Dissemination of wear particles to the liver, spleen, and abdominal lymph nodes of patients with hip or knee replacement.[see comment].* Journal of Bone & Joint Surgery - American Volume, 2000. 82(4): p. 457-76.
128. Hirakawa, K., et al., *Mechanisms of failure of total hip replacements - Lessons learned from retrieval studies.* Clinical Orthopaedics and Related Research, 2004(420): p. 10-17.
129. Wroblewski, B.M., *Osteolysis due to particle wear debris following total hip arthroplasty: the role of high-density polyethylene.* Instructional Course Lectures, 1994. 43: p. 289-94.
130. De Jong, P.T., et al., *Polyethylene wear particles do not induce inflammation or gelatinase (MMP-2 and MMP-9) activity in fibrous tissue interfaces of loosening total hip arthroplasties.* Acta Histochem, 2010.
131. Baxter, R.M., et al., *Do Tissues from THA Revision of HXLPE Liners Contain Wear Debris and Associated Inflammation?* Clin Orthop Relat Res, 2010. In Review(Aug 2010).
132. Baxter, R.M., et al., *Distinct immunohistomorphologic changes in periprosthetic hip tissues from historical and highly crosslinked UHMWPE implant retrievals.* J Biomed Mater Res A, 2010. 95(1): p. 68-78.
133. Kobayashi, A., et al., *Number of polyethylene particles and osteolysis in total joint replacements. A quantitative study using a tissue-digestion method.* Journal of Bone & Joint Surgery - British Volume, 1997. 79(5): p. 844-8.
134. Wilkinson, J.M., et al., *Polyethylene wear rate and osteolysis: critical threshold versus continuous dose-response relationship.* Journal of Orthopaedic Research, 2005. 23(3): p. 520-5.
135. Edwards, J., et al., *Absence of lymphatics at the bone-implant interface: implications for periprosthetic osteolysis.* Acta Orthopaedica, 2008. 79(2): p. 289-94.
136. Elfick, A.P.D., et al., *The nature and dissemination of UHMWPE wear debris retrieved from periprosthetic tissue of THR.* J. Viomws. Mater. Res., 2003. 65A: p. 95-108.
137. Glyn-Jones, S., et al., *The creep and wear of highly cross-linked polyethylene - A three-year randomised, controlled trial using radiostereometric analysis.* Journal of Bone and Joint Surgery-British Volume, 2008. 90B(5): p. 556-561.
138. Dumbleton, J.H., M.T. Manley, and A.A. Edidin, *A literature review of the association between wear rate and osteolysis in total hip arthroplasty.* Journal of Arthroplasty, 2002. 17(5): p. 649-61.

139. Harris, W.H., *"The lysis threshold": an erroneous and perhaps misleading concept?* Journal of Arthroplasty, 2003. 18(4): p. 506-10.
140. Gallo, J., M. Slouf, and S.B. Goodman, *The relationship of polyethylene wear to particle size, distribution, and number: A possible factor explaining the risk of osteolysis after hip arthroplasty.* J Biomed Mater Res B Appl Biomater, 2010. 94(1): p. 171-7.
141. Ries, M.D., M.L. Scott, and S. Jani, *Relationship between gravimetric wear and particle generation in hip simulators: conventional compared with cross-linked polyethylene.* Journal of Bone & Joint Surgery - American Volume, 2001. 83-A Suppl 2 Pt 2: p. 116-22.
142. Williams, P.A., et al., *Highly Crosslinked Polyethylenes in Hip Replacements: Improved Wear Performance of Paradox?* STLE Tribology Transactions, 2007. 50(2): p. 227-290.
143. Yamamoto, K., et al., *Microwear phenomena of ultrahigh molecular weight polyethylene cups and debris morphology related to gamma radiation dose in simulator study.* Journal of Biomedical Materials Research, 2001. 56(1): p. 65-73.

1. Comparison of Tissue Digestion Methods for Polyethylene Wear Particle Analysis[1]

Abstract

There is considerable interest in characterization of wear debris from ultra-high molecular weight polyethylene (polyethylene) bearing components used in total joint replacement (TJR). To isolate polyethylene wear debris, tissue samples must be excised from regions adjacent to revised polyethylene implant components, followed by exposure to one of many available tissue digestion methods. Numerous studies demonstrate successful digestion, but the relative efficiency of each method is not clear. In this first chapter, a variety of conditions for tissue digestion were evaluated to provide a quantitative comparison of methods. Porcine and human hip tissues were exposed for 24 hours to basic, acidic or enzymatic agents, filtered and digestion efficiency calculated based on the percentage of initial to final tissue weight. Of the conditions tested, 5*M* NaOH, 5*M* KOH, 15*M* KOH or 15.8*M* HNO_3 yielded the most complete porcine hip tissue digestion (<1% residual tissue weight). Proteinase K and Liberase Blendzyme 3 did not effectively digest tissue in a 24 hour period. Similar to results from the porcine dataset, human tissues digestion was most efficient using 5*M* NaOH, 5*M* KOH or 15.8*M* HNO_3 (<1% residual tissue weight). To verify that particle surface modifications did not occur after prolonged reagent exposure, GUR415 and Ceridust 3715 particles were immersed in each

---

[1] Baxter RM, Tipper JL, Parvizi J, Marcolongo M, Kurtz SM, Steinbeck MJ. Comparison of Periprosthetic Tissue Digestion Methods for Ultra-High Molecular Weight Polyethylene Wear Extraction. J Biomed Mater Res B Appl Biomater. 2009 Oct;91(1):409-18.

solution for 24 hours. Overall, this study provides a framework for thorough and efficient digestive methods for polyethylene wear debris extraction.

Introduction

There is considerable interest in characterization of wear debris from ultra-high molecular weight polyethylene (polyethylene) bearing components used in total joint replacement (TJR). The generation of polyethylene wear particles and the ensuing development of particle-induced osteolysis is a significant complication of total joint replacement (TJR), which contributes to decreased implant fixation and limits the long-term survival of joint replacement components [1, 2]. To understand particle characteristics, analysis of wear debris is often performed after wear simulation of TJR components *in vitro*; however, the true complexity of wear that occurs *in vivo* has yet to be achieved by simulator studies [3]. Thus, to obtain a clinically-relevant assessment of wear debris necessitates the collection of tissues from TJRs obtained at revision surgery or autopsy [4-7]. In the tissues surrounding the implanted joint, particle-induced macrophage activation marks the beginning of a chronic inflammatory response and the release of various cytokines and factors that promote adverse biological responses and/or bone loss. The formation of osteoclasts, bone resorbing cells, as well as a partial reduction in bone formation, leads to a predominance of bone loss at the prosthesis-bone interface [8-11]. The polyethylene wear particle-induced activation and progression of chronic inflammation, and the potential for osteolysis, is dependent on several aspects of particle generation, which include particle accumulation, size, shape and number

[12-20].

Particulate wear debris results from the motion between opposing implant bearing surfaces. The generation of wear debris is a function of several variables, which include lubrication, sliding distance, specifics of the manufacturing of the polyethylene component and level of patient activity [21]. Shanbhag et al., (2000) showed that wear particle size also varies by joint type based on differences in the loading and conformity of mating bearing surfaces [16]. In addition, implant exposure to oxygen-rich biological fluid can cause *in vivo* degradation of the mechanical properties of polyethylene components, which leads to an increase in the overall wear rate [21, 22]. As new polymer bearing components are introduced, such as highly-crosslinked polyethylene, a detailed understanding of the polyethylene wear behavior is necessary.

The process of studying clinically relevant wear debris begins at the time of implant removal and the surgical excision of adjacent or periprosthetic tissue. This is followed by tissue digestion to extract embedded polyethylene, metal, ceramic and/or bone cement debris. Previous tissue digestive approaches to isolate polyethylene wear debris include the use of basic, acidic and enzymatic reagent solutions (Table 1-1). In general, periprosthetic tissue digestion has been accomplished using a range of reagents, temperatures, solution concentrations, and digestive time periods. Sodium hydroxide (NaOH) and potassium hydroxide (KOH) are common basic reagents used for tissue digestion. Campbell et al. (1994) digested tissue at 65°C for 1–5 hours with 5*M* NaOH, and these conditions have been

subsequently widely used by others [18, 23, 24]. The digestion time was then extended to 24 hours by other investigators to achieve complete digestion of formalin-fixed tissues [25, 26]. Shanbhag et al., (2000) used 4*M* KOH at 56°C for 48 hours to digest formalin-fixed tissue, whereas Tipper et al. (2000) and Howling et al., (2001) used 12*M* KOH at 60°C for 2–5 days [16, 27, 28]. Tissue digestion to extract polyethylene wear debris has also been achieved using acid reagent solutions. Margevicius et al., (1994) digested formalin-fixed tissue at room temperature for 48 hours using concentrated nitric acid (HNO_3), which were also conditions used by others to digest fresh tissue [29-32]. Hydrochloric acid (HCl) has been used in limited instances, but with poor efficiency compared to tissue digestion in concentrated HNO_3 [29]. Another approach has been to use enzymatic solutions to digest tissue. Maloney et al. (1995) exposed tissue to 7 mg/mL of papain in phosphate buffer (pH 6.5) containing 2 mM N-acetylcysteine at 65°C, and other investigators used 0.3 mg/mL of papain [33-36]. The use of papain required 2–3 days and daily addition of fresh enzyme stock. In another study, tissue was digested in 2 mg/mL of collagenase in phosphate buffer (pH 7.0) for 24 hours at 37°C [37].

While each of these approaches have been used to isolate wear debris, the relative digestive efficiency of these agents remains unclear. Based on many of the previous studies, the ASTM standard document for particle analysis suggests a number of digestion solutions can be used to extract polyethylene particles [38]. However, these standards provide neither conclusive guidance nor comparative assessment of particle isolation techniques. In the current chapter, a variety of

conditions for tissue digestion were evaluated to provide a quantitative and comparative assessment of digestion efficiency. The primary hypothesis was that among previously utilized methods, one would provide thorough, efficient digestion of periprosthetic tissues.

Methods

The following materials were used: sodium hydroxide (NaOH, Catalog: S3181), potassium hydroxide (KOH, Catalog: 1310-58-3) (Fisher Scientific, Hampton, NH), Proteinase K (Catalog: BIO-37037, Bioline, Randolph, MA) Liberase Blendzyme 3 (Catalog: 1814184, Roche Applied Science, (Indianapolis, IN), nitric acid (HNO_3 Catalog A483-212) and Nucleopore® polycarbonate membranes with a pore size of 1 μm (Catalog: 110410, Whatman, Florham Park, NJ). Proteinase K is a serine protease that cleaves peptide bonds in proteins; Liberase Blendzyme 3 contains collagenase and neutral protease to cleave both collagen and peptide bonds in proteins.

Tissue Collection

Porcine hip tissue was obtained from six regions of a single animal cadaver. Human hip capsule tissue was collected from eight patients at the time of primary total hip replacement surgery. All tissue samples were wrapped in saline-wetted gauze, transported to the laboratory in a sterile container on wet ice, flash-frozen and stored at -80°C until the time of testing. Tissue collection and storage procedures were in accordance with the IRB guidelines of each participating

institutions.

Tissue Digestion Conditions

Tissue samples were cut into 1 gram tissue pieces, which were then cut into 0.25- *x* 0.25-cm cubes and exposed for 24 hours to basic, acidic or enzymatic solutions to compare digestion efficiency. Digestion procedures were performed by a single researcher, and all efforts were made to ensure the resultant size of each tissue was consistent by using a 0.25 cm grid. The digestion agents were prepared in 10 mL aliquots of distilled water for bases and acids, and PBS pH 7.4 for enzymes. After 24 hours, each tissue digestive solution combination was diluted to a total volume of 200 mL by addition of dH_20. Dilution was necessary to avoid exposure of the polycarbonate membrane to strong alkalinity (>6M NaOH), which can compromise the structural integrity of the membrane. Nucleopore® polycarbonate membranes with a pore size of 1 μm were weighed before sample filtration. Samples were vacuum-filtered (Figure 1-1), transferred to Petri dishes and dried for 1 hour by convection heat lamps followed by 4–6 hours at ambient temperature. Membranes were reweighed and weight measurements were recorded. All samples were weighed on a calibrated scale with precision to four decimal places.

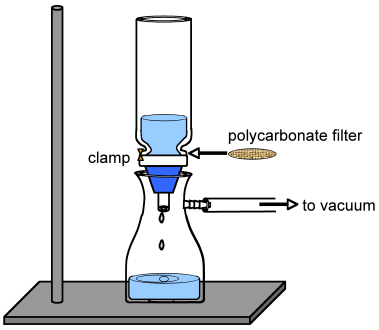

Figure 1-1. Schematic of Filtration Apparatus

Table 1-1. Summary of Tissue Digestion Approaches to Isolate Polyethylene Wear Debris

Digestion Method	Timing	Temperature	Tissue Specifics	Reference
5*M* NaOH	1-5 hours	65°C	Fresh	[37]
5*M* NaOH	1-5 hours	65°C	Fresh	[18]
5*M* NaOH	1-5 hours	65°C	Fresh	[24]
5*M* NaOH	24 hours	65°C	Stored in 10% v/v formalin	[25]
5*M* NaOH	24 hours	65°C	Stored in 10% v/v formalin	[26]
4*M* KOH	48 hours	56°C	Fresh	[39]
12*M* KOH	2-5 days	65°C	Stored in 10% v/v formalin	[27]
12*M* KOH	2-5 days	60°C	Stored in 10% v/v formalin	[28]
70% HNO_3	24 hours	25°C	Stored in 10% v/v formalin	[29]
70% HNO_3	24 hours	25°C	Freeze-dried prior to digestion	[30]
70% HNO_3	24 hours + 48 hours	25°C	Stored in 10% v/v formalin	[32]
Papain 7 mg/ml 0.05M PBS, pH 6.5, 2mM NAC, fresh papain daily	2 days	65°C	Stored in 10% v/v formalin	[33]
Papain 0.3 mg/ml 0.05M PBS, pH 6.5, 2mM NAC, fresh papain daily	3 days	65°C	Stored in 10% v/v formalin	[34]
Papain 0.3 mg/ml 0.05M PBS, pH 6.5, 2mM NAC, fresh papain daily	3 days	65°C	Stored in 10% v/v formalin	[35]
Papain 0.3 mg/ml 0.05M PBS, pH 6.5, 2mM NAC, fresh papain daily	3 days	65°C	Stored in 10% v/v formalin	[36]
Collagenase 2 mg/ml 0.1M phosphate buffer, pH 7.0	24 hours	37°C	Fresh	[37]

To compare the efficacy of basic, enzymatic, and acidic digestion methods, porcine or human hip tissues were subjected to several different agents. For basic digestion, three concentrations of NaOH and KOH were assigned to create a 2 *x* 3

array with six test conditions (Table 1-2; human, Table 1-3). Digestion using 5, 10, and 15M concentrations was tested for each basic reagent. Each test condition was repeated six times.

Table 1-2. Solutions and Concentrations Used for Digestion of Porcine Hip Tissue

Digestion Method	Concentration		
NaOH	5M	10M	15M
KOH	5M	10M	15M
Proteinase K	1 mg/mL	2 mg/mL	3 mg/mL
Liberase Blendzyme 3	0.1 mg/mL	0.2 mg/mL	0.3 mg/mL
HNO_3	–	11M	15.8M

For enzymatic digestion, Proteinase K and Liberase Blendzyme 3 were chosen for porcine tissue digestion. Three protease concentrations were assigned to a 2 *x* 3 array with six total test conditions (Table 1-2). The concentrations for Proteinase K were 1, 2, and 3 mg/mL; concentrations for Liberase Blendzyme 3 were 0.1, 0.2, and 0.3 mg/mL. Enzyme concentrations were selected based on amounts of proteinase and collagenase used in previous wear debris isolation studies [25, 26]. Each test condition was repeated six times.

For acid digestion, two concentrations of HNO_3 were used to digest tissue. The concentrations for each acid digestion were 11M (~49%) and 15.8M (concentrated, 70%) (porcine, Table 1-2; human, Table 1-3). Each test condition was repeated three times. For all treatments, 1 g of porcine or human hip tissue was digested in an oscillating water bath for 24 hours at 65°C, 37°C, or 25°C for basic, enzymatic, or acidic digestion, respectively. Chloroform/methanol extraction was

not performed prior to digestion.

Table 1-3. Solutions and Concentrations Used for Digestion of Human Hip Capsular Tissue

Digestion Method	Concentration		
NaOH	5M	10M	15M
KOH	5M	10M	15M
HNO_3	–	11M	15.8M

Tissue Digestion Efficiency Calculations

To evaluate digestion efficiency, initial and final membrane and tissue weights were measured, and the percentage of residual or undigested tissue was determined for each test condition. The differences in the final membrane weight represented the amount of residual digested tissue that did not pass through the 1 μm filter pores during vacuum-filtration.

Environmental Scanning Electron Microscopy

To check for surface modifications, GUR415 polyethylene powder and Ceridust 3715 HDPE particles were exposed to optimal digestive conditions, 5M NaOH, 5M KOH, and 15.8M HNO_3. Filtered samples were mounted on aluminum stubs with double-sided adhesive tape. Using a 208HR High Resolution Cressington Sputter Coater, filtered particulate samples were coated with Pt-Pd for 10 seconds to achieve an approximate coating thickness of 4 nm. Samples were imaged at 3500X or 5000X magnification with a beam intensity of 3 kV using an Environmental Scanning Electron Microscope at Drexel University's Centralized

Research Facility (Philips, XL-30).

Statistical Analysis

Statistical analysis was performed in JMP 7.0 (SAS, Cary, NC) using one-way ANOVA with a significance level of $p<0.05$. Figures were plotted in KaliedaGraph 3.6 (Synergy Software, Reading, PA). A post-hoc analysis was used to calculate the power associated with the observed differences between concentrations and digestive methods. The statistical power was 0.970 for the porcine tissue, 0.830 for the formalin-fixed tissue and 0.977 for the human tissue digestions, which is greater than the standard of ≥0.8 for sufficiently powered analyses.

Results

Porcine Pseudocapsular Hip Tissue Digestion Comparisons

For porcine hip tissue, results of each digestion condition are shown in Figure 1-2. The residual tissue percentages after 24 hours of digestion were statistically lowest for 5*M* NaOH, 5*M* KOH and 15*M* KOH ($p<0.05$). These treatments resulted in final tissue weights of <1% of the initial tissue weight.

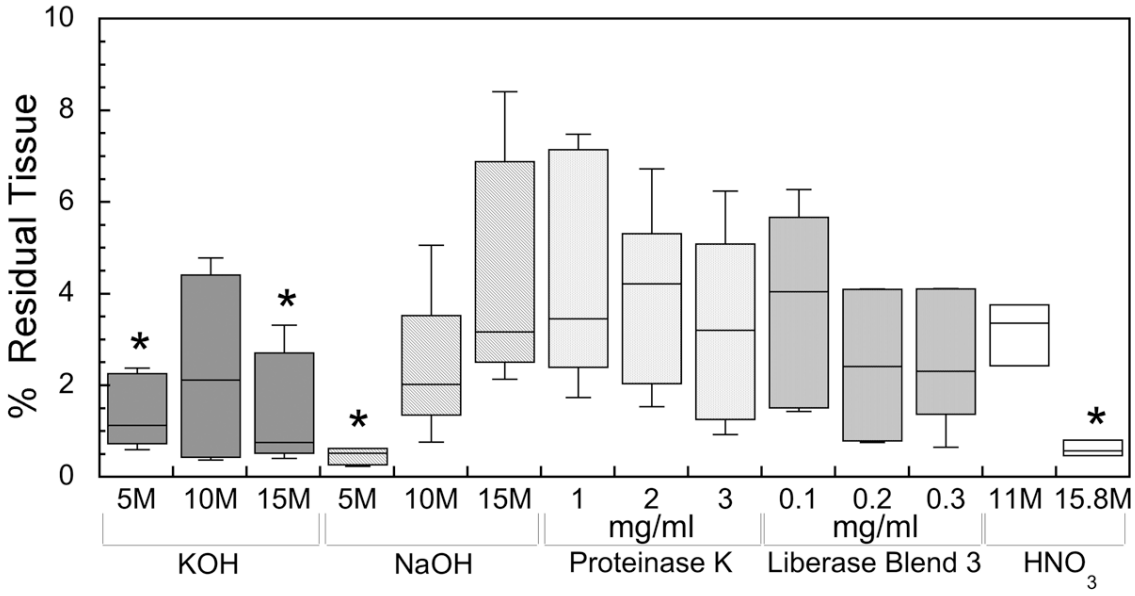

Figure 1-2. Box plot representation of percent residual tissue weight following porcine hip tissue digestion and vacuum filtration. Digestion results were statistically significant for 5*M* NaOH, 5*M* KOH, 15*M* KOH (n=6) and 15.8*M* HNO_3 (n=3) solutions, as compared to enzymatic and other solutions ($p<0.05$).

However, based on photodocumentation, only membranes from the 5*M* NaOH and 15.8*M* HNO_3 digested samples showed minimal amounts of undigested tissue material (Figure 1-3). All other samples, including the 5, 10, and 15*M* KOH treated samples, contained undigested cellular material. Polycarbonate membrane images in Figure 1-3 are representative of the amount of residual tissue debris.

Porcine tissue digested with enzymatic solutions yielded varied results after 24 hours at 37°C. Tissue samples were digested to a very limited extent by all concentrations of Proteinase K, and most of the original tissue pieces were still visible after 24 hours (Figure 1-2). Moderate improvements in digestion efficiency were observed with increased enzyme concentration (3 mg/mL), although the improvements were not statistically significant. For Liberase Blendzyme 3 improved levels of tissue digestion were observed compared to Proteinase K, but the digestion did not reach the lowest residual tissue weight of <1% (Figure 1-2). Porcine tissue digested in 15.8*M* HNO_3 resulted in very thorough digestion ($p<0.05$) (Figure 1-2). The residual tissue weight was less than 1% of the initial tissue weight, and little or no cellular material was observed on the membranes (Figure 1-3). Tissue digestion with 11*M* HNO_3 (50% v/v) was not as complete, and both residual tissue clumps and the polycarbonate membrane had a yellowed appearance.

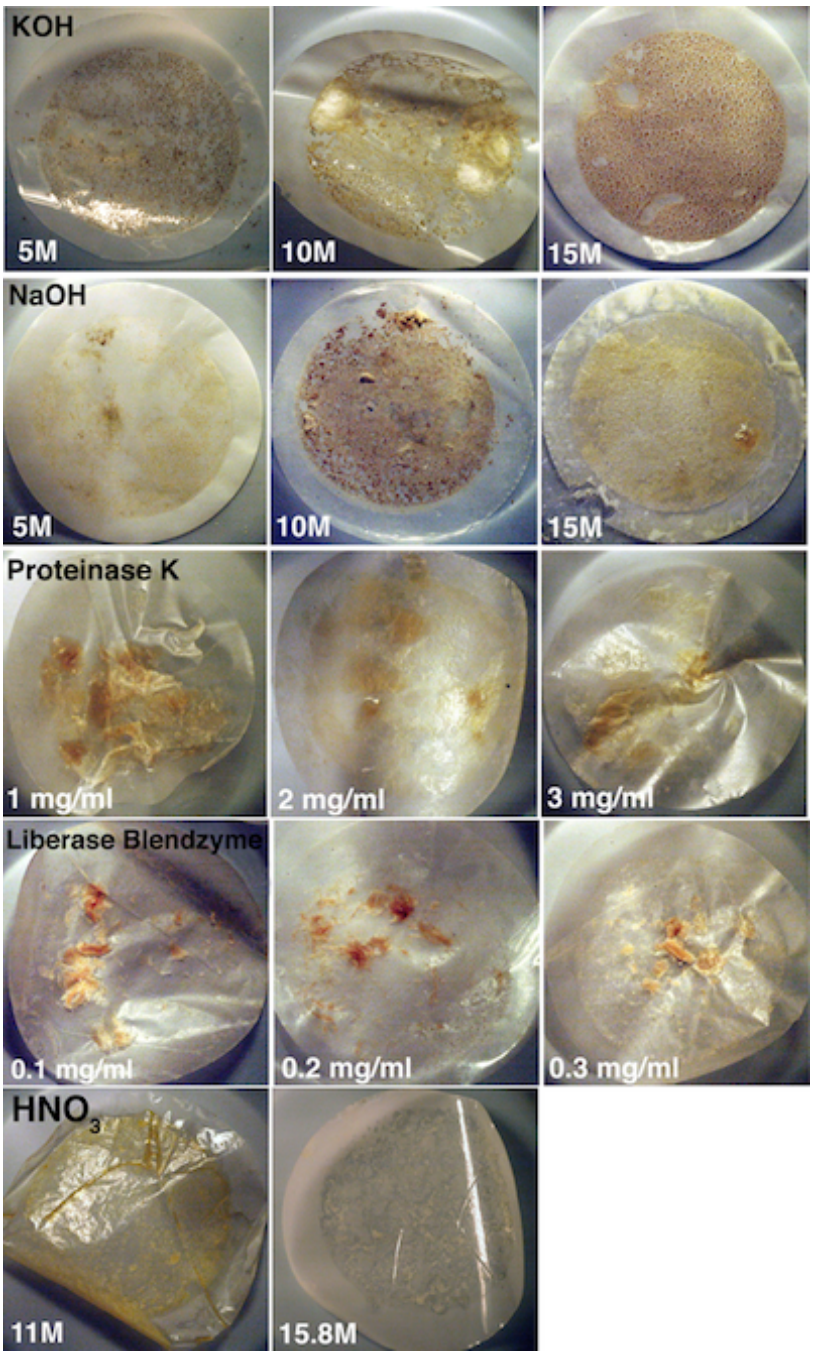

Figure 1-3. Representative images of porcine tissue digests following vacuum filtration. Qualitatively, large residual tissue debris were not observed on membranes from tissues digested in 5*M* NaOH and 15.8*M* HNO_3.

Formalin-Fixed Porcine Pseudocapsular Hip Tissue Digestion

To evaluate fixed tissue digestion, porcine tissue was placed in formalin fixative (10% (v/v) neutral buffered formalin) for 2 weeks. One gram of porcine tissue was cut into small pieces (0.25 *x* 0.25 cm) and placed into either 5*M* NaOH, 5*M* KOH, or 15.8*M* HNO_3 for 24 hours. Digested samples were filtered and the percentage of undigested tissue was calculated based on the initial and final membrane weight along with starting tissue weight. Formalin-fixed tissue samples yielded increased residual weights when digested using 5*M* NaOH or 5*M* KOH compared to non-fixed tissue ($p<0.05$)(Figure 1-4). Whereas, digestion of formalin-fixed tissues was highly efficient using HNO_3, resulting in less than 1% of the original tissue weight. This trend was similar for the results of both fixed and non-fixed tissue digestion.

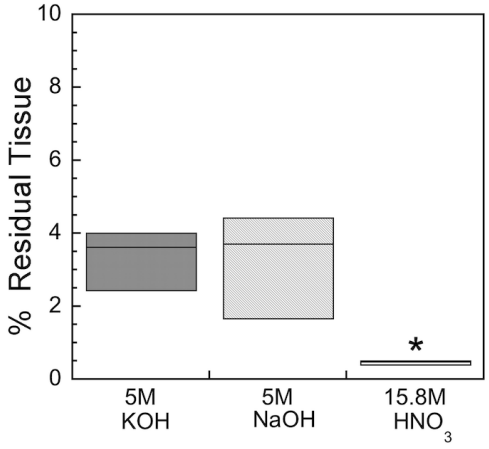

Figure 1-4. Box plot representation of percent residual tissue weight following formalin-fixed porcine hip tissue digestion and vacuum filtration. Digestion of formalin-fixed porcine tissue samples was most complete in 15.8*M* HNO_3, whereas 5*M* NaOH and 5*M* KOH had statistically higher amounts of residual tissue weight following vacuum filtration (n=3, $p<0.05$).

The overall percentage of residual tissue weight was statistically lower for HNO_3 digestion of formalin-fixed tissue as compared to basic digestion ($p<0.05$) (Figure 1-4). Representative images of formalin-fixed porcine tissue digests following vacuum filtration are shown in Figure 1-5.

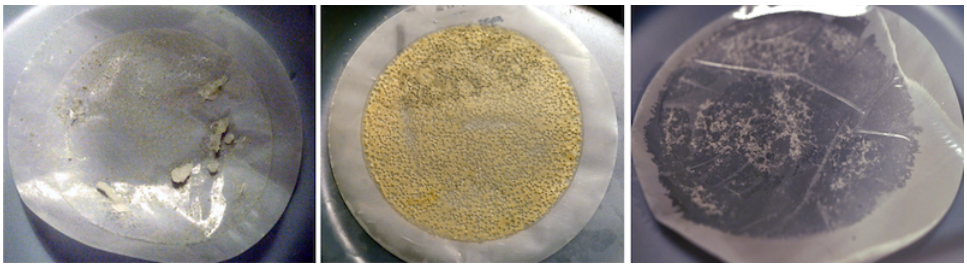

Figure 1-5. Representative images of formalin-fixed porcine tissue digests following vacuum filtration. Qualitatively, large residual tissue debris were not observed on membranes from tissues digested in 15.8*M* HNO_3.

Human Pseudocapsular Hip Tissue Digestion Comparisons

Based on the most efficient digestion of porcine tissues, human capsule tissue samples were exposed to basic and acidic digestion using conditions outlined in Table 1-3. Digestion was highly effective with 5*M* NaOH, 5*M* KOH or 15.8*M* HNO_3 when compared to other concentrations ($p<0.05$) (Figure 1-6). These treatments resulted in final tissue weights of less than 1% of the initial tissue weight. Digestion results for higher concentrations of NaOH and KOH were more variable; for NaOH, higher molar concentrations did not effectively digest human capsule tissue after 24 hours.

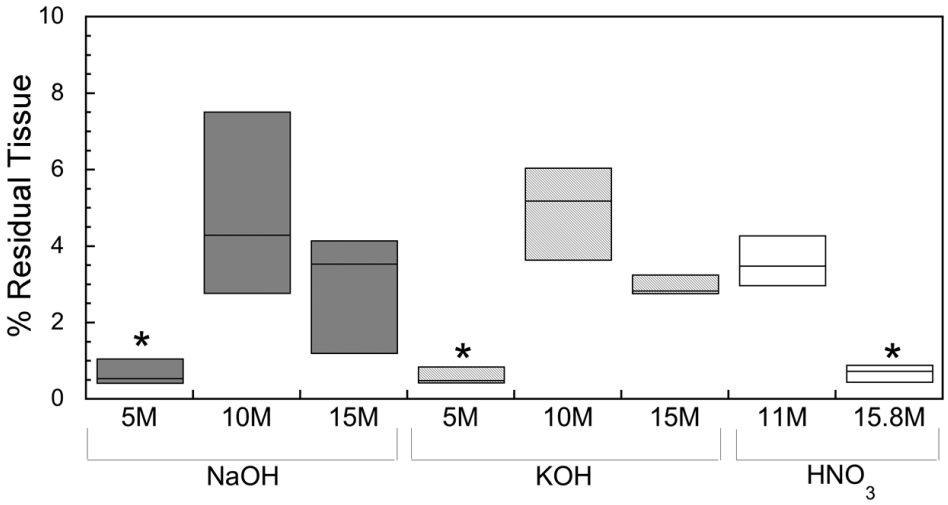

Figure 1-6. Box plot representation of percent residual tissue weight following human hip capsule tissue digestion and vacuum filtration. Digestion was most efficient for 5*M* NaOH, 5*M* KOH or 15.8*M* HNO_3 solutions, as compared to other treatments, <1% residual weight; (n=3; p<0.05)

Environmental Scanning Electron Microscopy Evaluation of Particle Surfaces

To verify that basic and acidic solutions did not alter the surface of polyethylene particles, GUR415 polyethylene powder and Ceridust 3715 particles were separately immersed in 5*M* NaOH, 5*M* KOH, or 15.8*M* HNO_3 for 24 hours. GUR 415 polyethylene powder and Ceridust 3715 particles were also immersed in distilled water for 24 hours as a comparative control. The selected GUR 415 powder is representative of resins used in conventional polyethylene implants, whereas Ceridust 3715 was selected as a representative example of commercially-available HDPE particles (5-10 μm). Recently, Ceridust particles have also been used during an *in vivo* study of osteolysis in a calvarial (mouse) animal model [40]. Reagent-exposed particles and the untreated control group were filtered onto polycarbonate membranes with a pore size of 1 μm, and dried overnight at room temperature in a Petri dish. After preparation for ESEM, the samples were imaged with a beam

intensity of 3 kV to avoid beam-induced melting of the polyethylene. The representative images presented in Figure 1-7 show that exposure of GUR415 polyethylene powder to 5*M* NaOH, 5*M* KOH, or 15.8*M* HNO_3 did not result in changes to the particle surface. Specifically, the treated particles retained the small fibril-like features that were visible on the untreated control group. Inspection of Ceridust particles from each of the reagent-exposed and control conditions revealed a similar appearance of the particle morphology (Figure 1-8). Both results verify that exposure to basic or acidic reagent solutions for a period of 24 hours does not etch or alter the polyethylene surface.

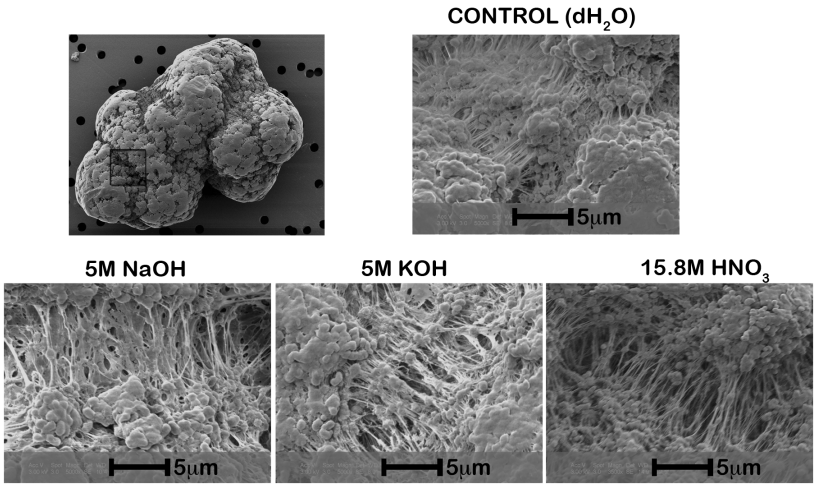

Figure 1-7. Environmental scanning electron microscopy (ESEM) of GUR415 polyethylene particles exposed to digestive solutions. A control polyethylene particle not subjected to digestion is shown at low magnification with an inset showing submicron-sized fibrillar structures. Fibrils are retained after immersion in 5*M* NaOH, 5*M* KOH, and 15.8*M* HNO_3 for 24 hours.

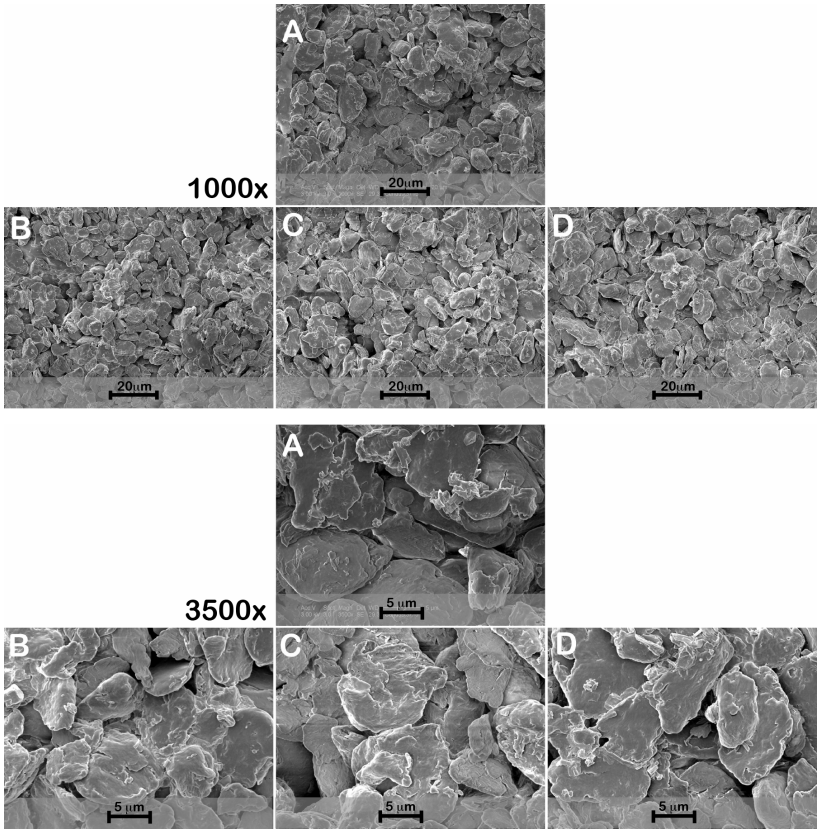

Figure 1-8. Environmental scanning electron microscopy (ESEM) of Ceridust HDPE particles exposed to digestive solutions at 1000X and 3500X. (A) Control Ceridust 3715 particles not subjected to digestion. Particles morphology is not altered following immersion in (B) 5*M* NaOH, (C) 5*M* KOH, (D) 15.8*M* HNO_3 for 24 hours.

Discussion

This study undertook a quantitative comparison of existing methods used to digest periprosthetic tissue for polyethylene wear debris analysis. First, a method for evaluating and comparing the efficiency of tissue digestion solutions by quantifying residual tissue weight was reported. Second, human tissues were most completely digested by 5*M* NaOH, 5*M* KOH or 15.8*M* HNO_3 solutions. All other concentrations of the acid and base digestive agents, as well as enzymatic solutions, contained large undigested pieces of tissue. Third, ESEM evaluation verified that GUR 415 polyethylene powder and Ceridust particles exposed to NaOH, KOH and

HNO_3 solutions do not undergo morphological changes. Finally, digestion of formalin-fixed tissue was most complete with 15.8*M* HNO_3.

The current findings suggest that, over a period of 24 hours, neither Proteinase K nor Liberase Blendzyme 3 effectively digested tissue. However successful enzymatic tissue digestion has been reported by a number of investigators (Table 1-1). Campbell et al., (1994) reported that successful digestion was achieved using bacterial collagenase over a 24 hour interval, which is the shortest enzymatic method presented in the literature [37]. In their study, successful digestion was based on a visual assessment of clumps or residual tissue in the digested solutions. Other researchers have used papain, which required the daily addition of fresh enzyme over 3 days to extract particles [33-36]. In the present study, digestion using Liberase Blendzyme 3 and Proteinase K concentrations was not extended beyond 24 hours, since the need for constant monitoring over extended periods of time as well as the high cost of materials make this approach less appealing.

Similar to other studies, lower molar solutions of NaOH or KOH were found to be effective digestive solutions. Studies by Campbell et al. showed that 5*M* NaOH effectively solubilized tissue within a 24 hour time period [18, 23, 24]. Shanbhag et al., (2000) used 4*M* KOH at 56°C for 48 hours to digest tissue [16]. Additionally, concentrated HNO_3 was an effective digestion solution, which agrees with the studies by Slouf et al., who used concentrated HNO_3 over a 48 hour time period [29, 30]. Overall, the present study shows that using 5*M* NaOH or KOH at 65°C or 15.8*M*

HNO_3 at room temperature resulted in ≥99% of tissue digestion after 24 hours.

Since many of the periprosthetic tissues are placed in formalin, this study evaluated digestion efficiency of the acid and base solutions on formalin-fixed porcine tissues. Digestion using concentrated HNO_3 was significantly more efficient than 5*M* NaOH or KOH solutions. Unlike the basic solutions, the digestive action of 15.8*M* HNO_3 did not appear to be affected by formalin fixation as compared with non-fixed tissues (Figure 1-4). Margevicius et al., (1994) and Hirakawa et al., (1996) previously used concentrated nitric acid for 48 hours to digest formalin-fixed tissue [29, 32]. The current finding that formalin-fixation decreases digestion efficiency is in agreement with methods employed by Hahn et al. (1997) and Wolfarth et al. (1997) who used 5*M* NaOH for 24 hours, and by Tipper et al. (2000) and Howling et al. (2001) who used 12*M* KOH for 2–5 days to achieve complete digestion [27, 28]. The authors do not wish to suggest formalin fixation as a general standard for collect collecting tissue retrieval, as this method of preservation can impose limits on complementary analyses of tissue samples by histological or immunohistochemical methods. However, this data suggests that thorough tissue digestion can be achieved using concentrated HNO_3 for cases where formalin fixation is the existing protocol of tissue collection.

The results of the current quantitative study highlight the variability of current tissue digestion methods. Of the fourteen conditions tested, three digestive solutions resulted in residual tissue weight less than 1% of the initial sample tissue weight: 5*M* NaOH, 5*M* KOH and 15.8*M* HNO_3. Several advantages of using HNO_3 are

that sample dilution and thus the final sample volume can be reduced because concentrated HNO_3 does not affect the polycarbonate membrane used to filter out the UHWMPE wear debris, and it does not affect the UHWMPE particle morphology. Additionally, concentrated HNO_3 has been used to isolate metal particles resulting in <1% of particle dissolution and no change in morphology after 48 hours, as previously confirmed by atomic absorption spectroscopy and ESEM, respectively [29]. In contrast, alkali solutions ranging from 2 to 12*M* have been shown to affect the size and ion composition of metal particles as early as 2 hours after exposure [41]. Based on the current evaluation of digestion efficiency, and previous wear debris analysis, concentrated HNO_3 is both effective and the least destructive digestive solution. These results provide a basic framework for expedited and efficient tissue digestion to extract polyethylene wear debris.

Acknowledgements

Special thanks to Dr. Michelle Marcolongo at Drexel University for access to her dedicated lab space during my initial experiments.

References

1. Purdue, P.E., et al., *The cellular and molecular biology of periprosthetic osteolysis.* Clin Orthop Relat Res, 2007. 454: p. 251-61.
2. Revell, P.A., *The combined role of wear particles, macrophages and lymphocytes in the loosening of total joint prostheses.* J R Soc Interface, 2008. 5(28): p. 1263-78.
3. Williams, P.A. and I.C. Clarke, *Understanding polyethylene wear mechanisms by modeling of debris size distributions.* Wear, 2009. 267(1-4): p. 646-652.
4. Agarwal, S., *Osteolysis: Science, incidence, and diagnosis.* Curr Orthop, 2004. 18(3): p. 220-231.

5. Amstutz, H.C., et al., *Mechanism and clinical significance of wear debris-induced osteolysis.* Clin Orthop Relat Res, 1992(276): p. 7-18.
6. Revell, P.A., N. al-Saffar, and A. Kobayashi, *Biological reaction to debris in relation to joint prostheses.* Proc Inst Mech Eng [H], 1997. 211(2): p. 187-97.
7. Willert, H.G., *Reactions of the articular capsule to wear products of artificial joint prostheses.* Journal of Biomedical Materials Research, 1977. 11(2): p. 157-64.
8. Greenfield, E.M., et al., *The role of osteoclast differentiation in aseptic loosening.* Journal of Orthopaedic Research, 2002. 20(1): p. 1-8.
9. Purdue, P.E., et al., *The central role of wear debris in periprosthetic osteolysis.* Hss J, 2006. 2(2): p. 102-13.
10. Sabokbar, A., O. Kudo, and N.A. Athanasou, *Two distinct cellular mechanisms of osteoclast formation and bone resorption in periprosthetic osteolysis.* Journal of Orthopaedic Research, 2003. 21(1): p. 73-80.
11. Teitelbaum, S.L., *Osteoclasts; culprits in inflammatory osteolysis.* Arthritis Research & Therapy, 2006. 8(1): p. 201.
12. Green, T.R., et al., *Effect of size and dose on bone resorption activity of macrophages by in vitro clinically relevant ultra high molecular weight polyethylene particles.* J Biomed Mater Res, 2000. 53(5): p. 490-7.
13. Green, T.R., et al., *Polyethylene particles of a 'critical size' are necessary for the induction of cytokines by macrophages in vitro.* Biomaterials, 1998. 19(24): p. 2297-302.
14. Schmalzried, T., et al., *Shapes and Dimensional Characteristics of Polyethylene Wear Particles Generated In Vivo by Total Knee Replacements Compared to Total Hip Replacements.* J Biomed Mater Res, Part B, 1997. 38: p. 203-210.
15. Kadoya, Y., et al., *Wear particulate species and bone loss in failed total joint arthroplasties.* Clin Orthop Relat Res, 1997(340): p. 118-29.
16. Shanbhag, A.S., et al., *Quantitative analysis of ultrahigh molecular weight polyethylene (UHMWPE) wear debris associated with total knee replacements.* J Biomed Mater Res, 2000. 53(1): p. 100-10.
17. Tipper, J., et al., *Isolation and characterization of UHMWPE wear particles down to ten nanometers in size from in vitro hip and knee joint simulators.* Journal of Biomedical Materials Research, 2006. 78A: p. 473-480.
18. Kobayashi, A., et al., *Number of polyethylene particles and osteolysis in total joint replacements. A quantitative study using a tissue-digestion method.* Journal of Bone & Joint Surgery - British Volume, 1997. 79(5): p. 844-8.
19. Yang, S., et al., *Diverse cellular and apoptotic responses to variant shapes of UHMWPE particles in a murine model of inflammation.* Biomaterials, 2002. 23: p. 3535-3543.
20. Ren, W., et al., *Distinct gene expression of receptor activator of nuclear factor-kappaB and rank ligand in the inflammatory response to variant morphologies of UHMWPE particles.* Biomaterials, 2003. 24(26): p. 4819-26.
21. Schmalzried, T.P. and J.J. Callaghan, *Wear in total hip and knee replacements.* J Bone Joint Surg Am, 1999. 81(1): p. 115-36.

22. Kurtz, S.M., et al., *In vivo degradation of polyethylene liners after gamma sterilization in air.* J Bone Joint Surg Am, 2005. 87(4): p. 815-23.
23. Campbell, P., et al., *Isolation of predominantly submicron-sized UHMWPE wear particles from periprosthetic tissues.* J Biomed Mater Res, 1995. 29(1): p. 127-31.
24. Mabrey, J.D., et al., *Standardized analysis of UHMWPE wear particles from failed total joint arthroplasties.* J Biomed Mater Res, 2002. 63(5): p. 475-83.
25. Hahn, D.W., D.L. Wolfarth, and N.L. Parks, *Analysis of polyethylene wear debris using micro-Raman spectroscopy: a report on the presence of beta-carotene.* J Biomed Mater Res, 1997. 35(1): p. 31-7.
26. Wolfarth, D.L., et al., *Separation and characterization of polyethylene wear debris from synovial fluid and tissue samples of revised knee replacements.* J Biomed Mater Res, 1997. 34(1): p. 57-61.
27. Tipper, J.L., et al., *Quantitative analysis of polyethylene wear debris, wear rate and head damage in retrieved Charnley hip prostheses.* J Mater Sci Mater Med, 2000. 11(2): p. 117-24.
28. Howling, G.I., et al., *Quantitative characterization of polyethylene debris isolated from periprosthetic tissue in early failure knee implants and early and late failure Charnley hip implants.* J Biomed Mater Res, 2001. 58(4): p. 415-20.
29. Margevicius, K.J., et al., *Isolation and characterization of debris in membranes around total joint prostheses.* J Bone Joint Surg Am, 1994. 76(11): p. 1664-75.
30. Slouf, M., et al., *Isolation, characterization and quantification of polyethylene wear debris from periprosthetic tissues around total joint replacements.* Wear, 2007. 262: p. 1171-1181.
31. Hallab, N.J., B.W. Cunningham, and J.J. Jacobs, *Spinal implant debris-induced osteolysis.* Spine, 2003. 28(20): p. S125-38.
32. Hirakawa, K., et al., *Characterization and comparison of wear debris from failed total hip implants of different types.* J Bone Joint Surg Am, 1996. 78(8): p. 1235-43.
33. Maloney, W.J., et al., *Isolation and characterization of wear particles generated in patients who have had failure of a hip arthroplasty without cement.* J Bone Joint Surg Am, 1995. 77(9): p. 1301-10.
34. Dean, D.D., et al., *The effect of ultra-high molecular weight polyethylene wear debris on MG63 osteosarcoma cells in vitro.* J Bone Joint Surg Am, 1999. 81(4): p. 452-61.
35. Wirth, M.A., et al., *Isolation and characterization of polyethylene wear debris associated with osteolysis following total shoulder arthroplasty.* Journal of Bone & Joint Surgery - American Volume, 1999. 81(1): p. 29-37.
36. Koseki, H., et al., *Analysis of polyethylene particles isolated from periprosthetic tissue of loosened hip arthroplasty and comparison with radiographic appearance.* J Orthop Sci, 2005. 10(3): p. 284-90.
37. Campbell, P., et al., *Tissue digestion for wear debris particle isolation.* J Biomed Mater Res, 1994. 28(4): p. 523-6.

38. *ASTM F561, 2005a, "Standard Practice for Retrieval and Analysis of Medical Devices, and Associated Tissues and Fluids," ASTM International, West Conshohocken, PA, www.astm.org.*
39. Shanbhag, A.S., et al., *Composition and morphology of wear debris in failed uncemented total hip replacement.* J Bone Joint Surg Br, 1994. 76(1): p. 60-7.
40. Illgen, R.L., 2nd, et al., *Highly crosslinked vs conventional polyethylene particles: relative in vivo inflammatory response.* Journal of Arthroplasty, 2009. 24(1): p. 117-24.
41. Catelas, I., et al., *Effects of digestion protocols on the isolation and characterization of metal-metal wear particles. II. Analysis of ion release and particle composition.* J Biomed Mater Res, 2001. 55(3): p. 330-7.

2. Time-dependent, Region-Specific and Wear Particle-Induced Changes in the Morphology of Revision Tissues from Conventional and Highly Crosslinked Polyethylene Implants[2]

Abstract

Assessment of the immune response to implant wear debris in periprosthetic tissue following total hip arthroplasty suggests that multiple factors are involved in the loss implant function. In this second chapter, ultra high molecular weight polyethylene (polyethylene) wear debris and the associated immunohistomorphologic changes in tissues were investigated from nine patients with conventional, gamma air-sterilized polyethylene (CPE) and nine highly crosslinked polyethylene (HXLPE) implant components. Paraffin embedded tissue sections were evaluated for the presence of histiocytes, giant cells, fibrocartilage/bone, and necrosis. To determine the incidence, degree and co-localization of immunohistomorphologic changes and wear, overlapping full-field tissue arrays were collected in brightfield and polarized light. The CPE cohort tissues predominantly showed histiocytes associated with significant accumulations of small wear (<2 μm), and giant cells associated with large wear (>2 μm). Frequently, focal regions of necrosis were observed in association with wear debris. For the HXLPE cohort, inflammation and associated wear debris were limited, but in

---

[2] Baxter RM, Ianuzzi A, Freeman TA, Kurtz SM, Steinbeck MJ. Distinct Immunohistomorphologic Changes in Periprosthetic Hip Tissues from Historical and Highly-crosslinked UHMWPE Implant Retrievals. J Biomed Mater Res A. 2010 Oct;95(1):68-78.

tissues from patients revised after implantation times of >2 years a response was observed; whereas significant amounts of fibrocartilage/bone were observed in patients at earlier implantation times. In both cohorts, tissue responses were more extensive in the retroacetabular or proximal femoral regions. The current findings suggest that wear debris-induced inflammation may be a major contributor to the loss of implant function for both the CPE and HXLPE cohorts, but it is not the primary cause of early implant loosening. This study highlights the importance of using a more quantitative and standardized assessment of immunohistomorphologic responses in periprosthetic tissues, and emphasizes differences in specific anatomical regions of individual patient tissues.

Introduction

Implant component wear and the associated immune reaction to ultra high molecular weight polyethylene (polyethylene) wear debris are among the most important factors in determining the longevity of a total joint replacement [1-5]. The major gross, clinical manifestation associated with polyethylene wear debris generation is osteolysis, which has been identified as a driving force in aseptic implant loosening and the need for revision surgery.

The overall immunohistomorphologic response to polyethylene wear debris is a complex process that involves multiple cell types, causes progressive local tissue damage, and increases with implantation time. Previous studies have demonstrated that accumulation of submicron and micron-sized wear debris initiates a foreign body inflammatory reaction. This reaction involves the activation of resident cells

within the tissue, such as fibroblasts and histiocytes, and the infiltration, maturation, and activation of predominantly monocytic phagocytes [1, 6]. The continuous influx of polyethylene wear particles, ingestion of the particles by phagocytosis and the resulting production of pro-inflammatory cytokines and chemokines, can ultimately cause inflammatory-mediated morphologic changes in the periprosthetic tissues. In addition, ingestion of wear debris causes cellular necrosis, a highly inflammatory form of cell death. The release of intracellular contents following cell death exacerbates and perpetuates inflammation, tissue necrosis, and osteoclast-mediated bone resorption [7]. Collectively, the immunohistopathologic changes in response to polyethylene wear debris contribute to tissue dysfunction, osteolysis, and implant component loosening.

Multiple characteristics of polyethylene wear debris, including size and number, can affect the inflammatory response in periprosthetic tissue [8-10]. Studies have shown that exposure to polyethylene wear debris within a specific size range (0.1–1 μm) results in enhanced macrophage activation *in vitro* [11-14]. In particular, submicron wear debris has been implicated as a potentially important contributor to the onset of osteolysis [9, 15, 16]. Others have shown the importance of particle number as a major contributor to the development of tissue morphological changes and osteolysis [12, 17, 18]. Evaluation of clinical data showed that patients revised for osteolysis consistently had polyethylene particle quantities in the order of 10^9 particles per gram weight of tissue [8, 17, 19]. Several *in vitro* studies have also shown a dependence of cytokine release to polyethylene

particle number [20, 21].

To date, studies performed on periprosthetic tissue, while informative, have predominantly been conducted on tissues from patients receiving gamma air-sterilized or inert-sterilized CPE components [22-30]. However, the current generation of implants is composed of HXLPE materials, and an understanding of the immunohistomorphologic response to the newer implant materials is crucial. In some circles, the prevailing scientific theory has been that the reduction in volumetric wear of HXLPE implants would contribute to the observation of fewer wear debris, resulting in fewer histiocytes and GCs *in vivo* [31-33]. Other researchers have argued, based on *in vitro* cell culture experiments, that HXLPE hip implants would produce wear debris that would provoke a stronger osteolytic response than CPE [34]. This chapter contains the first quantitative assessment of human tissues to test which theory describing the clinical performance of HXLPE is most accurate. To provide a context of differences between the inflammatory potential of wear debris from these materials, the current study compared immunohistomorphologic changes in hip tissues from patients with gamma air-sterilized CPE implants to HXLPE implant components revised for aseptic loosening. This study tested the hypothesis that distinct immunohistomorphologic responses would be observed in tissues from CPE and HXLPE components.

Methods

Tissue procurement

This multicenter study used a standardized tissue retrieval protocol allowing collection and analysis of periprosthetic hip tissues from patients undergoing revision arthroplasty. Informed consent was obtained before tissue collection, and all procedures were performed in accordance with Institutional Review Board guidelines of the participating institutes. Tissue samples were collected from 18 patients undergoing revision arthroplasty of uncemented, metal-on-polyethylene hip components. Polyethylene components were classified into two cohorts: conventional gamma air-sterilized (CPE, n=9) and gamma inert-sterilized highly crosslinked polyethylene (HXLPE, n=9). Tissues were excised from locations adjacent to the implant, which included the pseudocapsule for all 18 THR revision surgeries, as well as retroacetabular tissue (acetabular loosening) or proximal femoral tissue (femoral loosening) (Figure 2-1). Tissues were collected as part of Drexel's Implant Research Center and represent samples that would otherwise be removed and discarded during revision surgery. All four regions are not routinely collected during revision surgery, particularly in the absence of severe osteolytic lesions (which represent minimal opportunity for fibrous tissue ingrowth). Pseudocapsular tissues represent the most frequently received region, followed by retroacetabular and proximal femoral tissues, with intramedullary femoral tissues

rarely received. The clinical details for these two tissue sample collections are summarized in Table 2-1 and Table 2-2 for the CPE and HXLPE materials, respectively.

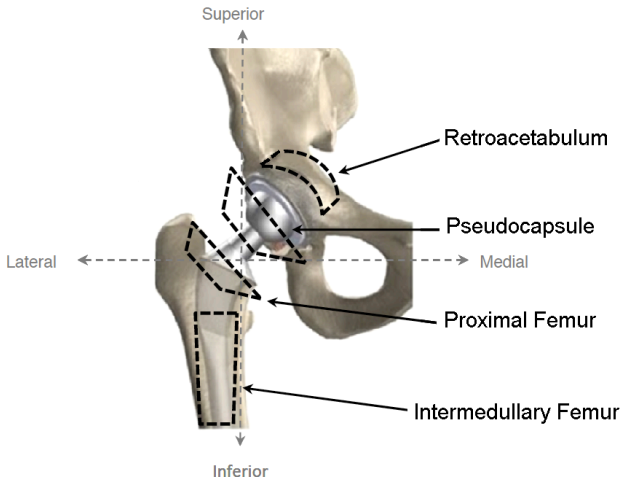

Figure 2-1. Schematic of regions for the collection of pseudocapsular and interfacial periprosthetic tissues.

Table 2-1. Clinical Information for gamma air-sterilized CPE Implant Revision Tissues

Patient #	Implantation Time (years)	Gender	Revision Reason	Implant Type
1	9.6	F	PE wear, osteolysis	Zimmer HGP II
2	11	M	Femoral loosening	Biomet Hexloc
3	12.7	F	Acetabular loosening	Biomet Hexloc
4	13.1	M	PE wear, osteolysis (femoral)	Zimmer HG II
5	13.4	F	Femoral loosening, PE wear	Biomet Hexloc
6	14.2	F	Femoral loosening	Zimmer HGP I
7	15.1	M	PE wear, osteolysis (acetabular)	Biomet Hexloc
8	15.4	M	PE wear, osteolysis (acetabular)	Zimmer HGP I
9	15.6	F	PE wear, osteolysis	Biomet Hexloc

Abbreviations: HG, Harris-Galante; HGP, Harris-Galante Porous

Table 2-2. Clinical Information for HXLPE Implant Revision Tissues

Patient #	Implantation Time (years)	Gender	Revision Reason	Implant Type

1	1.5	F	Acetabular loosening	Stryker Trident
2	1.6	M	Femoral loosening	Stryker Trident
3	1.7	F	Acetabular & Femoral loosening	Zimmer Longevity
4	2.0	M	Femoral loosening	Stryker Trident
5	2.7	F	Acetabular loosening	Stryker Trident
6	3.7	F	Femoral loosening	Stryker Omnifit
7	5.2	F	Acetabular loosening	Stryker Trident
8	5.2	F	Subluxation	Stryker Trident
9	5.9	M	Femoral loosening	Stryker Trident

Brightfield and Polarized Light Microscopy Protocols

Fixed tissues were embedded in paraffin and sections (6 μm) were mounted on Fisher Superfrost/Plus slides, dewaxed, rehydrated, and stained with hematoxylin and eosin (Fisher Scientific; 245–678) to evaluate tissue morphology. To determine co-localization of histomorphologic changes and wear debris, overlapping full-field tissue arrays were collected in brightfield and polarized light using an Olympus BX50 microscope, equipped with a stepper motor controlled stage (±2 μm positioning accuracy) and elliptically polarized light imaging system (EPLIS) filters. The EPLIS system relies on the use of a ¼-wavelength birefringent quartz retardation plate, a calibrated rotating polarizing element, and a rotating interference filter, which were adjusted to achieve maximum particle/tissue contrast and to eliminate collagen and other non-particle birefringence, allowing us to ensure that only polyethylene particles were observed. Images were captured at a magnification of 100X using a PixeLINK microscope camera both in brightfield and polarized modes. Pixel resolution was determined using a calibrated scale to be 0.5

μm/pixel (note, this is not the optical resolution). Brightfield images were scored for the presence of histiocytes, giant cells, necrosis, and fibrocartilage/bone. Histomorphologic changes were expressed as a percentage of images that contained each morphological parameter relative to the total number of images. The incidence of these morphological changes was evaluated using a set of established histologic grading criteria: 0, none; 1 rare, <10% of fields; 2 occasional, 10–30% of fields; 3 moderate, 30–50% of fields; 4 frequent, >50% of fields [23, 24]. In addition, the degree of the histiocyte and giant cell response was determined for each image using a modified semi-quantitative tissue scoring classification (Table 2-3)[30]. The corresponding polarized light images were evaluated to qualitatively determine the presence of small (<2 μm) polyethylene particles, and to quantitatively determine the number of large (≥2 μm) polyethylene particles per mm^2.

Table 2-3. Histiocyte and Giant Cell Scoring Criteria Based on a Modification of the Method by Mirra et al. (1976).

Histiocytes	
0	0 Cells
1+	1-9 Cells/low-power field (100X)
2+	10-49 Cells/low-power field (100X)
3+	≥50 Cells/low-power field (100X)
Giant Cells	
0	0 Cells
1+	1-2 Cells/low-power field (100X)
2+	3-8 Cells/low-power field (100X)
3+	≥9 Cells/low-power field (100X)

The presence of small wear debris was expressed as a percentage of images that contained particles relative to the total number of images. Images were then analyzed to determine large polyethylene particle number and tissue area using customized image threshold operations programmed in Matlab™ (Mathworks, Inc.) (Appendix I). To calculate particle number per mm^2 tissue area, we first applied a threshold to separate tissue from the white background (Figure 2-2A). Pixels associated with the tissue were replotted in a new window as a gray layer, and pixels associated with the background were replotted as a green/gold layer (Figure 2-2C). Polyethylene particles from the corresponding polarized light image (Figure 2-2B) were replotted as a white layer (Figure 2-2C). Note that for the sake of demonstration, the background was replaced with a green/gold color to distinguish it from the white mask representative of polyethylene particles. The average particle number per mm^2 was typically analyzed from 15 to 20 images per section (Table 2-4 and Table 2-6).

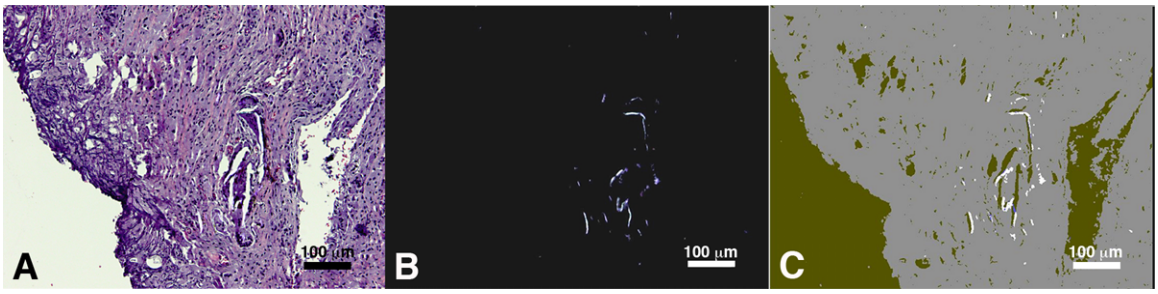

Figure 2-2. Polyethylene wear debris characterization in revised hip tissue. A: Brightfield image showing the tissue area, (B) polarized light image showing polyethylene particles, and (C) a composite of A and B generated as layers using customized threshold operations programmed in Matlab™ to determine the particle number per mm^2 area of tissue (100X).

To initially validate the elliptically polarized light imaging system (EPLIS), polyethylene particles were isolated from hip tissues, imaged using environmental scanning electron microscopy (ESEM) in variable pressure mode, and then imaged with EPLIS at 100 and 400X. Particle statistics confirmed that the same particles were observed using both methods. Measurements of particle size/area were performed for the EPLIS image by manually counting pixels, and comparing the size of the same particle in the ESEM image. For small versus large particles, the use of a single threshold value did not preferentially increase the error in determining particle size, which was steadily observed at ~3%.

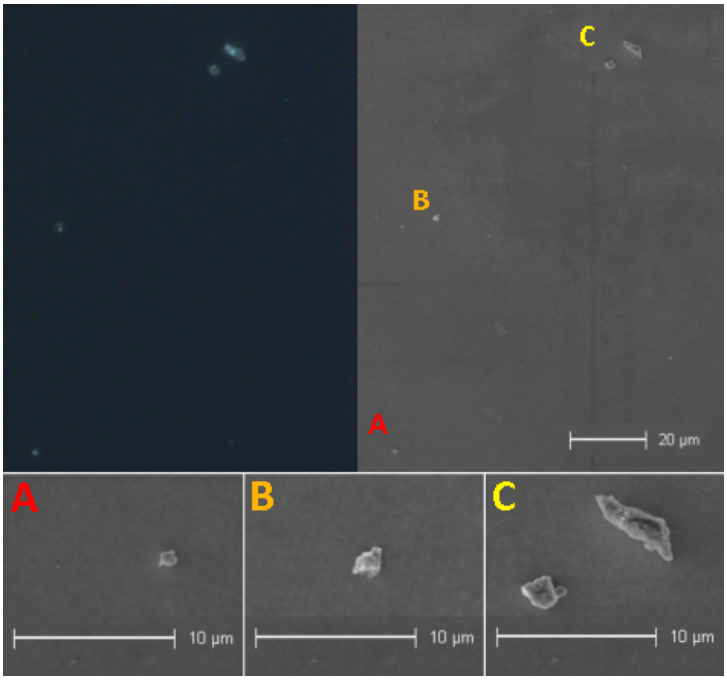

Figure 2-3. Matched polarized light microscopy and ESEM imaging of polyethylene. Magnified insets of A, B and C are shown below.

To further evaluate the accuracy of the EPLIS method, particle distributions obtained from environmental scanning electron microscopy (ESEM) and polarized light microscopy were compared. First, the tissue sections were analyzed using the EPLIS method described above. The corresponding serial sections from both patients were then digested, filtered, and analyzed using ESEM. Ten images were collected from each of three filter locations at a magnification of 2000X. The particle number and size were determined for both systems using a custom macro in NIH ImageJ (additional detailed particle analysis methods are outlined in Chapter 4). For both ESEM and EPLIS methods, the number of particles within each equivalent circle diameter (ECD) particle size range (1.0 μm increments) was determined as a percentage of the total number of particles. Equivalent circular diameter is a common representation of particle size by which the area of the particle is converted to a perfect circle. The frequency distribution of ECD particle sizes agreed within 5% of each other using a 1 μm cutoff (Figure 2-4). Upon further inspection of particles in the 0.5-1 μm range, we again observed an agreement in frequency distributions between polarized light and ESEM, which were consistently within 25% for both patient tissues. In the current chapter, particles in the smaller size range (<2 μm) were evaluated qualitatively and are defined as *small* polyethylene wear debris in the remainder of Chapter 2.

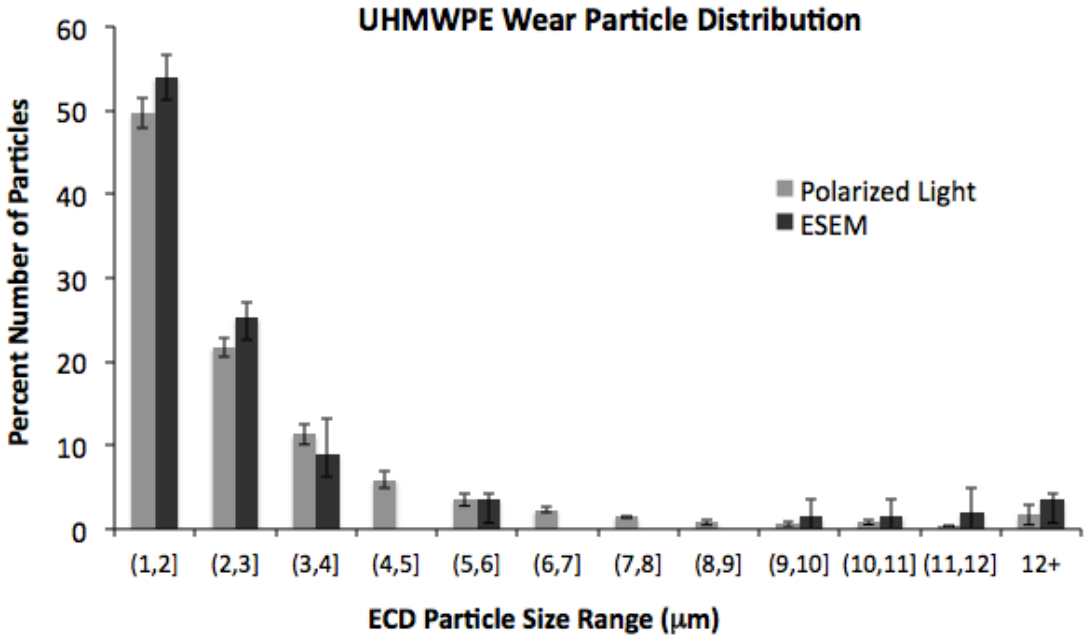

Figure 2-4. Average frequency distributions of particle size showing agreement between ESEM and polarized light methods. Comparison of distributions revealed an average difference of 2.1 ± 1.7%. Symbols showing (1,2] represent ranges of particle size, where $1 \leq x < 2$. Abbreviation: ECD, equivalent circular diameter.

Statistical analysis

To determine whether the tissue responses (represented by the presence of histiocytes, giant cells, necrosis, fibrocartilage/bone) were proportional to implant-related variables (small polyethylene wear particles, large polyethylene wear particle number, revision reason, implantation time), statistics were performed using JMP 6.0 (SAS Institute Inc., Cary, NC). Data were collected from each of 226 images in the CPE cohort, and 192 images in the HXLPE cohort. Statistically significant correlates were evaluated using ordinal logistic regression or nominal logistic regression. Separate analyses were conducted for comparison of necrosis and fibrocartilage/bone, and for differences across implant cohort using Fisher's

Exact Test. Two-factor analysis of variance (ANOVA) was conducted to evaluate whether small or large (≥2 μm) polyethylene wear debris were significantly correlated with polyethylene liner type (CPE versus HXLPE) or tissue region (capsular versus noncapsular tissue). There were nine patients in each cohort and gender was equally represented.

Results

Histomorphologic Changes and Polyethylene Wear Debris in Tissues from Conventional Polyethylene Implant Components

The present study was conducted to compare the immunohistology of periprosthetic tissues from patients with conventional (CPE) or highly crosslinked polyethylene (HXLPE) implant components, and to correlate these changes with wear debris, implantation time, and reason for revision. For the CPE component revisions, the average implantation time was 13.3 years (range 9.6–15.6 years). Pseudocapsular tissue was available for all nine patients and proximal femoral tissues and/or retroacetabular tissue was collected from patients revised for component loosening, femoral (n=3), acetabular (n=2) or both loosened components (n=1). The other reason for revision in this cohort was wear debris and associated osteolysis (n=2).

In evaluating the pseudocapsular tissue response to CPE wear debris, histiocytes with intracellular small polyethylene wear debris were observed in four of the nine patient tissues (Figure 2-5A–D) (Table 2-4). Individual data for all three scores (1+, 2+ or 3+) can be viewed within Appendix III (Note: *for the purpose of*

Table 2-4*, the summed % that encompasses the majority of tissue responses is shown for both histiocytes and GCs).* The remaining five pseudocapsular tissues were completely devoid of wear debris and histiocytes. When histiocytes were present, there were correlations with increasing implantation time (ordinal logistic regression, $p=0.0036$), small polyethylene wear debris (ordinal logistic regression, $p<0.0001$), and large polyethylene particle number (ordinal logistic regression, $p=0.0346$). Of the four patient tissues with histiocytes, two had the maximum score of 3+ (>50 cells/field) in >50% of the tissue section images. The other two had a score of 2+ (10–49 cells/field) in at least 40% of the fields. With the exception of patient 4, histiocytes were always observed when small wear debris was present. However, some small wear debris was found in the pseudocapsular tissue from patient 4 (<25% of the fields); no large wear was observed, but 100% of the pseudocapsular fields showed histiocytic necrosis. Regions of focal necrosis were also observed in five other pseudocapsular tissues (Table 2-4). These regions showed correlations with the presence of small wear debris (nominal logistic regression, $p<0.0001$).

Table 2-4. Pseudocapsular Scoring for CPE Implant Revision Tissues

Patient #	Histiocyte (%)* 2+ and 3+	Small Polyethylene Wear (%)	Necrosis (%)	Giant Cell (%)* 1+, 2+, 3+	Large (≥2 μm) Polyethylene Particle Number/mm^2	Fibrocartilage /Bone (%)
1 (C)	70	60	50	0	14.5±5.0	0
2 (C)	0	0	0	0	0.1±0.1	0
3 (C)	53	80	60	20	12.4±3.4	0
4 (C)	0	22	100	0	1.3±0.4	0
5 (C)	0	0	0	0	0.1±0.1	0
6 (C)	40	65	90	0	3.2±0.4	0
7 (C)	0	0	0	0	0	0
8 (C)	0	0	7	0	1.2±0.2	0
9 (C)	100	100	21	58	19.2±3.2	0

Abbreviations: C, pseudocapsule. *Summed responses for the indicated inflammation ranges

Table 2-5. Noncapsular Scoring for CPE Implant Revision Tissues

Patient #	Histiocyte (%) 2+ and 3+	Small Polyethylene Wear (%)	Necrosis (%)	Giant Cell (%) 1+, 2+, 3+	Large (≥2m) Polyethylene Particle Number/mm^2	Fibrocartilage /Bone (%)
2 (PF)	100	100	27	55	67.1±14.2	0
3 (RA)	100	100	30	14	181.8±31.4	86
4 (PF)	100	92	8	42	6.9±2.0	0
6 (PF)	7	93	0	0	3.0±0.6	0
8 (PF)	84	100	32	5	37.2±6.5	0
8 (RA)	100	100	7	53	82.8±7.3	7

Abbreviations: PF, proximal femur; RA, retroacetabulum. * Summed responses for the indicated inflammation ranges

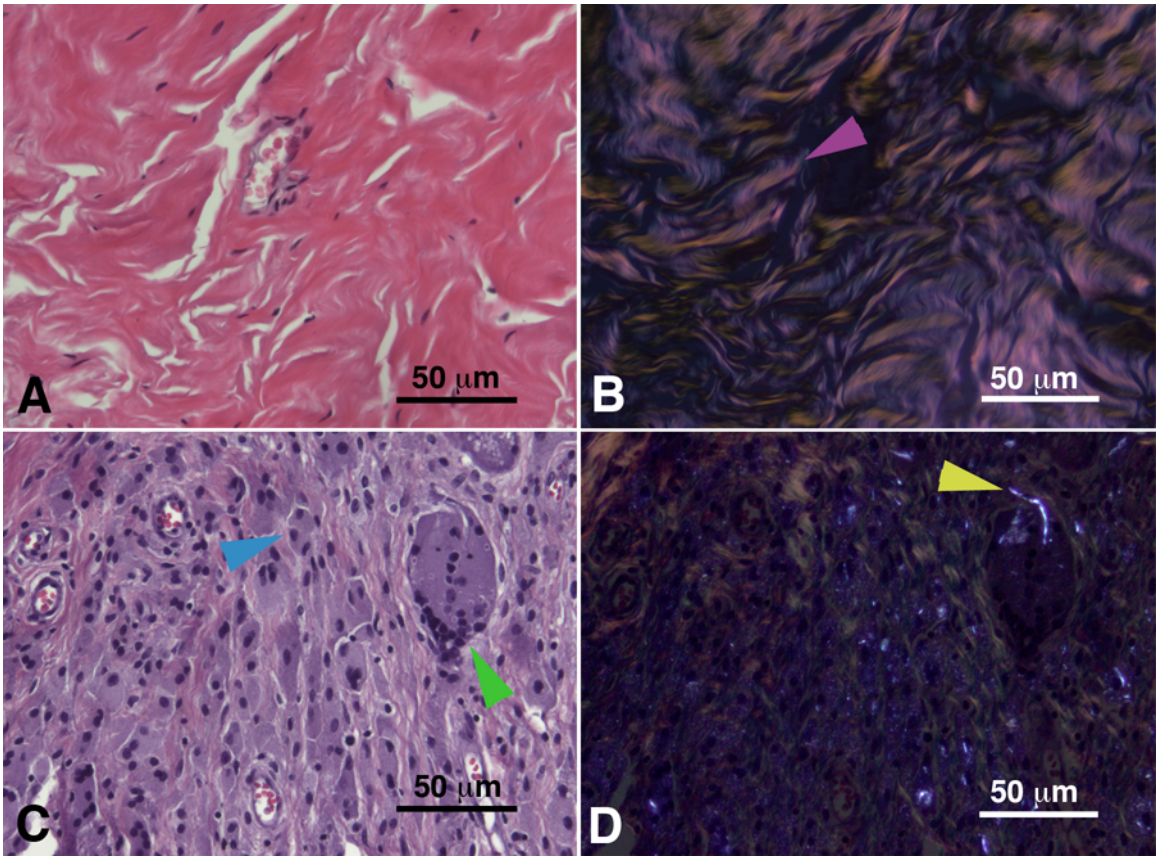

Figure 2-5. Representative images of H&E-stained pseudocapsule tissues from revised CPE liners. (A) Normal morphology observed in 5/9 pseudocapsular tissues, and (B) the corresponding polarized light image showing multidirectional collagen fibers (pink arrow) C: Histiocytes (blue arrow) observed in 4/9 pseudocapsular tissues, and giant cells (green arrow) observed in 2 of those 4 tissues, and (D) the corresponding polarized light image showing large (yellow arrow) and small polyethylene debris associated with giant cells and histiocytes, respectively (200X).

A less frequent finding in the CPE cohort pseudocapsular tissues was the presence of giant cells (GCs), which were observed in only two of the nine tissues (Figure 2-5A–D) (Table 2-4). When GCs were present, there was a significant correlation with large polyethylene particle number (ordinal logistic regression, p=0.0004). In addition, the two patient tissues with GCs had the maximum histiocyte score.

For the RA and PF tissues, histiocytes were observed in all six tissues and 67% had a score of 3+ in >50% of the tissue section images (Figure 2-6A). Five of the six noncapsular tissues showed the concomitant presence of GCs and necrosis (Figure 2-6A). Similar to the pseudocapsular tissue, histiocytes, GCs, and necrosis were observed in the presence of small and large polyethylene wear debris (Figure 2-6B). However, the number of histiocytes (ordinal logistic regression, $p<0.0001$), the GCs (ordinal logistic regression, $p<0.0001$), and the amount of wear debris (ANOVA, $p<0.001$) was higher than in the pseudocapsule. Whereas, the number of fields with necrosis was significantly lower than in the pseudocapsular tissue (Fisher's exact test, $p=0.0296$). A patient-specific response was observed for patient 6, in which the number of histiocytes in the pseudocapsule tissue was lower than other patient tissues with similar incidence of small wear. This phenomenon was more pronounced in the noncapsular tissue from the same patient. Fibrocartilage/bone was observed in two of the noncapsular tissues, but was not associated with the amount of wear debris, revision reason, or length of implantation time.

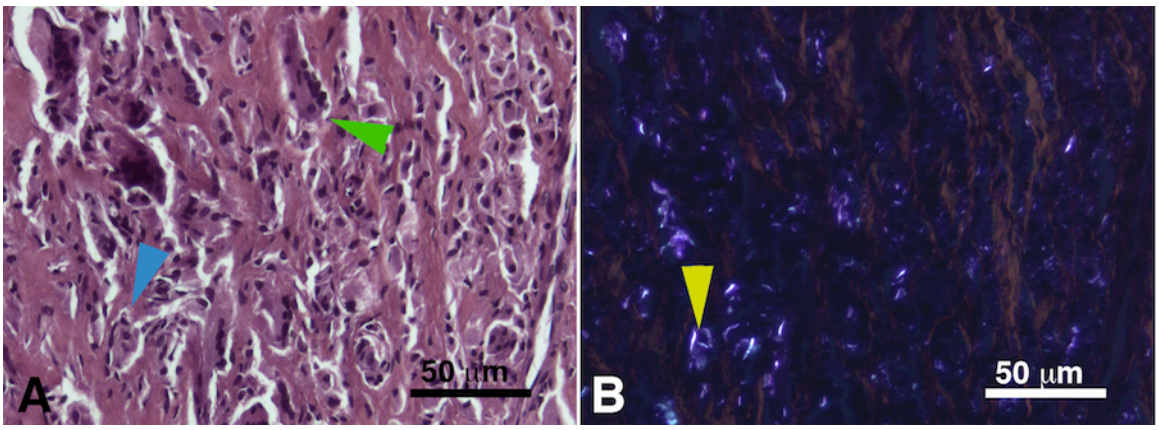

Figure 2-6. Representative images of H&E-stained proximal femoral tissues from revised CPE liners. (A) Histiocytes (blue arrow) observed in 6/6 noncapsular tissues and giant cells (green arrow) observed in 5/6 tissues; (B) the corresponding polarized light image showing polyethylene wear debris (yellow arrow) (200X).

Histomorphologic Changes and Polyethylene Wear Debris in Tissues from Highly Crosslinked Polyethylene Implant Components

For the HXLPE component revisions, the average implantation time was 3.3 years (range 1.5–5.9 years). Pseudocapsular tissue was available for all nine patients and proximal femoral tissues and/or retroacetabular tissue were collected from patients revised for component loosening, femoral (n=4), acetabular (n=3), or both loosened components (n=1). The other reason for revision in this cohort was subluxation after 5.21 years post-implantation. In evaluating the pseudocapsular response, seven of nine patient tissues were completely devoid of histiocytes and detectable small polyethylene wear debris (Table 2-6, Figure 2-7A). Of the two patient tissues with histiocytes, small polyethylene wear debris was also present. Only tissue from patient 7 contained tissue fields with a histiocyte score of 2+ (10–49 cells/field), which was observed in 33% of the tissue section images. Pseudocapsular tissue from patient 3 had a score of 1+ (<10 cells/field) in 17% of the fields. Similar to the limited presence of histiocytes, neither giant cells (GCs) nor

significant amounts of large polyethylene wear debris were observed in the pseudocapsular tissues (Table 2-6).

Table 2-6. Tissue Scoring for HXLPE Implant Revision Tissues

Patient #	Histiocyte (%)* 2+ and 3+	Small Polyethylene Wear (%)	Necrosis (%)	Giant Cell (%)* 1+, 2+, 3+	Large (≥2 μm) Polyethylene Particle Number/mm^2	Fibrocartilage /Bone (%)
1 (C)	0	0	8	0	0.7 ± 0.2	60
2 (C)	0	0	0	0	0.7 ± 0.3	0
3 (C)	0	25	0	0	2.9 ± 0.7	0
4 (C)	0	0	0	0	0.3 ± 0.1	0
5 (C)	0	0	67	0	0.0	67
6 (C)	0	0	0	0	0.1 ± 0.1	0
7 (C)	33	44	56	0	2.5 ± 0.4	22
8 (C)	0	0	0	0	0.3 ± 0.1	0
9 (C)	0	0	0	0	0.8 ± 0.22	0

Abbreviations: C, pseudocapsule. * Summed responses for the indicated inflammation ranges

Table 2-7. Tissue Scoring for HXLPE Implant Revision Tissues

Patient #	Histiocyte (%)* 2+ and 3+	Small Polyethylene Wear (%)	Necrosis (%)	Giant Cell (%)* 1+, 2+, 3+	Large (≥2 μm) Polyethylene Particle Number/mm^2	Fibrocartilage /Bone (%)
2 (PF)	20	10	10	0	0.8 ± 0.3	60
4 (PF)	0	33	33	0	0.4 ± 0.2	6
6 (PF)	5	15	5	0	1.9 ±0.4	15
7 (RA)	28	50	6	6	2.9 ± 0.4	6

Abbreviations: PF, proximal femur; RA, retroacetabulum. * Summed responses for the indicated inflammation ranges

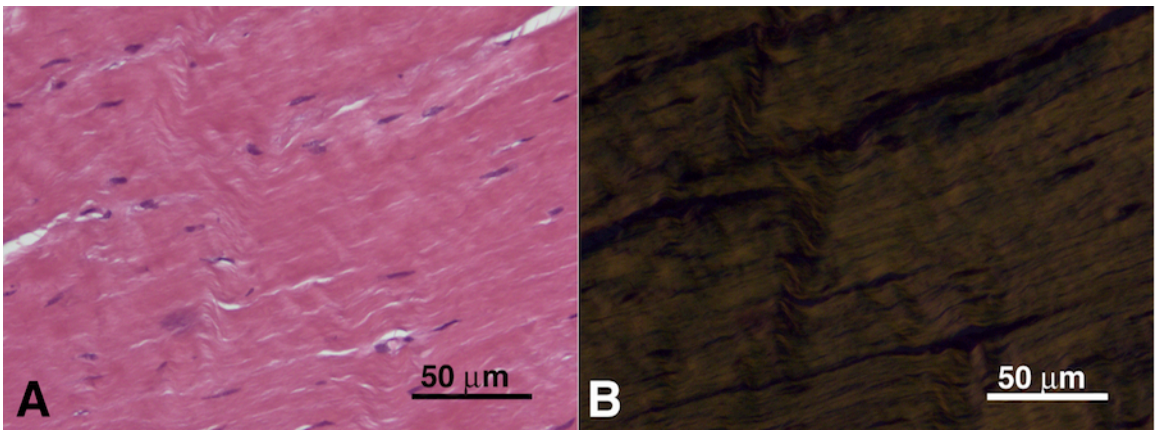

Figure 2-7. Representative images of H&E-stained pseudocapsule tissues from revised HXLPE liners. (A) Normal immunohistomorphology observed in 7/9 pseudocapsular tissues; (B) the corresponding polarized light image showing no visible polyethylene wear debris in a region of organized collagen fibers (200X).

Necrosis and regions of fibrocartilage/bone were detected in three of the pseudocapsular tissues (Table 2-6). For patient 7, the combined presence of necrosis and small wear debris was observed; however, this was not a consistent finding for the other two patients. Regions of fibrocartilage/bone were detected in the same three pseudocapsule tissues (Table 2-6). When fibrocartilage/bone was present, there was a correlation with implantation time, so that patients with shorter implantation times had a higher probability of having fibrocartilage (nominal logistic regression, $p<0.02$).

For the RA and PF tissues, histiocytes were observed in three of four patient tissues. Of the three patient tissues with histiocytes, only the RA tissue from patient 7 was given a score of 3+, which was observed in 17% of the tissue section images. In these three noncapsular tissues, a histiocyte score of 2+ was observed in >20% of the fields, and two of these three patients were revised after implantation times of >2 years. In all noncapsular tissues, histiocytes and small wear debris were

observed, except for tissue from patient 4, which contained small wear debris but no histiocytes. In contrast to histiocytes, GCs were only observed in the RA tissue from patient 7, which contained one of the higher percentages of large polyethylene wear debris. Necrosis was observed in all four of the noncapsular tissues in association with small polyethylene wear debris, but unlike the pseudocapsular tissue, the association was not significant. Fibrocartilage/bone was also observed in all of the noncapsular tissues; a higher incidence was consistently observed at earlier implantation times (nominal logistic regression, $p<0.0001$) (Figure 2-8A).

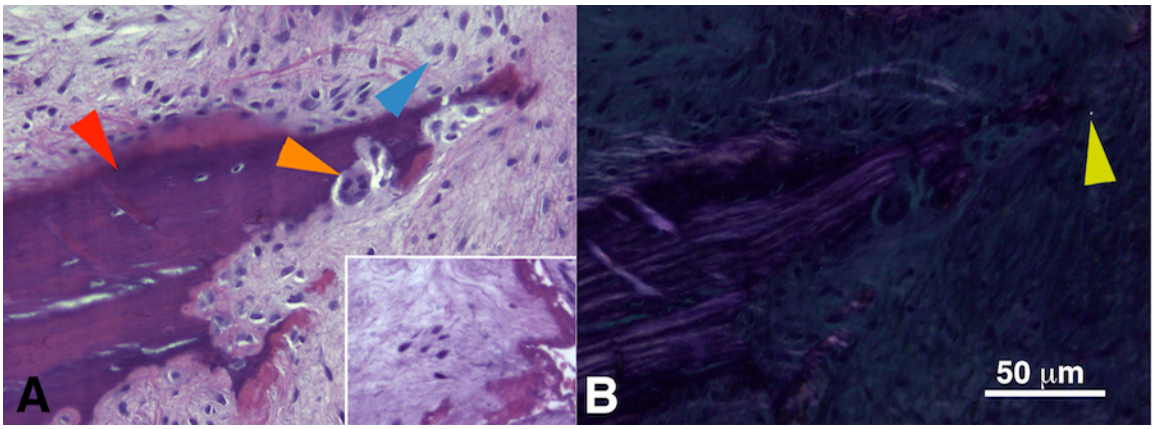

Figure 2-8. Representative image of fibrocartilage/bone in RA tissues from the HXLPE implant cohort. (A) A segment of bone (red arrow) with outer regions of fibrocartilage embedded within loose connective tissue. Visible within the tissue is an osteoclast (orange arrow) in a resorption lacuna, and necrosis (inset) associated with histiocytes. Histiocytes (blue arrow) are visible near the top edge of the bone; (B) the corresponding polarized light image showing a small polyethylene particle (yellow arrow) (200X).

Histomorphologic Changes and Polyethylene Wear Debris in Tissues from Revised Conventional and Highly Crosslinked Polyethylene Implant Components

In comparing the responses of the pseudocapsular and noncapsular tissues from the CPE cohort, there was an increased presence of histiocytes (ordinal logistic regression, $p<0.0001$), GCs (ordinal logistic regression, $p<0.0001$), and polyethylene wear particle number (ANOVA, $p<0.001$) in the noncapsular tissues, whereas

necrosis was observed more frequently in the pseudocapsule (Fisher's exact test, $p<0.0296$). The incidence and average percentage of pseudocapsular and noncapsular tissue responses are summarized for both cohorts in Table 2-8.

Table 2-8. Summary of Pseudocapsular and Noncapsular Tissue Responses for CPE and HXLPE Implant Cohorts

	Historical Polyethylene		HXLPE	
	n/N	Average (min-max)	n/N	Average (min-max)
Pseudocapsular tissue				
Histiocytes	4/9	32% (0-100)	2/9	8% (0-55)
Giant cells	2/9	8% (0-58)	0/9	0%
Necrosis	6/9	33% (0-100)	3/9	15% (0-67)
Fibrocartilage	0/9	0%	3/9	17% (0-67)
Small (<2μm) polyethylene	5/9	33% (0-100)	2/9	8% (0-44)
Large (≥2 μm) polyethylene	8/9	6/mm² (0-19)	8/9	1/mm² (0-3)
Noncapsular Tissue				
Histiocytes	6/6	77% (6-100)	3/4	33% (0-56)
Giant cells	5/6	25% (0-55)	1/4	1.5% (0-6)
Necrosis	5/6	16% (0-32)	4/4	14% (5-33)
Fibrocartilage	2/6	14% (0-86)	2/4	22% (6-60)
Small (<2μm) polyethylene	6/6	84% (6-100)	3/4	27% (10-50)
Large (≥2 μm) polyethylene	6/6	55/mm² (3-182)	4/4	1.5/mm² (0.4-2.9)

Presented is the average percentage of fields (minimum and maximum) containing histiocytes, GCs, necrosis, fibrocartilage, and small polyethylene wear for pseudocapsular and non-capsular regions. Large polyethylene wear is presented as the average particle number/mm². n, the incidence; N, total number of tissues.

In comparing the responses of pseudocapsular and non-capsular, periprosthetic tissues from the HXLPE cohort, one dominant histomorphologic change in non-capsular tissues was the presence of necrosis associated with small wear. The second frequently observed change was the presence of fibrocartilage/bone, which showed a correlation with decreasing implantation time

(nominal logistic regression, $p<0.0001$). In general, the Immunohistomorphologic responses of pseudocapsular and non-capsular tissues (for either the ≤ or > 2-year implants) were not distinctly different (Table 2-6). The exception was an increased presence of histiocytes in the non-capsular regions (ordinal logistic regression, $p=0.0002$), which were predominantly from patients with implantation times of >2 years. The incidence and average percentage of pseudocapsular and non-capsular tissue responses are summarized for both cohorts in Table 2-8. Overall, in comparing the responses of the CPE and HXLPE cohorts, the quantity of polyethylene wear debris (ANOVA, $p<0.001$), and subsequently, the presence of histiocytes (ordinal logistic regression, $p<0.0001$), GCs (ordinal logistic regression, $p<0.0001$), and necrosis (Fisher's exact test, $p<0.001$) were significantly lower in the HXLPE cohort.

Discussion

The current study presents the wear particle characteristics and histomorphology of revision tissues for a cohort of patients that received highly crosslinked UHMWPE (HXLPE) implant components. Tissues from this cohort showed a significant reduction in polyethylene wear debris, histiocytes, and necrosis as compared with a conventional (CPE) implant cohort, and the presence of GCs was only observed in one patient tissue. However, the presence of small wear and a histiocytic response was evident, and this correlated with increasing times of implantation. For those patients revised at time points ≤2 years, there was an increased incidence of focal fibrocartilage/bone, suggesting that implant fixation

was incomplete, and the contribution of wear debris was secondary. A detailed comparison of wear debris and tissue responses to a cohort implanted with conventional polyethylene components revealed extensive tissue histiocytosis and GC formation associated with the presence of small and large polyethylene wear debris, respectively, all of which were predominantly observed in retroacetabular and proximal femoral tissues.

The current chapter contained the following limitations: (i) There is a difference between the two patient cohort implantation times. The average implantation time was 13.3 years (range, 9.6–15.6) for the conventional cohort and 3.3 years (range, 1.5–5.9) for the HXLPE cohort. However, for the current cohorts, the observed tissue morphology and wear debris are representative of the end-stage reason for revision for each cohort. In one of the few early cadaveric studies evaluating tissue responses for uncemented conventional polyethylene (six patients), extensive polymeric wear, and associated histiocytosis were observed after an average of only 4.8 years [35]. Thus, the current findings for the HXLPE cohort also imply a lesser role of polyethylene wear debris than has previously been shown for CPE bearing couples at similar time points. (ii) Compared to particles isolated from periprosthetic tissues, the *in situ* observation of polyethylene wear debris using polarized light is limited by the lower resolution of the system. The birefringent characteristic of wear debris may be obscured by dense tissue morphology or, separately, by the hematoxylin and eosin stains used to identify morphological features of the tissue. However, based on the validation shown

earlier in the current chapter, the application of a 2 μm cutoff represents a cautious estimate of the lower limit for quantification. (iii) A pre-programmed focus routine was used to enable rapid, high-throughput imaging of tissue sections in both brightfield and polarized light. This focus routine performed an optimization of the visible edges in each image and was limited by the sensitivity of the minimum motor increment controlling the z-axis of the stage. Nevertheless, the optimized focus determined by the program consistently represented an improvement over user-defined focal planes. Because submicron particles are an important part of the assessment of wear products from artificial joints, their characteristics are further explored in Chapter 5.

Findings for the CPE cohort are, for the most part, in agreement with those reported by others [23-25, 30]. However, the current characterization of tissue histomorphology from loosened hip prostheses is unique in that it included a combined description of the incidence [23, 24] and degree [25, 30] to which the morphological changes and polyethylene wear debris were observed. In addition, by analyzing full-field tissue sections, the distinct regional variations of morphological changes and polyethylene wear debris in each tissue section could be determined. This study highlights the importance of evaluating tissues from multiple regions and emphasizes the need to quantify tissue responses in a more comprehensive manner to ascertain the predominant histomorphologic changes in localized areas, anatomical regions, and individual patient tissues.

In agreement with Ito et al., (2004), heterogeneity was observed in the

distribution of histiocytes, GCs, and wear debris within individual tissue sections [24]. In addition to heterogeneity, the current study separately evaluated the presence of both small and large wear debris, which were associated with histiocytes and GCs, respectively. In contrasting regional differences, these current observations also agree with those of Ito et al., (2004) that the number of histiocytes and GCs and the presence of wear debris were predominantly observed in non-capsular tissues from the proximal femur and behind the acetabulum. In a separate study of proximo-femoral tissues from uncemented hip prostheses, Kim et al. (1994) reported the presence of histiocytes with a score of 2+ or 3+ in 80% of tissues, and GCs in 40% of tissues using a modified Mirra tissue classification, and polyethylene wear debris [30]. Similarly, in the current study, images with 2+ or 3+ histiocyte scores were observed as a dominant feature in 83% of PF tissues. However, a similar increase was not observed in the number of GCs or the amount of wear debris, which may reflect the difference in scoring all fields versus the average of only five fields in their study.

The finding that small, rather than large polyethylene wear debris was localized to RA and PF tissues is consistent with the current understanding of particle migration [36-39]. Large particles are trapped in dense, collagen-rich joint connective tissue, whereas smaller particles are able to move more freely and migrate both locally and to more remote sites along the implant interface, as well as other organs. Multiple studies have demonstrated the migration of polyethylene wear debris to the lymph nodes, spleen, and liver [36, 37]. However, particle

migration and the implications of long-term systemic exposure, are generally poorly exposure, are generally poorly understood aspects of joint arthroplasty. If the ability to migrate through tissue is size dependent, then it could be speculated that the submicron-sized wear debris species from HXLPE components have a greater potential for diffusion, and a reduced likelihood of initiating a periprosthetic tissue reaction.

Early revisions within 2 years of implantation represent a potentially distinct patient subgroup for the HXLPE cohort. Specifically, a histiocytic response to wear debris was only observed in patients 6 and 7 from the HXLPE cohort, which were revised after an implantation time of >2 years. This increase was predominantly observed in the non-capsular tissues obtained from regions adjacent to loosened implant components. These results are in agreement with Knahr et al., (2007), who reported the presence of histiocytes, GCs, and a few submicron wear particles in pseudocapsular tissues from two patients with HXLPE implants revised after 4 and 5 years [33]. Thus, similar to the previous findings for the CPE implants, wear debris and inflammation are evident after implantation times longer than 2 years.

Recent clinical studies have reported that the majority of bedding-in and creep of HXLPE components occurs during the first 2 years after implantation, and relatively low-wear rates are observed at a 5-year follow-up [31, 40]. However, as shown by several studies *in vitro*, the lower wear rates may be associated with the generation of smaller particles, which are thought to be more biologically active [11, 41, 42]. The biological activity is a measure of cytokine release after ingestion of the

small wear debris particles by macrophages, but these smaller cells may not be readily observed in tissues due to the decreased histiocyte swelling/hypertrophy after ingestion of nanometer-sized particles. The current findings agree, in that histiocytes and small polyethylene particles were observed in tissues from the HXLPE patient cohort, and that GCs and large wear debris were less frequently observed in these tissue samples. Given the reduced amount of wear debris and inflammation in the HXLPE cohort tissues, particularly those revised at ≤2 years, revision surgery for component loosening may be more dependent on mechanical factors. Previous studies have shown that instead of bone formation or osseo-integration, a fibrous membrane can form at the implant-bone interface [43]. This membrane is characteristically thin or absent in well-fixed implants, whereas loose components generate thickened, dense membranes that contain fibrocartilage. The presence of fibrocartilage and lack of detectable wear debris in the HXLPE cohort revised after implantation times of ≤2 years is suggestive of decreased implant fixation, representing the possible contribution of micro-motion as a contributor to component loosening and/or fibrocartilage formation. Although patient 5 was revised at 2.7 years, which is outside of the 2 year cutoff, the tissue response was primarily fibrocartilage, which is consistent with loosening as a result of poor implant fixation. However, for patients revised after implantation times of >2 years, the presence of detectable wear debris and undetected nanometer-sized polyethylene wear may collectively contribute to the tissue response and implant loosening. Most previous studies have been performed during a discipline-wide focus of factors contributing to osteolysis, but do not provide a sufficient context of

differences between the osteolytic potential of wear debris from new and existing polyethylene bearing surface materials. The current observations suggest that size and number of wear debris particles generated from CPE and HXLPE implants contribute to a distinct immunohistomorphologic response that results in the loss of implant function, and that the primary cause of early implant loosening is not due to wear-debris induced inflammation. These observations underscore the need to evaluate pseudocapsular and non-capsular tissues to characterize wear debris and immunohistomorphologic responses that may contribute to implant loosening. The following chapter expands on the initial assessment of tissue responses, and investigates the role of innate and adaptive immune cells for these same polyethylene cohorts.

Acknowledgements

Special thanks to Dr. Todd Doehring for many hours of training and subsequent access to his dedicated microscopy suite at Drexel University, which contributed to the quality of the work performed in the current chapter. In addition, thanks to Dr. Dawn Elliot and David Beason from the McKay Orthopedic Laboratory at the University of Pennsylvania for the access to their polarized light microscopy facility. Thanks to Allison Morris for her contribution to the statistical analysis of the data.

References

1. Goodman, S.B., *Wear particulate and osteolysis.* Orthop Clin North Am, 2005. 36(1): p. 41-8.

2. Abu-Amer, Y., I. Darwech, and J.C. Clohisy, *Aseptic loosening of total joint replacements: mechanisms underlying osteolysis and potential therapies.* Arthritis Res Ther, 2007. 9 Suppl 1: p. S6.
3. Purdue, P.E., et al., *The cellular and molecular biology of periprosthetic osteolysis.* Clin Orthop Relat Res, 2007. 454: p. 251-61.
4. Looney, R.J., et al., *Periprosthetic osteolysis: an immunologist's update.* Curr Opin Rheumatol, 2006. 18(1): p. 80-7.
5. Goldring, S.R., C.R. Clark, and T.M. Wright, *The problem in total joint arthroplasty: aseptic loosening.* Journal of Bone & Joint Surgery - American Volume, 1993. 75(6): p. 799-801.
6. Ingham, E. and J. Fisher, *The role of macrophages in osteolysis of total joint replacement.* Biomaterials, 2005. 26(11): p. 1271-86.
7. Milosev, L., et al., *Extensive metallosis and necrosis in failed prostheses with cemented titanium-alloy stems and ceramic heads.* J Bone Joint Surg Br, 2000. 82(3): p. 352-7.
8. Margevicius, K.J., et al., *Isolation and characterization of debris in membranes around total joint prostheses.* J Bone Joint Surg Am, 1994. 76(11): p. 1664-75.
9. Shanbhag, A.S., et al., *Quantitative analysis of ultrahigh molecular weight polyethylene (UHMWPE) wear debris associated with total knee replacements.* J Biomed Mater Res, 2000. 53(1): p. 100-10.
10. Revell, P.A., *The combined role of wear particles, macrophages and lymphocytes in the loosening of total joint prostheses.* J R Soc Interface, 2008. 5(28): p. 1263-78.
11. Ingram, J., et al., *The influence of molecular weight, crosslinking and counterface roughness on TNF-alpha production by macrophages in response to ultra high molecular weight polyethylene particles.* Biomaterials, 2004. 25: p. 3511-3522.
12. Green, T.R., et al., *Effect of size and dose on bone resorption activity of macrophages by in vitro clinically relevant ultra high molecular weight polyethylene particles.* J Biomed Mater Res, 2000. 53(5): p. 490-7.
13. Green, T.R., et al., *Polyethylene particles of a 'critical size' are necessary for the induction of cytokines by macrophages in vitro.* Biomaterials, 1998. 19(24): p. 2297-302.
14. Ingham, E. and J. Fisher, *Biological reactions to wear debris in total joint replacement.* Proc Inst Mech Eng [H], 2000. 214(1): p. 21-37.
15. Schmalzried, T., et al., *Shapes and Dimensional Characteristics of Polyethylene Wear Particles Generated In Vivo by Total Knee Replacements Compared to Total Hip Replacements.* J Biomed Mater Res, Part B, 1997. 38: p. 203-210.
16. Lapcikova, M., et al., *Nanometer size wear debris generated from ultrahigh molecular weight polyethylene in vivo*, in *EMC 2008 14th European Microscopy Congress 1-5 September 2008, Aachen, Germany*, S. Richter and A. Schwedt, Editors. 2008, Springer Berlin Heidelberg: Berlin. p. 767-8.
17. Kobayashi, A., et al., *Number of polyethylene particles and osteolysis in total joint replacements. A quantitative study using a tissue-digestion method.* Journal of Bone & Joint Surgery - British Volume, 1997. 79(5): p. 844-8.

18. Kadoya, Y., et al., *Wear particulate species and bone loss in failed total joint arthroplasties.* Clin Orthop Relat Res, 1997(340): p. 118-29.
19. Tipper, J.L., et al., *Quantitative analysis of polyethylene wear debris, wear rate and head damage in retrieved Charnley hip prostheses.* J Mater Sci Mater Med, 2000. 11(2): p. 117-24.
20. Matthews, J.B., et al., *Evaluation of the Response of Primary Human Peripheral Blood Mononuclear Phagocytes to Challenge with In Vitro Generated Clinically Relevant UHMWPE Particles of Known Size and Dose.* J Biomed Mater Res 2000. 52: p. 296-307.
21. Matthews, J.B., et al., *Comparison of the response of primary human peripheral blood mononuclear phagocytes from di!erent donors to challenge with model polyethylene particles of known size and dose.* Biomaterials, 2000. 21: p. 2033-2044.
22. Willert, H.G., H. Bertram, and G.H. Buchhorn, *Osteolysis in alloarthroplasty of the hip. The role of ultra-high molecular weight polyethylene wear particles.* Clinical Orthopaedics & Related Research, 1990(258): p. 95-107.
23. Goodman, S.B., et al., *A clinical-pathologic-biochemical study of the membrane surrounding loosened and nonloosened total hip arthroplasties.* Clinical Orthopaedics & Related Research, 1989(244): p. 182-7.
24. Ito, S., et al., *Histological analysis and biological effects of granulation tissue around loosened hip prostheses in the development of osteolysis.* J Orthop Sci, 2004. 9: p. 478–487.
25. Kim, K.J., J. Chiba, and H.E. Rubash, *In vivo and in vitro analysis of membranes from hip prostheses inserted without cement.* Journal of Bone & Joint Surgery - American Volume, 1994. 76(2): p. 172-80.
26. Kim, K.J., et al., *A histologic and biochemical comparison of the interface tissues in cementless and cemented hip prostheses.* Clin Orthop Relat Res, 1993(287): p. 142-52.
27. Chun, L., et al., *The Characterization of Macrophages and Osteoclasts in Tissues Harvested from Revised Total Hip Prostheses.* J Biomed Mater Res, Part B, 1999. 48: p. 5.
28. Hansen, T., et al., *New aspects in the histological examination of polyethylene wear particles in failed total joint replacements.* Acta Histochemica, 2002. 104(3): p. 263-9.
29. Goodman, S.B., et al., *Heterogeneity in cellular and cytokine profiles from multiple samples of tissue surrounding revised hip prostheses.* J Biomed Mater Res, 1996. 31(3): p. 421-8.
30. Mirra, J.M., et al., *The pathology of the joint tissues and its clinical relevance in prosthesis failure.* Clin Orthop, 1976. 117: p. 221-240.
31. Digas, G., et al., *5-year experience of highly cross-linked polyethylene in cemented and uncemented sockets: two randomized studies using radiostereometric analysis.* Acta Orthopaedica, 2007. 78(6): p. 746-54.
32. Minoda, Y., et al., *Wear particle analysis of highly crosslinked polyethylene isolated from a failed total hip arthroplasty.* Journal of Biomedical Materials Research, 2008. Part B, Applied Biomaterials. 86B(2): p. 501-5.

33. Knahr, K., et al., *Retrieval analyses of highly cross-linked polyethylene acetabular liners four and five years after implantation.[erratum appears in J Bone Joint Surg Br. 2008 Apr;90(4):543].* Journal of Bone & Joint Surgery - British Volume, 2007. 89(8): p. 1036-41.
34. Illgen, R.L., 2nd, et al., *Highly crosslinked vs conventional polyethylene particles--an in vitro comparison of biologic activities.* Journal of Arthroplasty, 2008. 23(5): p. 721-31.
35. Santavirta, S., et al., *Aggressive granulomatous lesions associated with hip arthroplasty. Immunopathological studies.* Journal of Bone & Joint Surgery - American Volume, 1990. 72(2): p. 252-8.
36. Basle, M.F., et al., *Migration of metal and polyethylene particles from articular prostheses may generate lymphadenopathy with histiocytosis.* J Biomed Mater Res, 1996. 30(2): p. 157-63.
37. Urban, R.M., et al., *Dissemination of wear particles to the liver, spleen, and abdominal lymph nodes of patients with hip or knee replacement.[see comment].* Journal of Bone & Joint Surgery - American Volume, 2000. 82(4): p. 457-76.
38. Mabrey, J.D., et al., *Standardized analysis of UHMWPE wear particles from failed total joint arthroplasties.* J Biomed Mater Res, 2002. 63(5): p. 475-83.
39. Elfick, A.P.D., et al., *The nature and dissemination of UHMWPE wear debris retrieved from periprosthetic tissue of THR.* J. Viomws. Mater. Res., 2003. 65A: p. 95-108.
40. Dorr, L.D., et al., *Clinical performance of a Durasul highly cross-linked polyethylene acetabular liner for total hip arthroplasty at five years.* Journal of Bone & Joint Surgery - American Volume, 2005. 87(8): p. 1816-21.
41. Endo, M., et al., *Comparison of wear, wear debris and functional biological activity of moderately crosslinked and non-crosslinked polyethylenes in hip prostheses.* Proc IME HJ Eng Med, 2002. 216(2): p. 111-22.
42. Fisher, J., et al., *A novel method for the prediction of functional biological activity of polyethylene wear debris.* Proceedings of the Institution of Mechanical Engineers. Part H - Journal of Engineering in Medicine, 2001. 215(2): p. 127-32.
43. Konttinen, Y.T., et al., *The microenvironment around total hip replacement prostheses.* Clinical Orthopaedics & Related Research, 2005(430): p. 28-38.

3. The Combined Role of Innate and Adaptive Immune Cells in Aseptic Loosening of Conventional and Highly Crosslinked Polyethylene Liners[3]

Abstract

Polyethylene wear debris is a major contributor to inflammation and the development of implant loosening, a leading cause of THA revisions. To reduce wear debris, highly crosslinked ultrahigh-molecular-weight polyethylene (HXLPE) was introduced to improve wear properties of bearing surfaces. As HXLPE revision tissues are only now becoming available, it is possible to examine the presence and association of wear debris with inflammation in early implant loosening. The current chapter evaluates potential correlations between polyethylene wear debris and the extent of innate and/or adaptive immune cells for both conventional gamma air-sterilized polyethylene (CPE) and HXLPE cohorts. In addition, the regional differences in the immune cell response were evaluated between CPE and HXLPE cohorts. Tissue samples were obtained during revision surgery of nine CPE and nine HXLPE liners. Polarized light microscopy was used to determine 0.5- to 2-μm polyethylene particle number/mm^2, and immunohistochemistry was performed to determine macrophage, T cell, and neutrophil number/mm^2. For the CPE cohort, correlations were observed between wear debris and the magnitude of individual patient macrophage (ρ = 0.70) and T cell responses (ρ = 0.71) and between the

[3] Baxter RM, Freeman TA, Kurtz SM, Steinbeck MJ. Do Tissues from THA Revision of HXLPE Liners Contain Wear Debris and Associated Inflammation? Clin Orthop Relat Res. Symposium: UHMWPE for Arthroplasty: From Powder to Debris. 2010 *Epub. Dec 7.*

overall number of macrophages and T cells (ρ = 0.77) in revision tissues. In comparison, the HXLPE cohort showed a correlation between polyethylene wear debris and the magnitude of macrophage responses (ρ = 0.57) and between the overall number of macrophages and T cells (ρ = 0.68). Although macrophages and T cells were present in both cohorts, the HXLPE cohort had lower numbers, which may be associated with shorter implantation times. These data show that although implant loosening is a complex process involving surgical, patient and implant-specific factors, the presence of polyethylene wear debris and inflammation in HXLPE revision tissues may contribute to the process of loosening at early- to mid-term implantation. The unknown effect(s) of HXLPE wear debris after long-term implantation remains of crucial interest for clinical performance.

Introduction

The generation of ultra high molecular weight polyethylene (polyethylene) wear debris is a major cause of aseptic loosening, which is among the most common reasons for THA revision surgery [1-3]. From a biological standpoint, it is rather well accepted that the interaction of particles and phagocytic antigen-presenting cells in periprosthetic tissue and surrounding bone contributes to the deregulation of bone homeostasis resulting in osteolysis at the bone–implant interface [2, 4, 5]. Consequently, highly crosslinked polyethylene (HXLPE) was introduced to improve wear properties of the bearing surface [6-9], and *in vitro* studies have shown 40% to 95% reductions in wear rate [10-12] and an 87% reduction in the risk of osteolysis [13] as compared to conventional polyethylene (CPE). However, the brittle nature of the HXLPE [14], generation of predominantly submicron-sized particles [15-17], and studies showing the effect of particle size, shape, and number raise concerns regarding the long-term clinical performance of HXLPE [18-21].

As was initially presented in the introduction, the initial inflammatory response to wear debris primarily involves monocytes/macrophages. These innate immune cells differentiate into histiocytes or fuse with other macrophages to form multinucleated giant cells [22-24]. The ingestion of wear debris by macrophages results in their activation, gene expression, and pro-inflammatory cytokine (e.g., IL-1β, TNF-α, IL-6, PGE2, IL-8) and chemokine (e.g., monocyte chemotactic protein (MCP)-1, macrophage inflammatory protein (MIP)-1α) secretion [5, 25-28]. Collectively, these factors induce infiltration, maturation, and activation of immune

cells and osteoclasts [5, 29, 30]. Another innate immune cell, the neutrophil, also ingests particles and releases pro-inflammatory factors; however, these cells are present only in low numbers in aseptic loosening [31].

The adaptive immune response includes several subgroups of T lymphocytes (T cells): T helper cells (TH), involved in activating and directing other immune cells; cytotoxic T cells (TC), which cause cell death in response to the recognition of a foreign or altered self-antigen; and regulatory T cells (Treg), which suppress activation of the immune system maintaining homeostasis [2, 32]. Specifically, TH cells play a major role in releasing cytokines (e.g., RANKL) that promote macrophage differentiation into osteoclasts [33, 34]. Although the role of T cells in aseptic loosening is controversial, a recent study has identified a functionally active subset of TC cells capable of down-regulating TH cells [35], which may explain the inconsistent detection of lymphokines in tissues around loosened prostheses [35, 36]. Additional studies showing correlations between increased numbers of TH and TC cells and radiographic osteolysis [5, 37] further implicate T cell involvement in bone remodeling. However, others only attribute a substantial involvement of T cells in the inflammatory Type IV hypersensitivity response to metal particles and/or ions [38-41]. Thus, understanding of adaptive immune responses contributing to osteolysis lacks a clear consensus.

Methodologically, these immune cells can be evaluated using immunohistochemistry. To identify cells of interest, surface antigens within or on the surface of those cells can by targeted and labeled. Initially, the primary antibody

containing a specific IgG molecule is used to detect and bind to the surface antigen on the cell of interest. The next step involves the addition of a secondary antibody that binds to the IgG molecule of the primary antibody. Finally, immunohistochemical staining is completed using a chromogenic substrate such as diaminobenzidine (DAB), which reacts with binding sites specific to the secondary antibody.

Chapter 2 reported on the presence of histomorphologic changes in HXLPE revision tissues [42]. Specifically, the results of Chapter 2 showed a prevalence of fibrocartilage in tissues from HXLPE revisions implanted for less than 3 years (4/9 patients), implicating poor osseo-integration in the development of loosening [43]. In Chapter 3, the role of polyethylene wear debris in promoting inflammation and implant loosening was investigated by quantitatively measuring the *in vivo* inflammatory response.

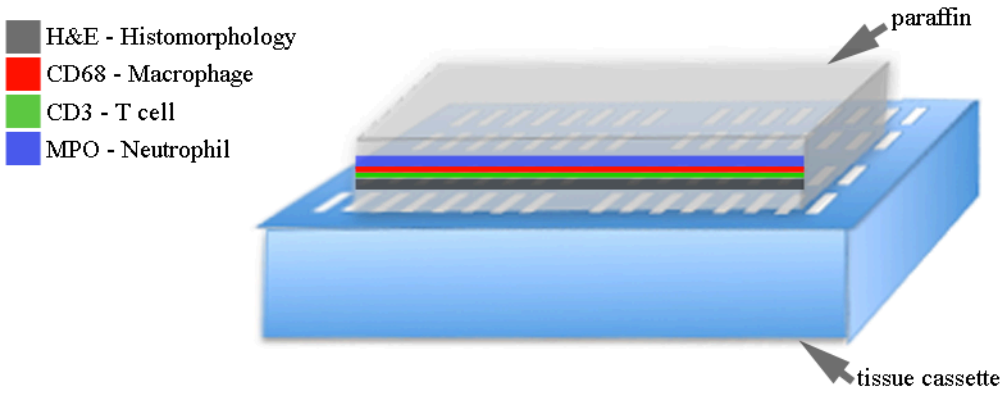

Figure 3-1. Schematic of tissue cassettes processed for histomorphologic and immunohistochemical analysis.

To evaluate immune cells, serial sections were obtained from the cassettes used in the analysis of histomorphologic changes in revision tissues from Chapter 2

(Figure 3-1). The current chapter addressed two main hypotheses. The first hypothesis was that the regional immune cell responses would differ when comparing tissues from CPE and HXLPE implant cohorts. The second hypothesis was that the presence of polyethylene wear debris in THA revision tissues would only correlate with innate immune cell numbers for the CPE cohort. The limited expectation for correlations between other immune cell types and polyethylene wear particles was based on several assumptions. First, based on animal models showing that T cells are dispensable in the development of osteolysis [44-46], correlations between T cells and polyethylene wear particle number were not expected. Next, for the HXLPE cohort, correlations between immune cells numbers and polyethylene wear particle numbers were not expected due to the relatively early implantation times (<5 years) and the categorical absence of radiographic osteolysis prior to revision surgery.

Methods

Tissue samples were obtained from 18 consenting patients undergoing revision arthroplasty of uncemented, metal-on-polyethylene hip components using a standardized tissue retrieval protocol; these are the same tissues used in the previous study [42]. Polyethylene liners were classified into two cohorts: conventional gamma air-sterilized polyethylene (CPE, n=9) and gamma inert-sterilized highly crosslinked polyethylene (HXLPE, n=9). For the CPE cohort, components were implanted for an average of 13.3 years (range, 9.6– 15.6 years) and revised for femoral loosening (n=3), acetabular loosening (n=2), loosening of

both components (n=1), or wear debris and associated osteolysis (n=2). For the HXLPE cohort, components were implanted for an average of 3.3 years (range, 1.5–5.9 years) and revised for femoral loosening (n=4), acetabular loosening (n=3), loosening of both components (n=1), or subluxation (n=1). Patients with known infection before surgery, implantation time less than 1 year, hepatitis, or cancer were excluded. Gender was represented equally in the two groups. We had prior IRB approval.

Tissues were excised from locations adjacent to the implant, which included the pseudocapsule for all 18 THA revision surgeries, and periprosthetic retroacetabular (acetabular loosening) or proximal femoral tissue (femoral loosening). The clinical details for the tissue samples are provided for the CPE (Table 2-1) and HXLPE (Table 2-2) materials, which are shown in Chapter 2.

To determine the quantity of polyethylene wear debris, overlapping full-field tissue arrays were collected in polarized light using an Olympus BX50 microscope (Olympus Corp, Tokyo, Japan), equipped with a stepper motor-controlled stage (± 2-lm positioning accuracy) and elliptically polarized light imaging system (EPLIS) filters. EPLIS relied on the use of a ¼-wavelength (λ) birefringent quartz retardation plate, an incremented rotating polarizing element, and a rotating interference filter, which were adjusted to achieve maximum particle/tissue contrast and to eliminate collagen and other non-particle birefringence. The initial EPLIS validation assumptions derived from scanning electron microscopy of wear debris shown in Chapter 2 were maintained for the methodology of the current chapter.

Immunohistochemistry Protocol

To evaluate the involvement of inflammatory cells in mediating implant failure, periprosthetic hip tissues were subjected to immunohistochemistry. For the current chapter, the following conditions were followed. Initially, three 6-μm serial sections from each tissue sample were mounted on Fisherbrand® Superfrost® Plus slides (ThermoFisher Scientific, Inc, Waltham, MA, USA), dewaxed, and rehydrated. A Dako automated slide stainer (Dako, Carpinteria, CA, USA) was used for the immunohistochemical staining reactions. All antibodies were diluted in 0.1 mol/L Tris/2% fetal bovine serum. For neutrophil detection, myeloperoxidase (MPO) rabbit polyclonal antibody (Dako) was used at a 1:4000 dilution for 30 minutes at room temperature. Prior epitope retrieval was for 10 minutes in pepsin (Dako). Secondary biotinylated anti-rabbit immunoglobulin (Ig) G (Vector Laboratories, Inc, Burlingame, CA, USA) was used at 1:200 dilution for 30 minutes at room temperature. For macrophage detection, cluster of differentiation 68 (CD68) mouse monoclonal antibody (Dako) was used at a 1:2000 dilution for 30 minutes at room temperature. Prior epitope retrieval was for 10 minutes in pepsin. Secondary biotinylated anti-mouse IgG (Vector Laboratories) was used at 1:200 dilution for 30 minutes at room temperature. For T cell detection, CD3 rabbit polyclonal antibody (Dako) was used at a 1:100 dilution for 30 minutes at room temperature. Prior epitope retrieval was for 20 minutes in Invitrogen™ (Life Technologies Corp, Carlsbad, CA, USA) EDTA epitope retrieval solution. Secondary biotinylated anti-rabbit IgG was used at 1:200 dilution for 30 minutes at room temperature. After rinsing, the slides were incubated with avidin-biotin complex (Vector Laboratories)

for 30 minutes at room temperature, rinsed, and incubated with diaminobenzidine (Dako) for 10 minutes at room temperature. Slides were counterstained with Harris hematoxylin (ThermoFisher Scientific). To determine the number of positive cells, total cells and polyethylene wear debris, overlapping full-field tissue arrays were collected in brightfield and polarized light, and an image analysis program was developed to threshold brightfield images based on predetermined criteria of cell size, nuclear color, and staining intensity using ImagePro™ Plus (Media Cybernetics Inc, Bethesda, MD, USA). Total cell numbers were also determined as a measure of tissue integrity and loose versus dense connective tissue.

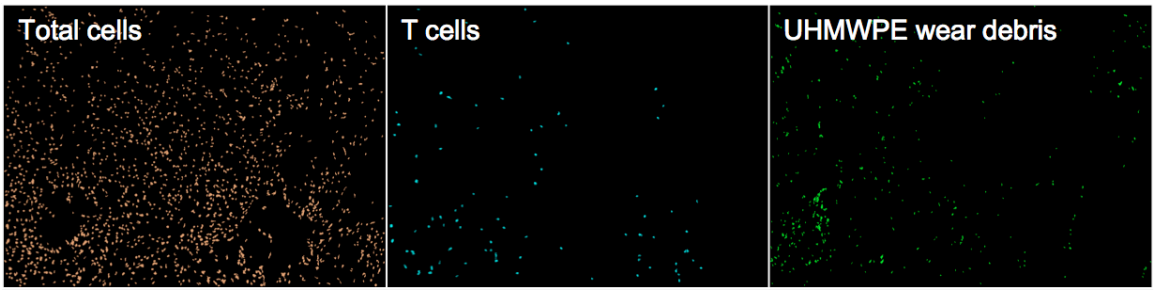

Figure 3-2. Representative images showing total cells (orange), T cells (blue) and polyethylene wear debris (green).

To calculate tissue area, a separate threshold was applied to distinguish between the tissue and the white background. A quantitative value of inflammatory response then was determined as the number of positive cells/mm^2 tissue area. Finally, polarized light images were analyzed to determine 0.5- to 2-μm polyethylene particle number using a customized image threshold operation programmed in MATLAB™ (The Mathworks Inc, Natick, MA, USA) (Appendix I). All imaging analyses were performed by three observers (RMB, TAF, LLJ) using the same software to threshold images from two patients to determine user variability.

The results agreed within 95% of each other.

For both cohorts, the number of polyethylene wear particles, macrophages, T cells, and neutrophils in each corresponding polarized light and brightfield image were determined, and the data were expressed as number/mm^2. Because the data were not normally distributed, nonparametric statistics were used throughout. Correlations between the number of macrophages, T cells, neutrophils, and polyethylene wear debris were evaluated using the Spearman rank correlation method for individual images and for the magnitude of individual patient responses (combined image results for each patient). When comparing all four data sets, the Kruskal-Wallis test was significant for macrophages and T cells, but not for neutrophils. Strictly where indicated, differences in the median number of immune cells/mm^2 were compared by the Wilcoxon Mann-Whitney test for each polyethylene cohort (CPE versus HXLPE) and tissue region (pseudocapsular versus periprosthetic). Based on the assessment of morphological changes for these same cohorts in the previous chapter, the sample sizes in the current study were sufficiently powered (>0.9) to identify similar differences in inflammatory cell responses [42]. Statistical analysis was performed using JMP 8.0 (SAS Institute Inc, Cary, NC, USA).

Results

Overview

For the conventional polyethylene (CPE) cohort, substantial inter-patient and intra-patient variability were observed in the number and location of polyethylene

wear particles and immune cells in pseudocapsular and periprosthetic tissues (Table 3-1 and Table 3-2, respectively). In general, the pseudocapsular and periprosthetic tissues from this cohort contained predominantly macrophages (Figure 3-3A), followed by T cells (Figure 3-3B), and a few neutrophils (Figure 3-3C) were observed in some tissues (<6/mm^2). For the HXLPE cohort, heterogeneous immune cell responses also were observed in pseudocapsular and periprosthetic tissues (Table 3-3 and Table 3-4, respectively). Similar to the CPE cohort, the inflammatory cells observed in tissues were predominantly macrophages (Figure 3-3D), then T cells (Figure 3-3E), and only a few neutrophils were observed (<8/mm^2) (Figure 3-3F).

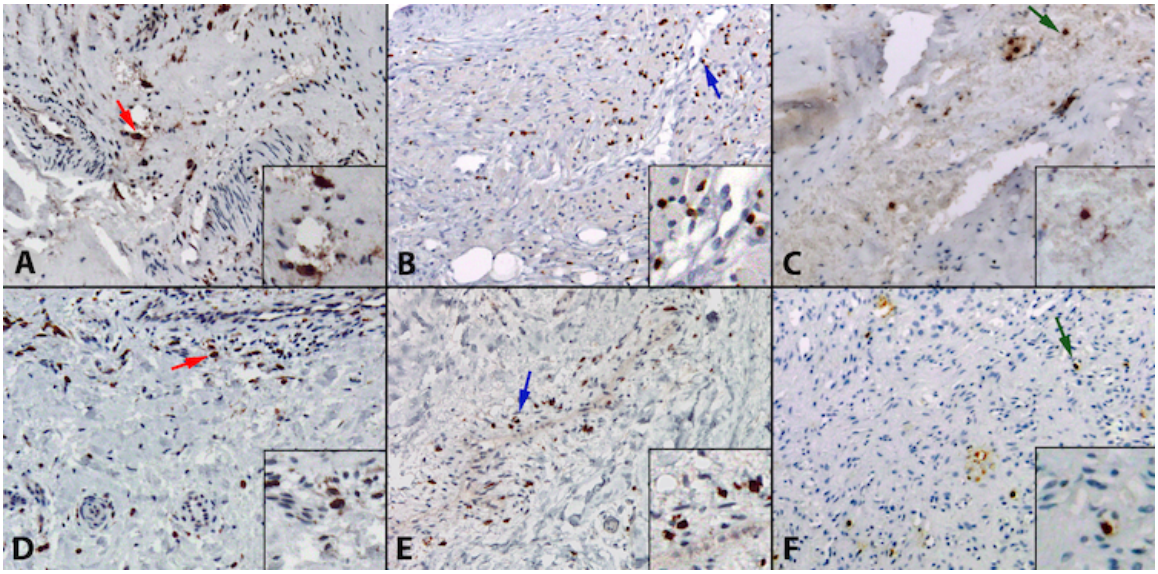

Figure 3-3. Representative images of immunohistochemistry for innate and adaptive immune cells in periprosthetic hip tissue are shown: (A) macrophages (CD68+, red arrow), (B) T cells (CD3+, blue arrow), and (C) neutrophils (MPO+, green arrow) in patient tissues from the CPE cohort; and (D) macrophages (red arrow), (E) T cells (blue arrow), and (F) neutrophils (green arrow) in patient tissues from the HXLPE cohort (nuclear stain, Harris hematoxylin; main image magnification, 100X; inset images, enlarged by 200%).

Table 3-1. Pseudocapsular Scoring for CPE Implant Revision Tissues

Patient #	PMN (MPO)/mm^2	MAC (CD68)/mm^2	T cell (CD3)/mm^2	Polyethylene wear/mm^2	Cell total/mm^2
1 (C)	5.6 ± 1.3	16.5 ± 5.1	0.6 ± 0.2	37.3 ± 11.7	629.7 ± 54.8
2 (C)	0.0 ±0.0	0.3 ± 0.1	0.0 ±0.0	3.8 ± 0.8	540.2 ± 14.2
3 (C)	0.2 ± 0.1	186.2 ± 25.2	6.4 ± 1.2	14.6 ± 3.0	1053.0 ± 45.4
4 (C)	0.0 ± 0.0	5.6 ± 1.2	6.0 ± 1.8	3.0 ± 1.3	1006.3 ± 173.6
5 (C)	0.1 ±0.1	491.8 ± 91.9	39.5 ± 9.9	5.5 ± 1.2	1405. 6 ± 85.6
6 (C)	3.2 ± 1.5	342. ± 60.4	0.0 ± 0.0	5.7 ± 2.0	934.3 ± 103.7
7 (C)	0.4 ± 0.2	8.6 ± 2.4	0.8 ± 0.6	1.9 ± 0.5	619.7 ± 21.7
8 (C)	1.5 ± 0.6	0.0 ± 0.0	0.0 ± 0.0	2.1 ± 0.4	231.3 ± 39.2
9 (C)	1.4 ± 0.4	370.1 ± 32.8	59.9 ± 12.7	35.5 ± 5.9	1353.3 ± 135.4

Notes: Values are presented as the average number of immunohistochemically positive cells, total cells, and 0.5-2 μm polyethylene particles/mm^2 ± standard error of the mean. Abbreviations: PMN, neutrophil polymorphonuclear leukocytes; MPO, myeloperoxidase; MAC, macrophage; CD, cluster of differentiation; C, pseudocapsule.

Table 3-2. Noncapsular Scoring for CPE Implant Revision Tissues

Patient #	PMN (MPO)/mm^2	MAC (CD68)/mm^2	T cell (CD3)/mm^2	Polyethylene wear/mm^2	Cell total/mm^2
2 (PF)	0.3 ± 0.2	559.3 ± 39.4	28.3 ± 4.6	48.8 ± 10.8	1167.0 ± 106.3
3 (RA)	0.0 ± 0.0	494.8 ± 55.4	53.0 ± 8.5	151.9 ± 32.0	1139.0 ± 47.8
4 (PF)	0.1 ± 0.1	491.8 ± 91.9	39.5 ± 9.9	5.0 ± 1.2	1405.6 ± 85.6
6 (PF)	1.5 ± 0.4	490.5 ± 44.5	9.1 ± 2.2	4.5 ± 0.8	839.3 ± 157.6
8 (RA)	8.4 ± 1.3	404.5 ± 23.2	33.6 ± 4.0	116.3 ± 20.7	1046.3 ± 99.9
8 (PF)	5.4 ± 1.2	475.0 ± 26.4	43.1 ± 7.3	546.4 ± 70.8	1242.3 ± 74.9

Notes: Values are presented as the average number of immunohistochemically positive cells, total cells, and 0.5-2 μm polyethylene particles/mm^2 ± standard error of the mean. Abbreviations: PMN, neutrophil polymorphonuclear leukocytes; MPO, myeloperoxidase; MAC, macrophage; CD, cluster of differentiation; PF, proximal femoral; RA, retroacetabulum

Correlations Between Immune Cells and Polyethylene Wear Debris

Generally, the strength of a correlation is associated with rho (ρ): values between 0.9-1.0 are considered very strong; 0.7-0.9, strong; 0.5-0.7, moderate; and 0.3-0.5, weak [47]. Values of ρ that fall below 0.3 are very weak and would represent little, if any, evidence to support a trend between two variables. Overall, when evaluating trends in the individual image values of all nine patients from each cohort, significant but weak and/or negative correlations were observed between the number of immune cells and the number of polyethylene particles. For macrophages, a statistically significant but very weak positive correlation was observed between macrophage number and polyethylene wear particle number in the CPE cohort (ρ=0.099; p=0.007). For the HXLPE cohort, statistically significant correlation indicating a weak and negative trend was also observed between the number of macrophages and the number of polyethylene wear debris (ρ=-0.329;

$p<0.001$). In addition, a statistically significant but very weak positive correlation was observed between T cell number and polyethylene wear particle number in the CPE cohort ($\rho=0.165$; $p<0.001$). For the HXLPE cohort, a significant but weak negative correlation was observed between the number of T cells and the number of polyethylene wear debris ($\rho=-0.329$; $p<0.001$) (Figure 3-4). For neutrophils, a statistically significant correlation was not observed between neutrophils and polyethylene wear debris in the CPE cohort ($\rho=0.081$; $p=0.084$). Finally, for the HXLPE cohort, a statistically significant but very weak negative correlation was observed between the number of neutrophils and the number of polyethylene wear debris ($\rho=-0.284$; $p<0.001$). These findings highlight variability in both polyethylene wear particle number and immune cells in the tissue sections.

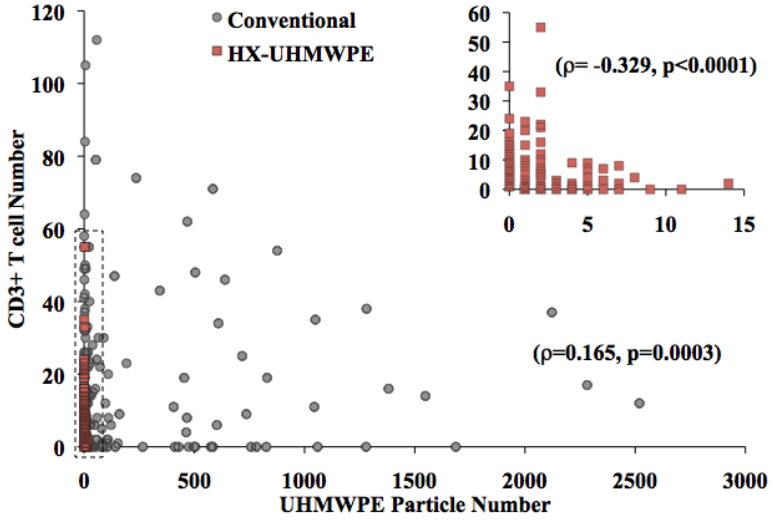

Figure 3-4. Representative trends observed for individual image correlation of immune cells and polyethylene wear debris. Shown are very weak and/or negative correlations between T cells and polyethylene particle number from CPE and HXLPE cohorts, respectively. Note: Data for images containing zero particles and zero cells are not included in this plot.

However, when considering the magnitude of individual patient responses (the combined image results for each patient), strong correlations were observed between macrophages and associated polyethylene wear debris (ρ=0.69; p=0.0042) (Figure 3-5A) and between polyethylene wear debris and T cells (ρ=0.71; p=0.0032) (Figure 3-5B). In addition, the magnitude of the macrophage and T cell responses was highly correlated for each of the nine patients and combined regions (ρ=0.77; p=0.0008) (Figure 3-5C). For the HXLPE polyethylene cohort, comparing trends in the magnitude of individual patient responses, a moderate correlation was observed between macrophages and polyethylene wear debris (ρ=0.57; p=0.0422) (Figure 3-6A). In addition, the magnitude of the macrophage and T cell responses was moderately correlated for each of the nine patients and combined regions (ρ=0.68;

p=0.0103), although the numbers for both were low in five of the patient tissues (Figure 3-6B).

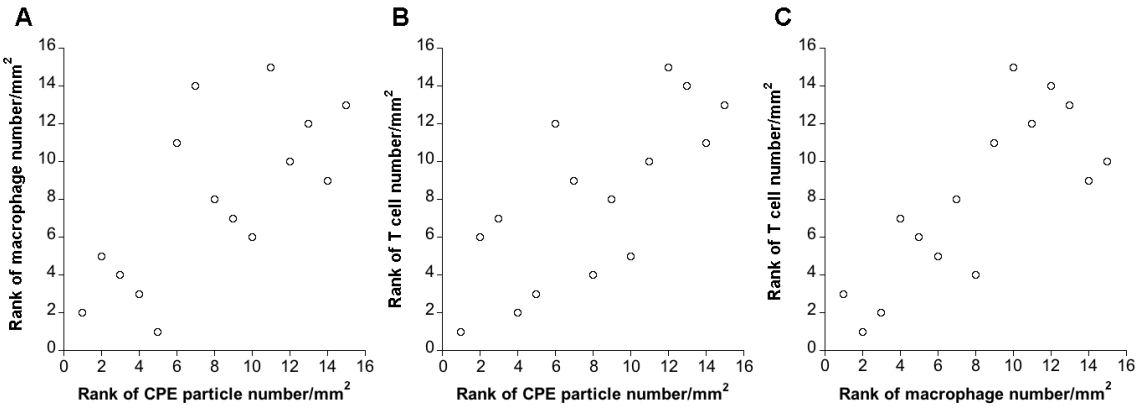

Figure 3-5. Polyethylene wear debris is associated with immune cells in pseudocapsular and periprosthetic tissues from revised CPE liners. Correlations were observed between wear particle number and individual patient responses for (A) CD68+ macrophages (ρ = 0.69; p = 0.0042) and (B) CD3+ T cells (ρ = 0.71; p = 0.0032) and (C) separately for macrophages and T cells (ρ = 0.77; p = 0.0008) using Spearman rank correlation tests. CPE = conventional polyethylene.

Table 3-3. Scoring for Pseudocapsular Tissues from Revised HXLPE Hip Implants

Patient #	PMN (MPO)/mm^2	MAC (CD68)/mm^2	T cell (CD3)/mm^2	Polyethylene wear/mm^2	Cell total/mm^2
1 (C)	0.9 ± 0.3	1.4 ± 0.4	1.3 ± 0.4	0.4 ± 0.1	539.6 ± 43.2
2 (C)	1.0 ± 0.1	1.7 ± 0.3	0.4 ± 0.2	0.5 ± 0.1	567.0 ± 13.5
3 (C)	8.6 ± 2.2	0.6 ± 0.4	0.7 ±0.4	1.1 ± 0.3	911.3 ± 72.9
4 (C)	0.4 ± 0.2	18.3 ± 8.1	3.3 ± 1.3	1.0 ± 0.2	854.3 ± 68.9
5 (C)	0.5 ± 0.2	15.0 ± 1.8	16.7 ± 3.4	1.0 ± 0.2	945.3 ± 72.6
6 (C)	0.2 ± 0.1	0.8 ± 0.3	0.9 ± 0.4	3.3 ± 0.6	609.6 ± 53.4
7 (C)	4.9 ± 1.1	50.9 ± 9.8	5.9 ± 1.2	4.7 ± 0.6	1304.6 ± 45.5
8 (C)	3.0 ± 0.9	1.5 ± 0.4	0.4 ± 0.2	0.5 ± 0.2	757.3 ± 49.4
9 (C)	0.5 ± 0.3	2.1 ± 0.3	2.3 ± 1.1	0.9 ± 0.3	666.3 ± 16.5

Notes: Values are presented as the average number of immunohistochemically positive cells, total cells, and 0.5-2 μm polyethylene particles/mm^2 ± standard error of the mean. Abbreviations: PMN, neutrophil polymorphonuclear leukocytes; MPO, myeloperoxidase; MAC, macrophage; CD, cluster of differentiation; C, pseudocapsule.

Table 3-4. Scoring for Noncapsular Tissues from Revised HXLPE Hip Implants

Patient #	PMN (MPO)/mm^2	MAC (CD68)/mm^2	T cell (CD3)/mm^2	Polyethylene wear/mm^2	Cell total/mm^2
2 (PF)	0.0 ± 0.0	3.5 ± 0.8	0.0 ± 0.0	1.4 ± 0.7	735.3 ± 15.2
4 (PF)	0.5 ± 0.2	69.6 ± 10.1	4.4 ± 0.9	0.2 ± 0.1	975.3 ± 43.9
6 (PF)	3.4 ± 1.0	108.3 ± 29.6	14.0 ± 3.5	8.8 ± 1.7	1196.7 ± 137.5
7 (RA)	2.9 ± 0.8	2.0 ± 0.8	2.4 ± 0.6	2.9 ± 0.6	1600.7 ± 86.5

Notes: Values are presented as the average number of immunohistochemically positive cells, total cells, and 0.5-2 μm polyethylene particles/mm^2 ± standard error of the mean. Abbreviations: PMN, neutrophil polymorphonuclear leukocytes; MPO, myeloperoxidase; MAC, macrophage; CD, cluster of differentiation; PF, proximal femoral; RA, retroacetabulum.

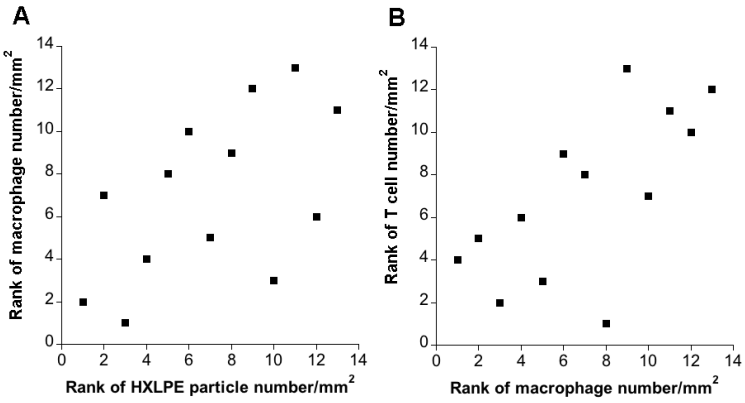

Figure 3-6. Polyethylene wear debris is associated with immune cells in pseudocapsular and periprosthetic tissues from revised HXLPE liners. Correlations were observed between polyethylene wear particle number and the individual patient response for (A) CD68+ macrophages (ρ = 0.57; p = 0.0422) and (B) separately for macrophages and CD3+ T cells (ρ = 0.68; p = 0.0103) using Spearman rank correlation tests.

Differences in Immune Cell Responses between Conventional and Highly Crosslinked Polyethylene Implant Components

For the CPE and HXLPE cohorts, variability in the immune cell responses in pseudocapsular and periprosthetic tissues was observed Table 3-5. However, comparison of the two cohort responses showed the average number of macrophages/mm^2 in periprosthetic tissue from the CPE cohort was higher than pseudocapsular tissue (p=0.0027) from the same cohort and pseudocapsular

(p=0.0018) and periprosthetic tissues (p=0.0142) from the HXLPE cohort (Figure 3-7). The average number of T cells/mm^2 also was greater in periprosthetic tissues from the CPE cohort as compared with pseudocapsular tissue (p=0.0148) from the same cohort and pseudocapsular (p=0.0027) and periprosthetic tissues (p=0.0252) from the HXLPE cohort. The number of neutrophils was low regardless of polyethylene cohort or tissue region.

Table 3-5. Summary of pseudocapsular and noncapsular tissue responses for CPE and HXLPE implant revisions

	CPE		HXLPE	
	n/N	Number/mm^2	n/N	Number/mm^2
Pseudocapsular tissue				
Neutrophils	7/9	1.4 (0.0-5.8)	9/9	2.2 (0.3-8.6)
Macrophages	8/9	111.6 (0.0-403.3)	9/9	10.0 (0.6-46.7)
T cells	5/9	33% (0.0-64.4)*	9/9	3.6 (0.4-17.9)
0.5-2.0 μm polyethylene particles	9/9	10.7 (0.3-34.2)	9/9	2.3 (0.5-8.6)
Total cells		791.6 (231.3-1353.3)	2/9	795.1 (539.7-1304.7)
Noncapsular Tissue				
Neutrophils	5/6	2.7 (0.0-8.4)	3/4	1.7 (0.0-3.2)
Macrophages	6/6	470.9 (401.1-581.6)	4/4	46.4 (2.1-118.6)
T cells	6/6	33.7 (9.6-51.6)	3/4	5.2 (0.0-13.7)
0.5-2.0 μm polyethylene particles	6/6	205.0 (4.0-642.5)	4/4	4.2 (0.4-13.3)
Total cells		1139.9 (839.3-1405.7)		1127.0 (735.3-1600.7)

Notes: Values are presented as the average number of immunohistochemically positive cells, total cells, and polyethylene particles/mm^2, with range in parentheses; *the number of pseudocapsular tissues showing a T cell response was lower in the CPE cohort than the incidence of other immune cell responses; n = incidence, N = total number of tissues.

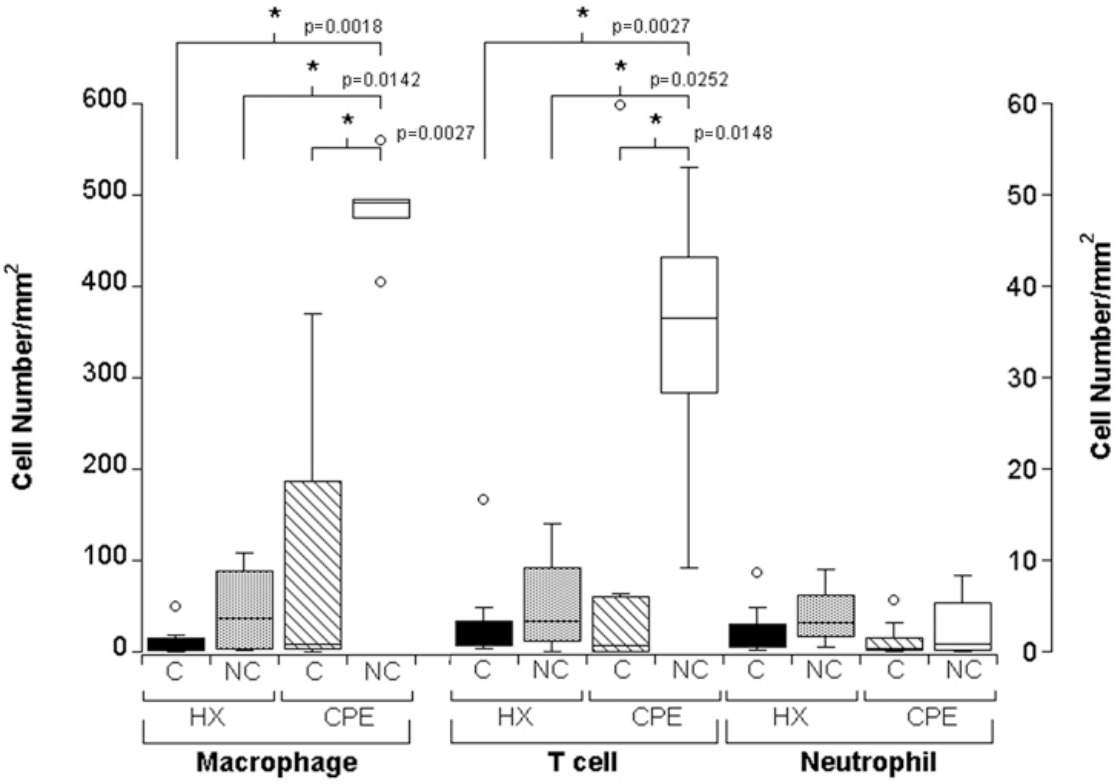

Figure 3-7. Box plots showing regional differences and inter-patient variability in the immune cell number/mm^2. The number of CD68+ macrophages and CD3+ T cells was higher in noncapsular, periprosthetic tissues from the CPE cohort. A secondary y-axis is provided for easier interpretation of the magnitude of T cell and neutrophil responses. Provided are medians, a boxed range of the 25th to 75th percentile, and whiskers showing the 10th and 90th percentile. Outliers are shown as open circles. C = pseudocapsule; NC = noncapsular periprosthetic.

Discussion

Polyethylene wear debris is a major contributor to inflammation in periprosthetic tissues and the development of osteolysis and loosening at the bone–implant interface. To reduce wear debris generation, highly crosslinked polyethylene (HXLPE) was introduced to improve wear properties of the bearing surface. However, only as THA revision tissues from HXLPE become available can the potential role of polyethylene wear debris and inflammation in implant

loosening be investigated. Based on the recent availability of tissues from revised HXLPE implants, the current study was performed to investigate potential correlations between polyethylene wear debris and immune cell responses in tissues that were representative of the end-stage reason for revision.

The current chapter contains the following limitations: (i) There is a difference between the two patient cohort implantation times. The average implantation time was 13.3 years (range, 9.6–15.6) for the conventional cohort and 3.3 years (range, 1.5–5.9) for the HXLPE cohort. Although implantation duration may affect the amount of wear debris and longevity of the immune response, the local cellular response was compared to the existing wear particle load. Therefore, Therefore, despite a reduced implantation time for the HXLPE cohort, the magnitude of the macrophage response was correlated with wear debris accumulation in pseudocapsular and periprosthetic tissues. (ii) There is an absolute lower resolution limit for detection of wear debris using polarized light microscopy (0.5 μm). Hip simulator studies of polyethylene wear debris observed by environmental scanning electron microscopy suggest the mean particle size range is 0.2 to 0.5 μm for HXLPE liners [48, 49] and 0.3 to 0.8 μm for CPE liners [50, 51]. Thus, there is a greater potential to underestimate particle number in the HXLPE cohort, which may account for the reduced correlation for wear debris and inflammatory cells. Compared to the previous chapter, the intensity of light contributing to particle birefringence was not decreased by eosin staining in these tissue sections. Nevertheless, to account for the full range of particle sizes, a detailed analysis of these submicron wear debris is

provided in the final chapter. (iii) The cohort sizes are small, but the differences observed in this and the previous chapter evaluating morphological changes in the same patient tissues were supported by a power analysis indicating a power of greater than 0.90 [42]. In addition, that the inclusion of additional tissue samples would not likely reduce the range of immune cell responses occurring due to individual patient variation. (iv) There is an unknown contribution of the variation along the z-axis of the embedded tissue. Based on the large amount of time involved in the imaging and analysis of individual tissue sections, it was not possible to identify the distribution of inflammatory cells along the depth of the entire tissue sample. More global assessments of cellular contents are available using methods such as FACS (fluorescent activated cell sorting). However, the *in situ* comparison of regional differences in particles and immune cells would be lost using a global approach, which was a primary objective of the work performed in this current chapter.

Our findings for the CPE cohort are similar to those reported in other immunohistochemical studies of periprosthetic tissues from uncemented, gamma air-sterilized polyethylene liners [52-57]. In general, the co-localization of wear debris and macrophages/histiocytes is well-established [37, 57]. In addition, several studies have identified the presence of T cells in periprosthetic tissues, with the incidence ranging from categorically absent to 30% [37, 56, 57]. However, in these studies, there was no attempt to correlate the presence of polyethylene wear debris with immune cells, to separately evaluate the presence of macrophages and

histiocytes using a size exclusion cutoff, or to determine macrophage and T cell number in the entire tissue section. Macrophages, unlike debris-laden histiocytes, have the potential to up-regulate pro-inflammatory cytokine expression [58], and only by determining the number of these cells in each section can their involvement be assessed given the known intra-tissue variability [42, 55, 56, 59]. In our study and others [37, 60], T cells were observed near blood vessels and in pseudocapsular and periprosthetic tissues associated with macrophages. Importantly, metal wear particles were not observed in patient tissues to account for the presence of T cells. Although animal models have shown T cells are dispensable in the development of osteolysis [44-46], a recent in vitro study showed depletion of T cells or the addition of RANK-Fc to human peripheral blood cell cultures equally reduced osteoclast formation in response to RANKL [35]. Additionally, the current findings and those of others [5, 37] support the potential involvement of T cells in human osteolytic responses after recruitment by chemotactic factors released from activated macrophages [2, 53, 60, 61].

For individual image comparisons, the effect of cellular chemotaxis may be the predominant reason for the lack of correlations between immune cells and polyethylene wear debris. In a recent article by Goodman et al., (2010), both local and systemic recruitment of inflammatory cells in response to wear debris is considered to be a paramount component in the development of a progressive biological response leading to osteolysis [62]. Importantly, as shown in Figure 3-4, increased numbers of particles and relatively low numbers of cells for an individual

image would not be explained by the resolution limit of light microscopy. Rather, it is more likely that the accumulation of polyethylene wear debris results in the formation of a cell transport gradient modulated by chemotactic cytokines (i.e. – MCP-1, MIP-1α, IL-8, IP-10, etc), which could contribute to cellular recruitment in neighboring tissue regions.

In agreement with other reports, distinct regional and patient differences in the immune cell responses were observed [37, 42, 56, 59] along with a corresponding heterogeneity in polyethylene particle number. The accumulation of polyethylene wear debris in periprosthetic tissue may depend on several factors, other than their rate of production, including tissue morphology, particle size, and particle migration [42, 63-65]. In general, wear debris was observed predominantly in periprosthetic tissues removed from the bone–implant interface. Similar to a previous study of two patient tissues from revised HXLPE liners, macrophages, lymphocytes, and polyethylene wear debris were infrequently observed [66]. However, immunohistochemistry was not performed to quantify individual cell types or evaluate co-localization of the inflammatory response with wear debris. Using this approach, the magnitudes of macrophage and T cell responses were moderately correlated for each of the nine patients and combined regions. The limited number of wear particles found in their study [66] and in the current study may represent the greater potential for smaller particles to migrate away from the implant site. Alternatively, or in addition, nanometer-sized polyethylene particles may be present and undetected as even a small wear volume would generate large

numbers of predominantly submicron-sized particles [10, 17, 67]. The regional and patient differences in the number of macrophages and T cells are supported by previous investigations of immune cells and cytokines in tissues from loosened conventional polyethylene prostheses [20, 42, 55]. In agreement with prior immunohistochemical [37, 52-54, 56, 57, 59] or histologic [31, 66] studies, the predominant cells in both cohorts were macrophages and T cells. The contribution of neutrophils was negligible, and even the largest neutrophil infiltration (8.4/mm^2; Table 3-2 and Table 3-4) represented only a fraction of what would be considered evidence of subclinical infection [68-71]. A detailed assessment of polyethylene wear debris and immune cells was performed to compare the inflammatory response in revision tissues from CPE implants revised for osteolysis and loosening and HXLPE implants revised for loosening in the absence of radiographic osteolysis. Taken together, these results suggest the release of pro-inflammatory factors by activated macrophages may contribute to the recruitment of macrophages and/or T cells, activation of osteoclasts, and osteolysis [5, 29, 33, 72, 73]. Alternatively, or in addition, it is possible submicron-sized particles induce poor osseo-integration by directly inhibiting osteoblast viability and proliferation [74, 75]. Based on radiograph information alone, it is impossible to distinguish between implant loosening attributable to poor osseo-integration and linear osteolysis. Furthermore, most cases of radiographic osteolysis are observed only after long-term (>5 years) implantation as originally determined for CPE implants [11, 76, 77]. Among the existing theories of factors that contribute to aseptic loosening, the current chapter represents the first indication that the presence of wear debris and inflammation in

HXLPE revision tissues, separately or in conjunction with osteoblast apoptosis, mechanical, and/or genetic factors [43, 74, 78-83], may contribute to early implant loosening. The following chapter (Chapter 4) investigates the influence of regional component surface damage on the characteristics of polyethylene wear debris. Subsequently, the full range of polyethylene wear particle characteristics are provided for first-generation remelted and annealed HXLPE cohorts in Chapter 5.

Acknowledgements

Special thanks to Daniel Martinez and the supporting staff of the Pathology Core Laboratories at the University of Pennsylvania.

References

1. Kurtz, S.M., et al., *Reasons for Revision of First-Generation Highly Cross-Linked Polyethylenes.* Journal of Arthroplasty, 2010.
2. Revell, P.A., *The combined role of wear particles, macrophages and lymphocytes in the loosening of total joint prostheses.* J R Soc Interface, 2008. 5(28): p. 1263-78.
3. Ulrich, S.D., et al., *Total hip arthroplasties: what are the reasons for revision?* Int Orthop, 2008. 32(5): p. 597-604.
4. Goodman, S.B., *Wear particles, periprosthetic osteolysis and the immune system.* Biomaterials, 2007. 28(34): p. 5044-8.
5. Purdue, P.E., et al., *The cellular and molecular biology of periprosthetic osteolysis.* Clin Orthop Relat Res, 2007. 454: p. 251-61.
6. Harris, W.H. and O.K. Muratoglu, *A review of current cross-linked polyethylenes used in total joint arthroplasty.* Clinical Orthopaedics & Related Research, 2005(430): p. 46-52.
7. Kurtz, S.M., *The UHMWPE Biomaterials Handbook: Ultra-High Molecular Weight Polyethylene in Total Joint Replacement and Medical Devices*. 2nd Edition ed. 2009, Burlington, MA Academic Press.
8. McKellop, H., et al., *Development of an extremely wear-resistant ultra high molecular weight polyethylene for total hip replacements.* J Orthop Res, 1999. 17(2): p. 157-67.
9. Muratoglu, O.K., et al., *A novel method of cross-linking ultra-high-molecular-weight polyethylene to improve wear, reduce oxidation, and retain mechanical*

properties. Recipient of the 1999 HAP Paul Award. J Arthroplasty, 2001. 2001: p. 149-160.

10. Jacobs, C.A., et al., *Clinical performance of highly cross-linked polyethylenes in total hip arthroplasty.* Journal of Bone & Joint Surgery - American Volume, 2007. 89(12): p. 2779-86.
11. Mall, N.A., et al., *The Incidence of Acetabular Osteolysis in Young Patients With Conventional versus Highly Crosslinked Polyethylene.* Clin Orthop Relat Res, 2010.
12. Olyslaegers, C., et al., *Wear in conventional and highly cross-linked polyethylene cups: a 5-year follow-up study.* Journal of Arthroplasty, 2008. 23(4): p. 489-94.
13. Kurtz, S.M., H.A. Gawel, and J. Patel, *History and Systematic Review of Wear and Osteolysis Outcomes for First-Generation Highly Crosslinked Polyethylene.* Clin Orthop Relat Res, 2011. Epub Mar 23.
14. Bradford, L., et al., *Wear and surface cracking in early retrieved highly cross-linked polyethylene acetabular liners.* Journal of Bone & Joint Surgery - American Volume, 2004. 86-A(6): p. 1271-82.
15. Minoda, Y., et al., *Wear particle analysis of highly crosslinked polyethylene isolated from a failed total hip arthroplasty.* Journal of Biomedical Materials Research, 2008. Part B, Applied Biomaterials. 86B(2): p. 501-5.
16. Purdue, P.E., et al., *The central role of wear debris in periprosthetic osteolysis.* Hss J, 2006. 2(2): p. 102-13.
17. Ries, M.D., M.L. Scott, and S. Jani, *Relationship between gravimetric wear and particle generation in hip simulators: conventional compared with cross-linked polyethylene.* Journal of Bone & Joint Surgery - American Volume, 2001. 83-A Suppl 2 Pt 2: p. 116-22.
18. Green, T.R., et al., *Polyethylene particles of a 'critical size' are necessary for the induction of cytokines by macrophages in vitro.* Biomaterials, 1998. 19(24): p. 2297-302.
19. Kobayashi, A., et al., *Number of polyethylene particles and osteolysis in total joint replacements. A quantitative study using a tissue-digestion method.* Journal of Bone & Joint Surgery - British Volume, 1997. 79(5): p. 844-8.
20. Shanbhag, A.S., et al., *Quantitative analysis of ultrahigh molecular weight polyethylene (UHMWPE) wear debris associated with total knee replacements.* J Biomed Mater Res, 2000. 53(1): p. 100-10.
21. Tipper, J.L., et al., *Isolation and characterization of UHMWPE wear particles down to ten nanometers in size from in vitro hip and knee joint simulators.* J Biomed Mater Res A, 2006. 78(3): p. 473-80.
22. Greenfield, E.M., et al., *The role of osteoclast differentiation in aseptic loosening.* Journal of Orthopaedic Research, 2002. 20(1): p. 1-8.
23. Haynes, D.R., et al., *The osteoclastogenic molecules RANKL and RANK are associated with periprosthetic osteolysis.* J Bone Joint Surg Br, 2001. 83(6): p. 902-11.
24. Sabokbar, A., et al., *Human arthroplasty derived macrophages differentiate into osteoclastic bone resorbing cells.* Ann Rheum Dis, 1997. 56(7): p. 414-20.

25. Abu-Amer, Y., I. Darwech, and J.C. Clohisy, *Aseptic loosening of total joint replacements: mechanisms underlying osteolysis and potential therapies.* Arthritis Res Ther, 2007. 9 Suppl 1: p. S6.
26. Goldring, S.R., C.R. Clark, and T.M. Wright, *The problem in total joint arthroplasty: aseptic loosening.* Journal of Bone & Joint Surgery - American Volume, 1993. 75(6): p. 799-801.
27. Goodman, S.B., *Wear particulate and osteolysis.* Orthop Clin North Am, 2005. 36(1): p. 41-8.
28. Looney, R.J., et al., *Periprosthetic osteolysis: an immunologist's update.* Curr Opin Rheumatol, 2006. 18(1): p. 80-7.
29. Ingham, E. and J. Fisher, *The role of macrophages in osteolysis of total joint replacement.* Biomaterials, 2005. 26(11): p. 1271-86.
30. Ren, W.P., et al., *Association between UHMWPE particle-induced inflammatory osteoclastogenesis and expression of RANKL, VEGF, and Flt-1 in vivo.* Biomaterials, 2006. 27(30): p. 5161-9.
31. Pandey, R., A.R. Berendt, and N.A. Athanasou, *Histological and microbiological findings in non-infected and infected revision arthroplasty tissues. The OSIRIS Collaborative Study Group. Oxford Skeletal Infection Research and Intervention Service.* Arch Orthop Trauma Surg, 2000. 120(10): p. 570-4.
32. Frost, S., et al., *The Role of Regulatory T Cells in Periprosthetic Osteolysis Following Primary Total Hip Arthroplasty.* J Bone Joint Surg Br, 2008. 90(Supplement 1): p. 38.
33. Boyle, W.J., W.S. Simonet, and D.L. Lacey, *Osteoclast differentiation and activation.* Nature, 2003. 423(6937): p. 337-42.
34. Gehrke, T., et al., *Receptor activator of nuclear factor kappaB ligand is expressed in resident and inflammatory cells in aseptic and septic prosthesis loosening.* Scand J Rheumatol, 2003. 32(5): p. 287-94.
35. Roato, I., et al., *Osteoclastogenesis in peripheral blood mononuclear cell cultures of periprosthetic osteolysis patients and the phenotype of T cells localized in periprosthetic tissues.* Biomaterials, 2010. 31(29): p. 7519-25.
36. Li, T.F., et al., *No lymphokines in T-cells around loosened hip prostheses.* Acta Orthop Scand, 2001. 72(3): p. 241-7.
37. Goodman, S.B., et al., *Cellular profile and cytokine production at prosthetic interfaces. Study of tissues retrieved from revised hip and knee replacements.* J Bone Joint Surg Br, 1998. 80(3): p. 531-9.
38. Davies, A.P., et al., *An unusual lymphocytic perivascular infiltration in tissues around contemporary metal-on-metal joint replacements.* Journal of Bone & Joint Surgery - American Volume, 2005. 87(1): p. 18-27.
39. Mahendra, G., et al., *Necrotic and inflammatory changes in metal-on-metal resurfacing hip arthroplasties.* Acta Orthop, 2009. 80(6): p. 653-9.
40. Park, Y.-S., et al., *Early osteolysis following second-generation metal-on-metal hip replacement.* Journal of Bone & Joint Surgery - American Volume, 2005. 87(7): p. 1515-21.

41. Willert, H.G., et al., *Metal-on-metal bearings and hypersensitivity in patients with artificial hip joints. A clinical and histomorphological study.* Journal of Bone & Joint Surgery - American Volume, 2005. 87(1): p. 28-36.
42. Baxter, R.M., et al., *Distinct immunohistomorphologic changes in periprosthetic hip tissues from historical and highly crosslinked UHMWPE implant retrievals.* J Biomed Mater Res A, 2010. 95(1): p. 68-78.
43. Sundfeldt, M., et al., *Aseptic loosening, not only a question of wear: a review of different theories.* Acta Orthop, 2006. 77(2): p. 177-97.
44. Goodman, S., et al., *T-lymphocytes are not necessary for particulate polyethylene-induced macrophage recruitment. Histologic studies of the rat tibia.* Acta Orthop Scand, 1994. 65(2): p. 157-60.
45. Jiranek, W., et al., *Tissue response to particulate polymethylmethacrylate in mice with various immune deficiencies.* Journal of Bone & Joint Surgery - American Volume, 1995. 77(11): p. 1650-61.
46. Taki, N., et al., *Polyethylene and titanium particles induce osteolysis by similar, lymphocyte-independent, mechanisms.* Journal of Orthopaedic Research, 2005. 23(2): p. 376-83.
47. Chen, P.Y. and P.M. Popovich, *Correlation: Parametric and Nonparametric Measures*. Quantitative Applications in the Social Sciences. 2002, Thousand Oaks, California: Sage Publications, Inc.
48. Saikko, V., O. Calonius, and J. Keranen, *Wear of conventional and cross-linked ultra-high-molecular-weight polyethylene acetabular cups against polished and roughened CoCr femoral heads in a biaxial hip simulator.* J Biomed Mater Res, 2002. 63(6): p. 848-53.
49. Williams, P.A., et al., *Highly Crosslinked Polyethylenes in Hip Replacements: Improved Wear Performance of Paradox?* STLE Tribology Transactions, 2007. 50(2): p. 227-290.
50. Endo, M., et al., *Comparison of wear, wear debris and functional biological activity of moderately crosslinked and non-crosslinked polyethylenes in hip prostheses.* Proc IME HJ Eng Med, 2002. 216(2): p. 111-22.
51. Yamamoto, K., et al., *Microwear phenomena of ultrahigh molecular weight polyethylene cups and debris morphology related to gamma radiation dose in simulator study.* Journal of Biomedical Materials Research, 2001. 56(1): p. 65-73.
52. Arora, A., et al., *The role of the TH1 and TH2 immune responses in loosening and osteolysis of cemented total hip replacements.* Journal of Biomedical Materials Research, 2003. Part A. 64(4): p. 693-7.
53. Baldwin, L., et al., *A study of tissue interface membranes from revision accord knee arthroplasty: the role of T lymphocytes.* Biomaterials, 2002. 23(14): p. 3007-14.
54. Chun, L., et al., *The Characterization of Macrophages and Osteoclasts in Tissues Harvested from Revised Total Hip Prostheses.* J Biomed Mater Res, Part B, 1999. 48: p. 5.

55. Goodman, S.B., et al., *Heterogeneity in cellular and cytokine profiles from multiple samples of tissue surrounding revised hip prostheses.* J Biomed Mater Res, 1996. 31(3): p. 421-8.
56. Jones, L., C. Frondoza, and D. Hungerford, *Immunohistochemical Evaluation of Interface Membranes from Failed Cemented and Uncemented Acetabular Components.* J Biomed Mater Res, Part B, 1999. 48: p. 889-898.
57. Kim, K.J., J. Chiba, and H.E. Rubash, *In vivo and in vitro analysis of membranes from hip prostheses inserted without cement.* Journal of Bone & Joint Surgery - American Volume, 1994. 76(2): p. 172-80.
58. Maitra, R., et al., *Immunogenecity of modified alkane polymers is mediated through TLR1/2 activation.* PLoS One, 2008. 3(6): p. e2438.
59. Ito, S., et al., *Histological analysis and biological effects of granulation tissue around loosened hip prostheses in the development of osteolysis.* J Orthop Sci, 2004. 9: p. 478–487.
60. Sandhu, J., et al., *The role of T cells in polyethylene particulate induced inflammation.* J Rheumatol, 1998. 25(9): p. 1794-9.
61. Gallo, J., et al., *Particle disease. A comprehensive theory of periprosthetic osteolysis: a review.* Biomedical Papers of the Medical Faculty of Palacky University in Olomouc, Czech Republic, 2002. 146(2): p. 21-8.
62. Goodman, S.B. and T. Ma, *Cellular chemotaxis induced by wear particles from joint replacements.* Biomaterials, 2010. 31(19): p. 5045-50.
63. Basle, M.F., et al., *Migration of metal and polyethylene particles from articular prostheses may generate lymphadenopathy with histiocytosis.* J Biomed Mater Res, 1996. 30(2): p. 157-63.
64. Elfick, A.P.D., et al., *The nature and dissemination of UHMWPE wear debris retrieved from periprosthetic tissue of THR.* J. Viomws. Mater. Res., 2003. 65A: p. 95-108.
65. Urban, R.M., et al., *Dissemination of wear particles to the liver, spleen, and abdominal lymph nodes of patients with hip or knee replacement.[see comment].* Journal of Bone & Joint Surgery - American Volume, 2000. 82(4): p. 457-76.
66. Knahr, K., et al., *Retrieval analyses of highly cross-linked polyethylene acetabular liners four and five years after implantation.[erratum appears in J Bone Joint Surg Br. 2008 Apr;90(4):543].* Journal of Bone & Joint Surgery - British Volume, 2007. 89(8): p. 1036-41.
67. Jacobs, J.J., et al., *How has the biologic reaction to wear particles changed with newer bearing surfaces?* Journal of the American Academy of Orthopaedic Surgeons, 2008. 16 Suppl 1: p. S49-55.
68. Athanasou, N.A., et al., *Diagnosis of infection by frozen section during revision arthroplasty.* J Bone Joint Surg Br, 1995. 77: p. 28-33.
69. Bauer, T.W., et al., *Diagnosis of periprosthetic infection.* J Bone Joint Surg Am, 2006. 88(4): p. 869-82.
70. Feldman, D.S., et al., *The role of intraoperative frozen sections in revision total joint arthroplasty.* Journal of Bone & Joint Surgery - American Volume, 1995. 77(12): p. 1807-13.

71. Mirra, J.M., R.A. Marder, and H.C. Amstutz, *The pathology of failed total joint arthroplasty.* Clin Orthop Relat Res, 1982(170): p. 175-83.
72. Altaf, H., *The inflammatory response to particlulate wear debris in the context of total hip replacement*. 2007 University of London.
73. Hercus, B. and P.A. Revell, *Phenotypic characteristics of T lymphocytes in the interfacial tissue of aseptically loosened prosthetic joints.* J Mater Sci Mater Med, 2001. 12(10-12): p. 1063-7.
74. Dean, D.D., et al., *The effect of ultra-high molecular weight polyethylene wear debris on MG63 osteosarcoma cells in vitro.* J Bone Joint Surg Am, 1999. 81(4): p. 452-61.
75. Lohmann, C., et al., *Phagocytosis of wear debris by osteoblasts affects differentiation and local factor production in a manner dependent on particle composition.* Biomaterials, 2000. 21: p. 551-561.
76. Beksac, B., et al., *Wear is reduced in THA performed with highly cross-linked polyethylene.* Clin Orthop Relat Res, 2009. 467(7): p. 1765-72.
77. Geerdink, C.H., et al., *Crosslinked polyethylene compared to conventional polyethylene in total hip replacement: pre-clinical evaluation, in-vitro testing and prospective clinical follow-up study.* Acta Orthopaedica, 2006. 77(5): p. 719-25.
78. Gallo, J., F. Mrazek, and M. Petrek, *Variation in cytokine genes can contribute to severity of acetabular osteolysis and risk for revision in patients with ABG 1 total hip arthroplasty: a genetic association study.* BMC Med Genet, 2009. 10: p. 109-19.
79. Gallo, J., et al., *Bone remodeling, particle disease and individual susceptibility to periprosthetic osteolysis.* Physiol Res, 2008. 57(3): p. 339-49.
80. Lohmann, C.H., et al., *Nitric oxide and prostaglandin E2 production in response to ultra-high molecular weight polyethylene particles depends on osteoblast maturation state.* Journal of Bone & Joint Surgery - American Volume, 2002. 84-A(3): p. 411-9.
81. Malik, M.H., et al., *Genetic susceptibility to total hip arthroplasty failure--positive association with mannose-binding lectin.* Journal of Arthroplasty, 2007. 22(2): p. 265-70.
82. Malik, M.H., et al., *Genetic susceptibility to hip arthroplasty failure--association with the RANK/OPG pathway.* Int Orthop, 2006. 30(3): p. 177-81.
83. Malik, M.H.A., et al., *Genetic susceptibility to total hip arthroplasty failure: a preliminary study on the influence of matrix metalloproteinase 1, interleukin 6 polymorphisms and vitamin D receptor.* Annals of the Rheumatic Diseases, 2007. 66(8): p. 1116-20.

4. Relationship Between Implant Wear Modes and Biological Activity of Polyethylene Wear Debris From Revised Total Disc Replacements[4]

Abstract

Wear, oxidation and particularly rim impingement damage have been observed following revision surgery of ultra-high molecular weight polyethylene (polyethylene) total disc replacement (TDR) components. However, neither *in vitro* testing nor retrieval-based evidence has shown the effect(s) of impingement on the characteristics of polyethylene wear debris. The current study was performed to determine differences in polyethylene particle size, shape, number or biological activity that correspond to intermittent (mild) or chronic (severe) rim impingement. In addition, for all TDRs regardless of impingement classification, potential correlations between the extent of regional damage and the characteristics of polyethylene wear debris were investigated. The extent of dome and rim damage was characterized for 11 retrieved polyethylene cores obtained at revision surgery after an average implantation of 9.7 years (range: 4.6-16.1 years). Polyethylene wear debris were isolated from corresponding periprosthetic tissues using nitric acid and imaged using ESEM. Subsequently, particle size, shape, number and biological activity were determined. Separation of particles by size ranges that represent high (<0.1-1 μm), intermediate (1-10 μm) and low (>10 μm) biological

---

[4] Baxter RM, MacDonald DW, Kurtz SM, Steinbeck MJ. Chronic Impingement of Lumbar Disc Arthroplasty Increases the Functional Biologic Activity of Polyethylene Wear Debris. JBJS. 2011 *In Review.*

relevance revealed an increased number of particles in the 1-10 μm size range and larger particles in the >10 μm size range for the chronic impingement group. For TDRs with intermittent impingement, the specific biological activity (SBA) per unit particle volume was increased in the <0.1-1 and 1-10 μm size ranges; whereas, in the chronic impingement group the >10 μm size range was increased. In contrast, when SBA was normalized by polyethylene particle volume (mm^3)/gram tissue, functional biological activity (FBA) of the chronic impingement group was increased in the >10 μm range and for the cumulative value of all three size ranges. For all TDRs, the extent of rim penetration positively correlated with increasing particle size (ρ=0.68), number (ρ=0.72) and FBA (ρ=0.75). The results of this study suggest that chronic rim impingement increases the production of biologically relevant polyethylene particles from mobile-bearing lumbar TDR components. *In vitro* test methods to simulate this unintended wear mode are warranted. In addition, these data highlight the potential clinical implications for the development of impingement in other total joint replacement components.

Introduction

For patients who suffer from degenerative disc disease, lumbar fusion of the affected vertebral segment has been the standard treatment of care. However, studies have shown that fusion of a single level results in an accelerated rate of degeneration in adjacent discs and vertebral levels due to altered biomechanics [1, 2]. Alternatively, total disc replacement (TDR) achieves both a resolution of pain and preserves the motion segment of the functional spine unit, and thus, represents

an appealing surgical alternative [3, 4]. Two lumbar TDR devices have been approved for use in the United States. The SB Charité III (Link/DePuy, Germany/USA), the first FDA-approved TDR device in the U.S., includes an ultra-high molecular weight polyethylene (UHMWPE) core articulating between two cobalt chromium (CoCr) endplates [5]. Currently, the short- and mid-term clinical results of the Charité TDR are at least equivalent to the clinical outcomes of lumbar interbody fusion, with a success rate of 65.2% and 57.8% at two and five years follow-up, respectively [3, 6-8]. Nevertheless, as several studies have identified a low quality of evidence supporting the efficiency of TDR over fusion, the long-term effectiveness of this relatively new medical device compared to lumbar fusion remains unclear [9-11].

Similar to larger joint replacement technologies in the hip and knee, motion-preserving TDRs are prone to generate wear debris during a patient's daily activities [12-18]. However, until recently the role of polyethylene wear debris as a limiting factor in the longevity of TDRs was limited to a few case studies [19-21]. Initially, it was thought that the generation of substantial amounts of polyethylene wear debris in the spine was unlikely due to a limited range of motion and the absence of a synovial joint [5, 22]. These views were based on an *in vitro* study of Serhan et al. [22], showing only minimal wear debris generation after 10 million cycles. However, in a recent immunohistological study by Punt et al., (2009), the concomitant presence of polyethylene particles ($\geq$2 μm), phagocytic cells and pro-inflammatory cytokines was identified in periprosthetic tissues around retrieved TDRs [13].

Interestingly, while osteolysis and loosening represent the most frequent reason for revision surgery of THA and TKA implants [23-27], the development of osteolysis around TDRs is rarely observed [20, 22, 28]. Thus, the clinical implications of polyethylene wear debris and the development of inflammation in tissues around the spine are still poorly understood [10, 13, 29].

Recently, TDR retrieval studies have also identified impingement patterns on the mobile-bearing polyethylene core [21, 30-33]. To date, these findings suggest that the kinematics of the superior bearing surface causes the core to become locked, resulting in an accumulation of rim damage, radial cracking and, in severe cases, rim fracture [12, 20, 30]. The effects of impingement have been addressed by numerous studies of revised artificial hip, knee and shoulder components [34-39]. Specifically, malfunctioning metal-on-metal [40-44] and ceramic-on-ceramic hip bearings [45-50], as well as rim fracture of highly-crosslinked polyethylene liners [51, 52] have been considered in the context of impingement.

Although the body of evidence implicating impingement as a clinical concern in TDR continues to expand, the extent to which impingement affects the production of polyethylene particles currently remains unanswered. Thus, the current study was performed to determine the characteristics of wear debris generated from mobile-bearing TDRs. Specifically, differences in polyethylene particle size, shape, number and biological activity were evaluated between two groups of TDRs with intermittent (mild) or chronic (severe). Lastly, for all TDRs regardless of impingement classification, correlations between the extent of regional damage and

the characteristics of polyethylene wear debris were investigated. This study tested the hypothesis that polyethylene components exhibiting chronic impingement would generate particles with increased biological activity.

Methods

Patient Selection

Forty-eight (48) SB Charité III total disc replacements were retrieved and analyzed during revision surgery between 2002 and 2008. The clinical information, oxidative properties and surface damage were previously published for a cohort of 48 revised TDR components [12, 53]. Of these 48 components, the current chapter evaluated 11 that were revised with periprosthetic tissue samples. For these patients, revision was indicated after an average of 9.7 years (range 4.6-16.1 years) due to persistent back and leg pain, and one patient was revised for osteolysis (Table 4-1). To confirm that the subset of TDRs was representative of the published collection, measurements of surface damage (Table 4-4) or oxidation (Table 4-5) were compared against all 48 TDRs, and no significant differences were observed. In addition, the frequency of retrieved components exhibiting chronic impingement (severe rim damage; 7/11 TDRs with tissues, 37/48 TDRs overall) was consistently higher than intermittent impingement (mild rim damage; 4/11 TDRs with tissues, 10/48 TDRs overall)(Figure 4-11). Although the TDR revised for osteolysis exhibited signs of chronic impingement, data from this patient were considered separately to eliminate this potential confounding patient variable.

Table 4-1. Summary of Clinical information (sorted by increasing implantation time within each impingement classification.

Case	Sample ID	Impingement Classification	Implantation Time (y)	Revision Reason	Level
1	Maa003	Chronic	6.2	Subsidence	L4/L5
2	Maa006	Chronic	6.5	Grossly loose with osteolysis in the sacrum	L5/S1
3	Maa002	Chronic	9.2	Persistent pain low back and both legs; flattening of the PE core; broken metal wire; subsidence	L5/S1
4	Maa018	Chronic	10.6	Persistent lumbar and right leg pain; disc degeneration L3/L4 above a successful posterior fusion L4/S1	L4/L5
5	Maa004	Chronic	12.7	Anterior position of L4/L5 disc	L4/L5
6	Maa013	Chronic	12.8	Instability/retrolisthesis L1/L2, L2/L3; pseudoarthrosis L4/L5; anterior position and possible wear	L3/L4
7	Maa019	Chronic	16.1	Progressive anterior migration; pressure against the aorta; back and leg pain	L4/L5
8	Maa023	Intermittent	4.6	Severe back pain; multiple disc degeneration above prosthesis; lateral displacement of upper endplate	L5/S1
9	Maa010	Intermittent	8.5	Persisting pain after failed posterior fusion	L5/S1
10	Sal007	Intermittent	9.7	Faulty PE	L5/S1
11	Maa009	Intermittent	10.2	Pain due to severe facet joint degeneration L4/L5 and disc degeneration L1/L2 and L3/L4	L4/L5

Notes: L, lumbar vertebra

Wear Particle Analysis Protocol

Wear Particle Isolation

At the time of surgery, tissue samples were fixed in 10% phosphate buffered formalin and the bone tissue was subsequently decalcified. During decalcification, the specimens were kept in a 3.5% sodium formate and 25% formic acid solution, until they were soft enough and could be embedded in paraffin. Wear particle

isolation was performed using methods modified from Margevicius et al., (1994) [54]. One or more small areas of the tissue were removed from the paraffin block. To remove paraffin, the tissue was placed in 10 ml xylene overnight at room temperature and then washed twice in xylene and twice in 100% ethanol for three minutes each. After drying for two hours, 0.02-0.03 grams of tissue were placed in a polypropylene tube and digested in 5 ml 65% HNO_3 at room temperature. After the first 24 hours, the tubes were agitated and left to digest for an additional 24 hours.

Following digestion, the solutions containing polyethylene wear debris were thoroughly mixed with a G560 vortex (Scientific Industries, Bohemia, NY) for three 30-second intervals. Finally, the tubes were placed in an ultrasonic bath (Cole-Parmer, Vernon Hills, Illinois) for two minutes to achieve uniform dispersion. Subsequently, the sample was vacuum-filtered through a polycarbonate membrane with a pore size of 1.0 μm (Whatman, Billerica, MA) and the filtrate containing submicron particles was collected and saved. After filtration, the membrane was washed with 10 ml of fresh 65% HNO_3, which was added to the membrane surface for 10 minutes and subsequently pulled through by a vacuum. Finally, using a separate side-arm flask, this washing process was repeated with methanol. To prevent particle agglomeration, the filtrate containing submicron particles was diluted with 15 ml of methanol containing 2% Nonidet P-40® (NP40 substitute) (AppliChem GmbH, Darmstadt, Germany), a non-ionic surfactant. The solution containing surfactant was mixed with a vortex for three 30-second intervals, and subsequently placed in an ultrasonic bath for two minutes to achieve uniform

particle dispersion and to further reduce agglomeration. After sonication, samples were immediately filtered through a membrane with a pore size of 0.05 μm. As with the first membrane, the second polycarbonate membrane was sequentially washed with 10 ml solutions of 65% HNO_3 followed by methanol, which were again collected in separate sidearm flasks. Based on the thorough digestion of small quantities of tissue selected, centrifugation steps were not employed during wear particle isolation; however, this practice may require modification for larger tissue samples. Each membrane was then dried for 2 hours at room temperature, and prepared for scanning electron microscopy.

Imaging

Polycarbonate membranes with isolated polyethylene wear debris were fixed onto aluminum stubs with double-sided carbon tape, and sputter coated with a 5-nm-thick layer of platinum/palladium using a 208 HR vacuum sputter coater (Cressington, Watford, England) in order to eliminate sample drift and/or damage by the electron beam at high magnifications (Figure 4-1) [55].

Figure 4-1. 208HR High Resolution Cressington Sputter Coater

Polyethylene wear debris was visualized using a XL30 environmental scanning electron microscope (FEI/Phillips, Hillsboro, OR) equipped with a Schottky field-emission gun (Figure 4-2). Imaging was performed at a working distance of 12 mm and a beam intensity of 5kV. All sample preparation and imaging were performed in the Drexel University Centralized Research Facilities.

Figure 4-2. XL30 environmental scanning electron microscope (FEI/Phillips, Hillsboro, OR).

Membranes with a pore size of 1.0 μm were imaged at magnifications of 500X and 1,000X; five and 10 images were collected, respectively. Polycarbonate membranes with a pore size of 0.05 μm were imaged at a magnification of 12,000X; 10 images were collected from three separate regions. A minimum of 1000 particles was characterized from each patient.

Wear Particle Analysis

Image analysis of ESEM micrographs was initially performed using a gray-scale level threshold in Adobe Photoshop (San Jose, CA). After analysis of the histogram, the threshold (grayscale value) corresponding to the right side of the main peak was chosen for all images. Subsequently, using a scale bar from each micrograph, the individual particle areas and dimensions were determined using a custom macro in NIH ImageJ (National Institutes of Health, USA) (Appendix II). The resulting areas and dimensions were used to characterize particle number, size (equivalent circular diameter, ECD) (Equation 1) and shape (aspect ratio, AR (Equation 2); roundness, R (Equation 3); form factor, FF (Equation 4)) based on guidelines for wear particle analysis outlined in ASTM F1877 [56].

$$ECD = \sqrt{\frac{4 \bullet A_P}{\pi}}$$

Equation 1. Equivalent circular diameter, ECD (μm), where A_P represents particle area. ECD is a measure of size represented by the diameter of a circle with an area that is equivalent to the particle area [56].

$$AR = \frac{L_P}{W_P}$$

Equation 2. Aspect ratio, AR (unitless), where L_P represents particle length and W_P represents particle breadth. AR is a measure of particle shape determined by the ratio of particle length to particle breadth, and has a minimum value of 1 [56].

$$R = \frac{4 \bullet A_P}{\pi \bullet (L_P)^2}$$

Equation 3. Roundness, R (unitless), where A_P represents particle area and L_P represents particle length. R is a measure of circularity ranging from 0 to 1, and is based on particle length [56].

$$FF = \frac{4 \bullet \pi \bullet A_P}{(\text{perimeter})^2}$$

Equation 4. Form factor, FF (unitless), where A_P represents particle area. FF is a measure of circularity ranging from 0 to 1, and is based on particle perimeter [56].

To determine particle number per gram of tissue, representative images were collected from a set of images that went from the center to the edge of the filter. To determine particle number per gram of tissue, the number of imaged particles was scaled by the total filter area and by the initial tissue weight (Equation 5).

$$N_P = N_I \bullet (A_F/A_I)/W_T$$

Equation 5. Particle Number (per gram of tissue), where N_I represents the number of particles imaged, A_F represents the total area of the filter, A_I represents the imaged area of the filter and W_T represents the starting tissue weight. Imaged area was determined separately for each magnification.

To characterize particle biological activity, the current study utilized equations originally developed by Fisher, et al. (2001), which were based on a model of cytokine expression from cultured macrophages in response to varying doses of particle size and volume [57, 58]. The biological activity function, B(r), which separately ranks the biological relevance of particles in <0.1-1, 1-10 and >10 μm size ranges, was assumed to be the same as previously published (Figure 4-3) [57]. *In vitro* scalars were determined by normalizing all three size ranges by the response observed for particles from the <1 μm size range. Results indicated that the biological response initiated by particles in the lowest size range was 5-fold larger than for particles in the 1-10 μm size range and 25-fold larger than for particles the >10 μm size range.

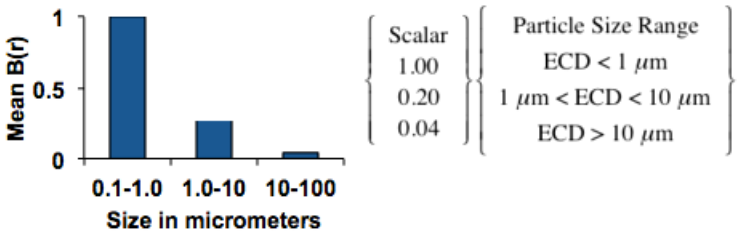

Figure 4-3. Biological activity scalar function, B(r), derived from an *in vitro* study by Fisher et al., (2001) [57].

To determine particle volume in the current study, V_P (Equation 6), calculations were based on the work of Scott, et al. (2005) [59]. Subsequently, the volume of particles within each size range (expressed as a fraction of the total

volume) was used to determine the volume fraction distribution, V(r) for the <1, 1-10 and >10 μm size ranges [57]. Previous studies that used gravimetric filter weights to determine V(r) had the advantage of much larger quantities of wear debris and a controlled environment from which to collect the particulates. In addition, the gravimetric method assumes a constant particle thickness and uses values of weight and polyethylene density to determine volume, which ignores the potential influence of individual particles. For the current study, gravimetric values were considered to be inaccurate given the small initial tissue weights.

$$V_P = \frac{1}{18} \bullet \pi \bullet (ECD)^3$$

Equation 6. Particle volume using an approximation of a prolate ellipsoid.

To determine the specific biological activity per unit volume, (SBA) (Equation 7), the dot-product of $B(r)$ and $V(r)$ was evaluated over each range of particle size. The lowest predicted value of specific biological activity, 0.04, would be obtained if particle volumes were all in the >10 μm size range; whereas, the highest value, 1, would be obtained if particle volumes were all in the <0.1-1 μm size range. Intermediate values would be achieved as the distribution of volume percentage was shared between all three particle size ranges. The dot-product matrix multiplications for determining the range of SBA are shown below in Figure 4-4.

$$SBA = \sum B(r) \bullet V(r)$$

Equation 7. Specific biological activity per unit volume (SBA), determined by the dot-product of biological activity scalars and particle volume fractions of 0.1-1 μm, 1-10 μm and >10 μm size ranges.

$$\begin{matrix} \text{B(r) scalar} & & \text{V(r)} & & \\ \left\{\begin{matrix} 1.00 \\ 0.20 \\ 0.04 \end{matrix}\right\} & \begin{matrix} 0.1-1\mu\text{m} \\ \{0 \end{matrix} & \begin{matrix} 1-10\mu\text{m} \\ 0 \end{matrix} & \begin{matrix} >10\mu\text{m} \\ 1\} \end{matrix} & = (1\bullet 0) + (0.2\bullet 0) + (0.4\bullet 1) \Rightarrow SBA = 0.04 \end{matrix}$$

$$\begin{matrix} & & & & \\ \left\{\begin{matrix} 1.00 \\ 0.20 \\ 0.04 \end{matrix}\right\} & \begin{matrix} 0.1-1\mu\text{m} \\ \{1 \end{matrix} & \begin{matrix} 1-10\mu\text{m} \\ 0 \end{matrix} & \begin{matrix} >10\mu\text{m} \\ 0\} \end{matrix} & = (1\bullet 1) + (0.2\bullet 0) + (0.4\bullet 0) \Rightarrow SBA = 1 \end{matrix}$$

Figure 4-4. Dot-product multiplication showing the representative range of specific biological activity (SBA)

Finally, to determine functional biological activity, FBA, SBA was scaled by the total particle volume (mm^3)/gram of tissue (Equation 8.). *In vitro* studies have previously determined FBA after normalizing by the volume of wear removed from the component. Such studies have the benefit of using a standardized number of cycles; whereas, for retrieval implants the level of patient activity is variable even after normalizing by implantation time. In addition, retrieved components often have some level of iatrogenic damage caused during revision surgery, which is potentially confounding when making determinations of total volume loss from the bearing surface. Other similarities and differences in the determination of particle biological activity are shown in Table 4-2 and Table 4-3.

$$FBA = SBA \bullet \sum V_P$$

Equation 8. Functional biological activity (FBA), determined by the product of SBA and the total particle volume (mm^3) per gram of tissue.

Table 4-2. Summary of variables used to determine particle biological activity showing the overlap with previous *in vitro* studies

Study	B(r)	V_P	V(r)	SBA	FBA
Fisher [57]	Biological Activity Scalars	n/a	Filter weight (gravimetric)	B(r)×V(r)	SBA×Volume (gravimetric)
Galvin [60]	Biological Activity Scalars	n/a	Filter weight (gravimetric)	B(r)×V(r)	SBA×Volume (gravimetric)
Scott [61]	Biological Activity Scalars	Prolate Ellipsoid	Individual Particle Volume	B(r)×V(r)	SBA×Volume (gravimetric)
Bowsher [62]	Biological Activity Scalars	Prolate Ellipsoid	Individual Particle Volume	B(r)×V(r)	SBA×Volume (gravimetric)
Current	Biological Activity Scalars	Prolate Ellipsoid	Individual Particle Volume	B(r)×V(r)	SBA×Volume (per gram of tissue)

Note: The current study was the only one to normalize by particle volume (mm^3) per gram of tissue since other studies were performed *in vitro.*

Table 4-3. Simplified summary of variables used to determine particle biological activity showing the overlap with previous *in vitro* studies

Study	B(r)	V_P	V(r)	SBA	FBA
Fisher [57]	×			×	
Galvin [60]	×			×	
Scott [61]	×	×	×	×	
Bowsher [62]	×	×	×	×	
Current	×	×	×	×	×

Particle Validation

To validate particle isolation techniques, two tissue samples (0.02-0.03 g) from primary spine surgery were selected. Control tissues were processed using the digestion and imaging methods from above. ESEM imaging revealed polycarbonate filters indicative of complete digestion (Figure 4-5).

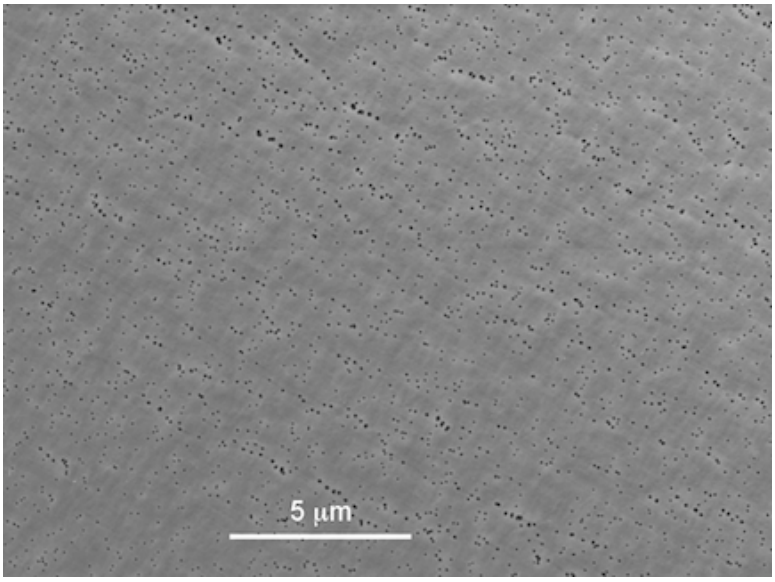

Figure 4-5. Representative micrograph of a polycarbonate filter obtained after digestion of control tissue obtained from primary spine surgery.

Validation of the methods used for determining particle size and morphology were performed using reference standard polyethylene particles (RM8385), which were generated by rubbing a gamma-irradiated polyethylene pin against a textured surface in a reciprocating pin-on-disk system (National Institute of Standards & Technology (NIST), Gaithersburg, MD). Initially, to evaluate the approximation of particle size, a solution containing polyethylene particles with a nominal diameter of 7 μm (from NIST RM8385 Ampoule R2) was vacuum-filtered through a

polycarbonate membrane with a pore size of 1 μm. Particles were analyzed using imaging and image processing methods described above and the obtained values of particle size were then compared to values provided in the reference standard. The mean difference (± standard error) in the frequency distributions of particle size was 1.3 ± 0.4%. Next, to validate the method of determining particle shape, a solution containing polyethylene particles with a nominal aspect ratio of 2.0 (from NIST RM8385 Ampoule E1) was vacuum-filtered through a polycarbonate membrane with a pore size of 1 μm. Particles were analyzed using imaging and image processing methods described above and the obtained values of particle aspect ratio were then compared to values provided in the reference standard. The mean difference (± standard error) in the frequency distributions of particle aspect ratio was 2.9 ± 0.8%.

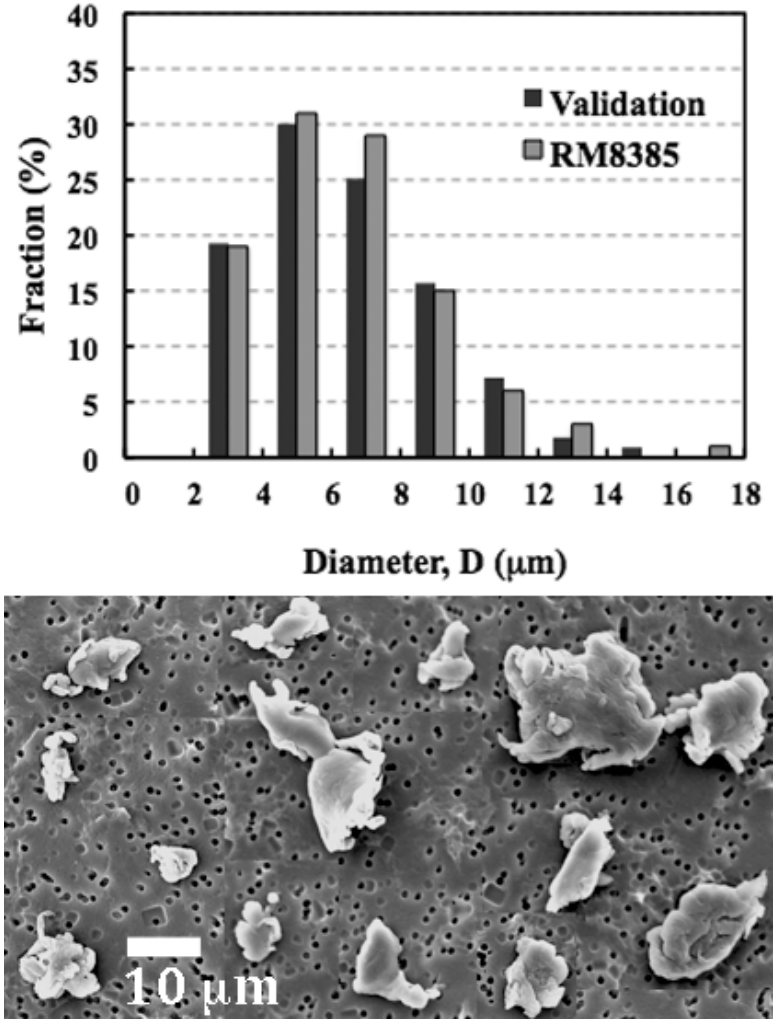

Figure 4-6. Validation of particle size distribution. Diameter was approximated using Equation 1 for equivalent circular diameter. Representative particles from the R2 ampoule in the NIST Traceable Standard (RM8385) are shown below the particle size distributions. The mean difference between frequency distributions of particle size was 1.3 ± 0.4 %.

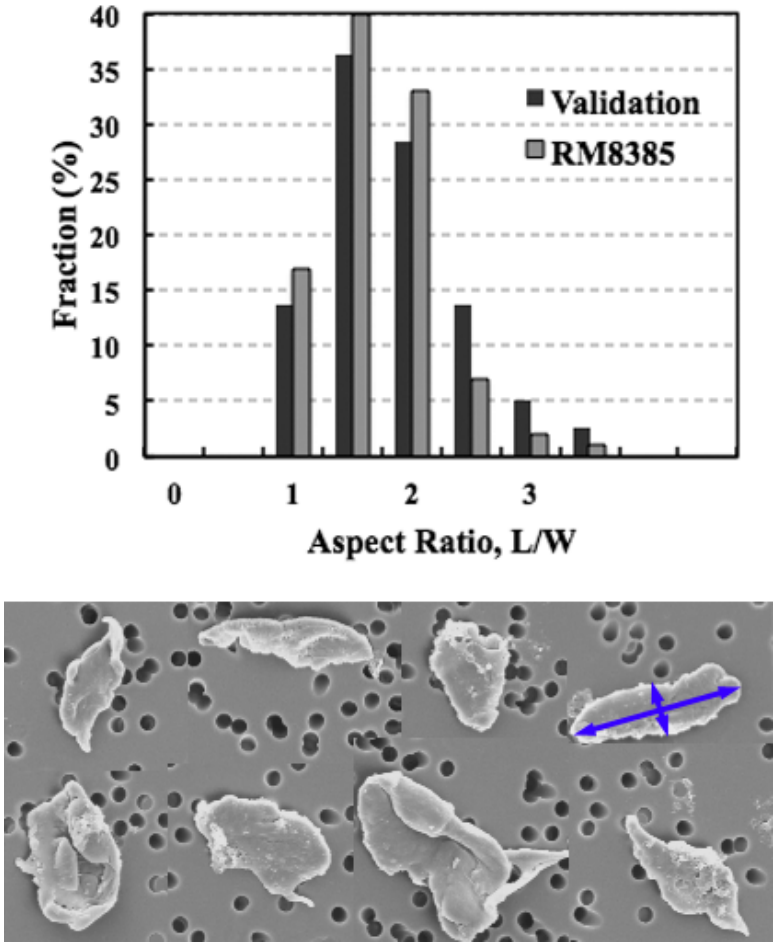

Figure 4-7. Validation of aspect ratio distribution. Representative particles from the E1 ampoule in the NIST Traceable Standard (RM8385) are shown below the aspect ratio distributions. The mean difference between the frequency distributions of aspect ratio was 2.9 ± 0.8%.

To validate the purity of polyethylene particles, multiple regions from polycarbonate membranes of two patients were scanned using Fourier Transform Infrared (FTIR) Spectroscopy (Nicolet/Thermo Fisher Scientific, Waltham, MA) in transmission. Reference spectra were also collected a negative (blank polycarbonate membrane) control. Comparison of the current findings with a previous publication by Lapcikova et al., (2009) reveal complete spectral agreement between absorbance

peaks, and reveal less intermediate noise between these characteristic vibrational peaks [63].

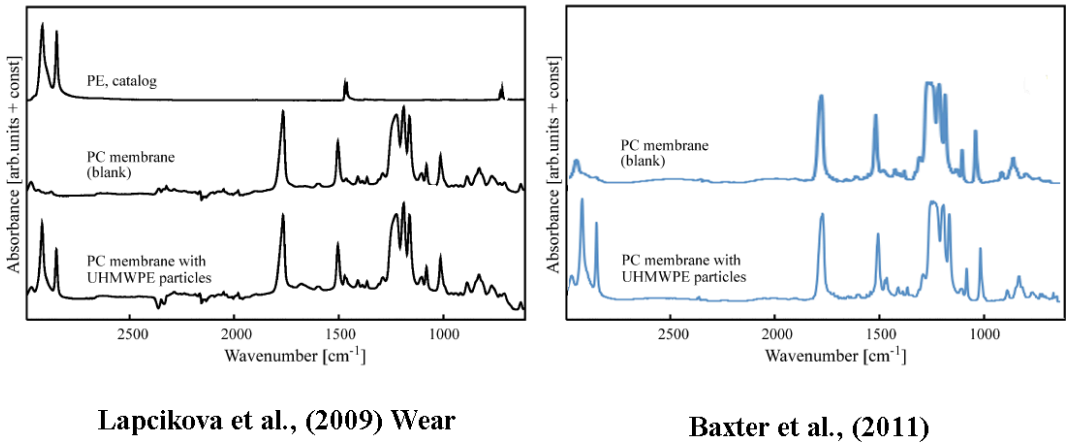

Lapcikova et al., (2009) Wear **Baxter et al., (2011)**

Figure 4-8. Representative spectra from previously published (black lines [63]) and current (blue line) FTIR evaluations of polycarbonate membranes with and without polyethylene wear debris.

Finally, for the calculation of particle number per gram, a scaling factor must be applied to account for the entire filter area. In order to justify the calculation of particle number per gram, the homogeneity of the particle distribution was evaluated along a radius of the polycarbonate filter. The first image was collected from the edge of the filter region that was exposed to particles during filtration. Subsequent images were collected at increments of five fields of view in the direction of the center of the filter. Trends in particle number were not observed based on the outer and inner regions of the filter (R^2=0.0167). Despite random variability, the distribution of particles were predominantly within 1 standard deviation from the mean and all values were within 2 standard deviations from the mean. The farthest value from the mean was observed at the outer-most edge. The

Shapiro-Wilk test was used to confirm the goodness of fit for a normal distribution (P<0.79), which can also be appreciated visually from the graph (Figure 4-9).

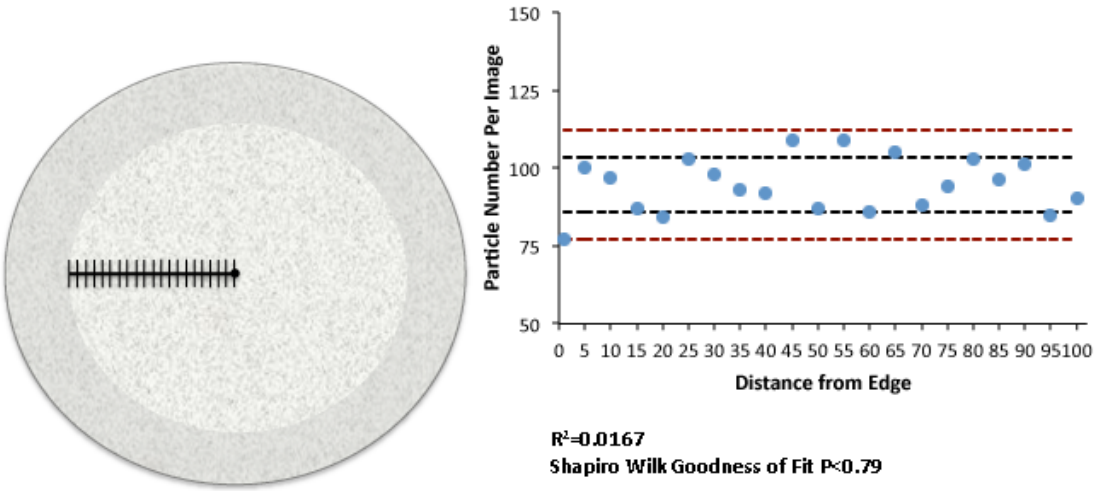

Figure 4-9. Validation of particle homogeneity along the radius of a polycarbonate filter. Black dotted lines represent the values extending 1 standard deviation from the mean; red dotted lines represent values extending 2 standard deviations from the mean. Trends in particle number were not observed between outer and inner regions of the filter. Overall, data were consistent with a normal distribution.

Penetration Analysis

Penetration was assessed at the rim and dome of each component by direct measurement using a calibrated micrometer (accuracy 0.001 mm) (Figure 4-10). The full details of this penetration analysis can be obtained in the original publication by Kurtz et al. (2008)[33]. Regional penetration values from the current cohort of TDRs was representative of the overall published cohort (Table 4-4), and showed increased rim penetration for TDRs with chronic impingement (Figure 4-11).

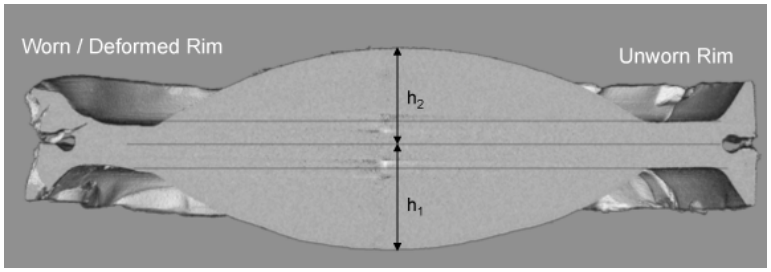

Figure 4-10. Representative cross-section of a mobile-bearing TDR from which maximum measurements of penetration were collected at the dome and the rim [33].

Table 4-4. Summary of Linear Penetration for Impingement Groups

Case	Impingement Classification	Linear Dome Penetration (mm)	Linear Rim Penetration (mm)
1	Chronic	0.11	0.42
2[ξ]	Chronic	0.92	0.81
3	Chronic	0.34	2.38
4	Chronic	0.33	0.06
5	Chronic	0.21	0.63
6	Chronic	0.36	0.10
7	Chronic	0.58	0.81
8	Intermittent	0.23	0.028
9	Intermittent	0.37	0.019
10	Intermittent	0.31	0.089
11	Intermittent	0.54	0.085
p-value (Chronic vs. Intermittent)		0.77	[#]**0.03**
p-value (Subset of 11 vs. all 48 TDRs)		0.65	0.68

Abbreviations: [ξ]TDR revised for osteolysis; [#], significantly higher in chronic impingement group

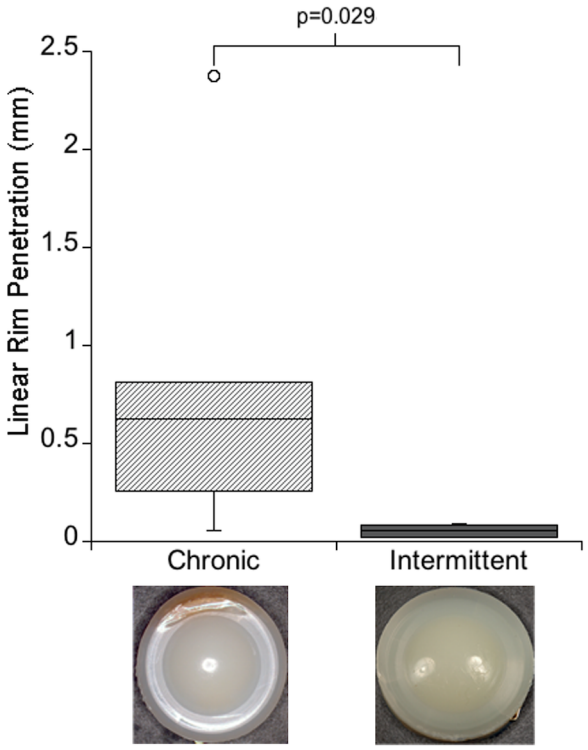

Figure 4-11. Linear rim penetration was increased for retrieved mobile-bearing TDR components exhibiting chronic impingement. Provided are boxed ranges of the 25th and 75th percentile and whiskers showing the 10th and 90th percentile. Outliers are shown as open circles. Representative images are also provided to illustrate both impingement classifications.

Oxidation Analysis

Thin sections were taken from the central axis of the cores to assess oxidation and oxidation potential[33]. Initially, lipids (which may interfere with the oxidation analysis) were extracted from the polyethylene by boiling the slices in heptane for 6 hours. Thin sections were then analyzed at the dome and the rim using Fourier Transform Infrared (FTIR) spectroscopy at both the dome and rim, and the oxidation index (OI) was calculated in accordance with ASTM F2102-06 [64]. To investigate the hydroperoxide content, section were then exposed to nitric oxide, thereby converting the hydroperoxides to nitrates, which are readily

identifiable and were measured using FTIR spectroscopy [65, 66]. A hydroperoxide index (HI) was calculated by normalizing the area under the peak located at 1630 cm^{-1} by the peak centered at 1368 cm^{-1}. The full details of this oxidation analysis can be obtained in the original publication by Kurtz et al., (2000)[33]. Regional oxidation and hydroperoxide indices from the current cohort of TDRs were representative of the overall published cohort (Table 4-5), and showed no significant differences between for TDRs with chronic or intermittent impingement.

Table 4-5. Summary of Oxidation Index and Hydroperoxide Index for Impingement Groups

Case	Impingement Classification	Max OI (Dome)	Max HI (Dome)	Max OI (Rim)	Max HI (Rim)
1	Chronic	0.70	0.30	2.22	0.78
2[ξ]	Chronic	1.00	0.55	1.69	0.92
3	Chronic	0.57	0.55	3.84	0.62
4	Chronic	0.39	0.36	1.62	0.41
5	Chronic	1.16	0.45	5.69	0.63
6	Chronic	0.72	0.39	4.65	0.58
7	Chronic	2.87	0.38	7.19	0.47
8	Intermittent	0.21	0.34	0.88	0.46
9	Intermittent	0.49	0.53	3.61	0.66
10	Intermittent	0.42	0.41	3.30	0.51
11	Intermittent	0.40	0.38	2.35	0.77
p-value (Chronic vs. Intermittent)		0.05	0.89	0.30	0.77
p-value (Subset of 11 vs. all 48 TDRs)		0.87	0.23	0.59	0.79

Abbreviations: [ξ]TDR revised for osteolysis

Statistical Analysis

After the first 6 samples were analyzed, a power calculation was performed to determine the number of samples required to detect a significant difference in functional biological activity. Using P=0.80 and α=0.05, 10 TDR samples were sufficient to detect a 1.5-fold change in functional biological activity between

impingement groups. An 11th TDR revised for osteolysis was analyzed separately to remove the potential confounding effect of this outlier. In addition, by including this patient separate from the others, it was used to test the applicability of the biological activity model for particles *in vivo*. Initially, Mann Whitney U Tests were used to evaluate differences in clinical data, regional surface damage and oxidation between the current subset of TDRs and the larger overall group of 48 TDRs (Table 4-4 and Table 4-5). Distributions of particle characteristics were assessed for normality using the Shapiro-Wilk test. For normally distributed data, differences between impingement groups were evaluated using independent t-tests. For non-parametric data, Mann Whitney U tests were used to evaluate differences in particle characteristics. Correlations between particle characteristics, clinical variables (i.e. implantation time), penetration and oxidation were determined using the Spearman rank correlation test.

Results

Differences in Particle Characteristics Between Intermittent or Chronic TDR Impingement

In general, no significant differences in the mean particle size, shape or number were observed on the basis of TDR impingement classification. For particle size, the mean values of equivalent circular diameter were 0.56±0.11 μm vs. 0.81±0.30 μm (p=0.15, Power=0.30) for the intermittent and chronic impingement groups, respectively (Table 4-6). In both impingement groups, characterization of particle shapes revealed a combination of granular and, to a lesser extent, fibrillar

morphologies (Fig. 2). Mean values of aspect ratio, the ratio of particle length to breadth, were not significantly different for the intermittent and chronic impingement groups (1.97±0.14 vs. 1.95±0.12, p=0.77, Power<0.10) (Table 4-7). Similarly for particle roundness, a measure of how closely a particle resembles a perfect circle ranging from 0-1, values were comparable between intermittent and chronic impingement groups (0.56±0.02 vs. 0.57±0.02, p=0.78, Power<0.10) (Table 4-7). Form factor, a descriptor of circularity that relies on particle perimeter, was also similar between intermittent and chronic impingement groups (0.57±0.07 vs. 0.54±0.11, p=0.58, Power<0.10) (Table 4-7); however, for both groups, form factor was increased (more rounded) for particles in the submicron size range as compared to the larger size ranges (p<0.01). Lastly, mean values of particle number were not significantly different between intermittent and chronic impingement groups (p=0.10, Power=0.37) (Table 4-6).

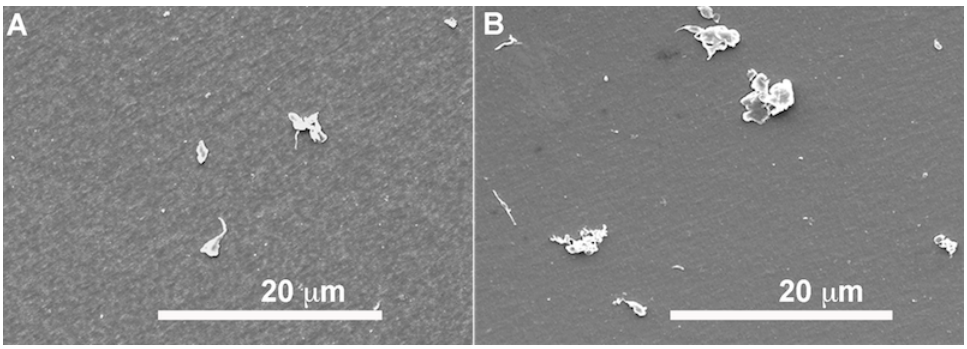

Figure 4-12. Polyethylene Wear Particles from Revised TDRs

Table 4-6. Summary of particle size and number characteristics for impingement groups

Case	Impingement Classification	ECD (μm) mean ± std. dev.	Particle Number (x10^9/gram)
1	Chronic	0.58 ± 1.35	1.80
2ξ	Chronic	0.61 ± 0.60	2.59
3	Chronic	1.37 ± 2.04	2.60
4	Chronic	0.52 ± 1.21	1.20
5	Chronic	1.01 ± 1.41	1.88
6	Chronic	0.89 ± 1.32	1.54
7	Chronic	0.69 ± 1.13	2.36
8	Intermittent	0.65 ± 1.09	0.98
9	Intermittent	0.40 ± 0.67	1.99
10	Intermittent	0.58 ± 0.70	1.19
11	Intermittent	0.59 ± 0.78	1.49
	p-value	0.15	0.10

Abbreviations: ECD, equivalent circular diameter.

ξTDR revised for osteolysis

Table 4-7. Summary of particle shape characteristics for impingement groups

Case	Impingement Classification	AR mean ± std. dev.	R mean ± std. dev.	FF mean ± std. dev.
1	Chronic	2.07 ± 0.80	0.54 ± 0.15	0.52 ± 0.26
2[ξ]	Chronic	1.84 ± 0.56	0.58 ± 0.14	0.32 ± 0.20
3	Chronic	2.11 ± 0.99	0.55 ± 0.19	0.58 ± 0.24
4	Chronic	1.81 ± 0.64	0.60 ± 0.15	0.55 ± 0.23
5	Chronic	1.93 ± 0.74	0.58 ± 0.17	0.65 ± 0.21
6	Chronic	1.85 ± 0.64	0.59 ± 0.15	0.57 ± 0.25
7	Chronic	2.03 ± 0.91	0.56 ± 0.18	0.60 ± 0.24
8	Intermittent	2.08 ± 0.89	0.55 ± 0.18	0.63 ± 0.21
9	Intermittent	1.85 ± 0.65	0.59 ± 0.15	0.47 ± 0.23
10	Intermittent	2.10 ± 1.02	0.55 ± 0.19	0.58 ± 0.24
11	Intermittent	1.86 ± 0.61	0.58 ± 0.15	0.61 ± 0.26
	p-value	0.77	0.78	0.58

Abbreviations: AR, aspect ratio; R, roundness; FF, form factor. [ξ]TDR revised for osteolysis

To further evaluate particle characteristic differences, the particles were evaluated according to size ranges with high (<0.1-1 μm), intermediate (1-10 μm) and low (>10 μm) biological relevance. This separation showed the mean equivalent circular diameter of particles in the >10 μm range was larger in the chronic impingement group (p=0.03) and tissues from this group contained more particles in the 1-10 μm size range (p=0.03) (Table 4-8 and Table 4-9). Several larger particles obtained from TDRs with chronic impingement are shown in Figure 4-13.

Table 4-8. Mean Particle Size for Individual Particle Size Ranges

Impingement Classification	ECD (μm), mean ± std. dev. <0.1-1 μm	1-10 μm	>10 μm
Chronic	0.42±0.05	1.97±0.21	18.70±4.83
Intermittent	0.38±0.08	1.91±0.11	12.86±3.35
p-value	0.26	0.54	[#]**0.03**

ECD, equivalent circular diameter. [#], significantly higher in chronic impingement group

Table 4-9. Mean Particle Number for Individual Particle Size Ranges

Impingement Classification	Particle Number, mean ± std. dev. <0.1-1 μm	1-10 μm	>10 μm
Chronic	$1.95\pm0.52 \times 10^{9}$	$4.52\pm3.04 \times 10^{7}$	$3.17\pm2.98 \times 10^{5}$
Intermittent	$1.40\pm0.44 \times 10^{9}$	$1.13\pm0.73 \times 10^{7}$	$0.71\pm0.28 \times 10^{5}$
p-value	0.11	**#0.03**	0.07

#, significantly higher in chronic impingement group

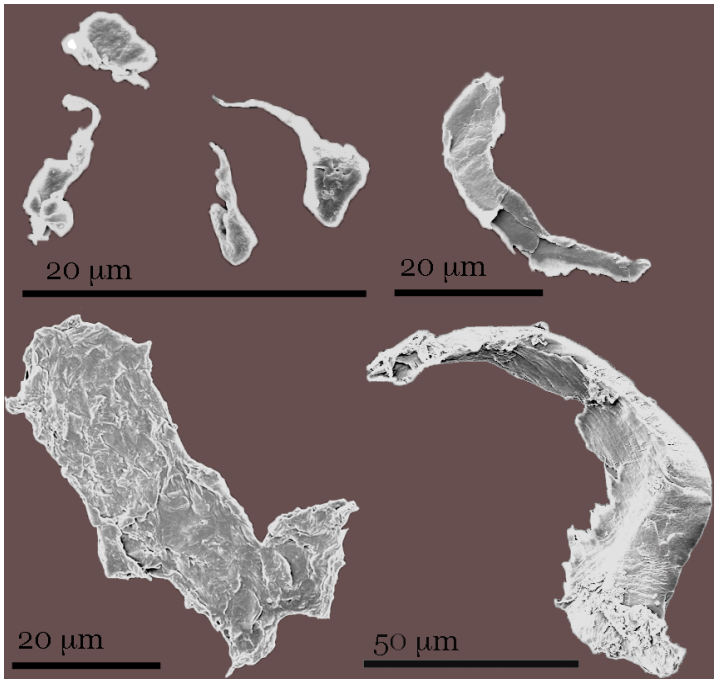

Figure 4-13. Representative images of particles from larger 1-10 and >10 micron size ranges for TDRs with chronic impingement.

Differences in Biological Activity of Particles for Intermittent and Chronic TDR Impingement

Major differences were observed between impingement groups for the polyethylene wear particle volume fraction, V(r), and the specific biological activity (SBA; biological activity per unit volume). For the comparison of the particle volume fraction, significant increases were observed for the <0.1-1 μm and 1-10 μm size ranges from TDRs with intermittent impingement (p=0.04 and p=0.03,

respectively); whereas, the volume fraction of >10 μm particles was increased in the chronic impingement group (p=0.01) (Figure 4-14). After applying ranked biological activity scalars, B(r), to each size range, particles from TDRs with intermittent impingement had increased values of SBA for the 0.1-1 μm and 1-10 μm size ranges (p=0.04 and p<0.01, respectively) and for the cumulative value of all three size ranges (p<0.01, Power=0.95) (Figure 4-15). For the >10 μm size range, SBA was increased in the chronic impingement group (p<0.01); however, for both groups, the biological relevance of particles from this size range was low (Figure 4-15). For particles from the single TDR revised for osteolysis, SBA_V was one of the highest values reported for either impingement group.

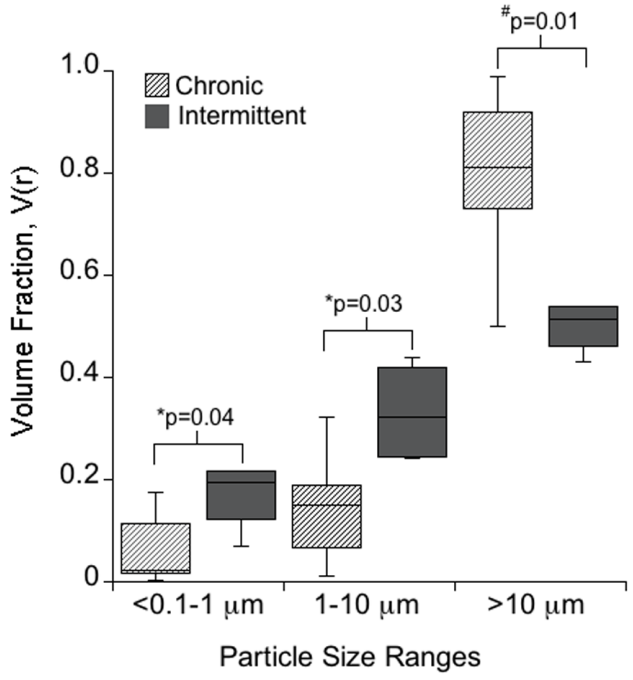

Figure 4-14. Differences in volume % were observed based on impingement group. For the TDRs with intermittent impingement, particle volume % was increased in the <0.1-1 and 1-10 μm size ranges; whereas, the volume % of >10 μm wear debris was increased for the chronic impingement group. Provided are boxed ranges of the 25th to 75th percentiles and whiskers showing the 10th and

90th percentile.

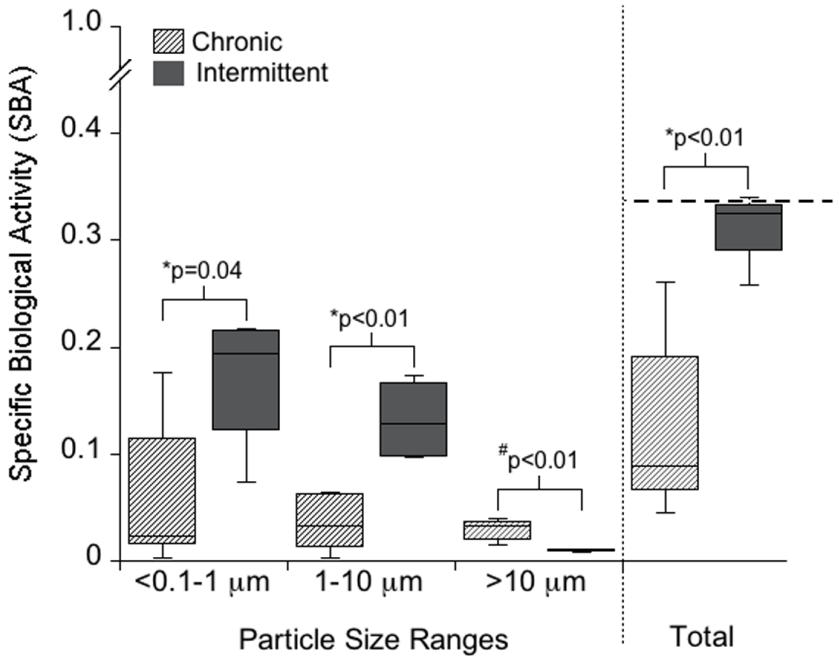

Figure 4-15. Differences in specific biological activity (SBA) were observed based on impingement classification. SBA was increased for the 0.1-1 μm and 1-10 μm size ranges and for the cumulative value from all three size ranges from the intermittent impingement group. For the >10 μm size range, SBA was increased in the chronic impingement group. Provided are boxed ranges of the 25th to 75th percentile and whiskers showing the 10th and 90th percentile. The dotted line represents the SBA of polyethylene wear debris from the single TDR revised for osteolysis.

Differences were also observed between impingement groups for the total particle volume and functional biological activity (FBA). For the chronic impingement group, particle volume (mm^3)/gram of tissue was elevated in the submicron and 1-10 μm size ranges, and significantly higher for both the >10 μm size range (p=0.01) and the cumulative value of all three size ranges (p=0.01) (Figure 4-16). Similarly, FBA (SBA normalized by particle volume (mm^3)/gram of tissue) was significantly higher for both the >10 μm size range (p=0.01) and the cumulative value of all three size ranges of particles from the chronic impingement

group (p=0.03, Power=0.73) (Figure 4-17). For the single TDR revised for osteolysis, FBA was one of the highest values in either impingement group.

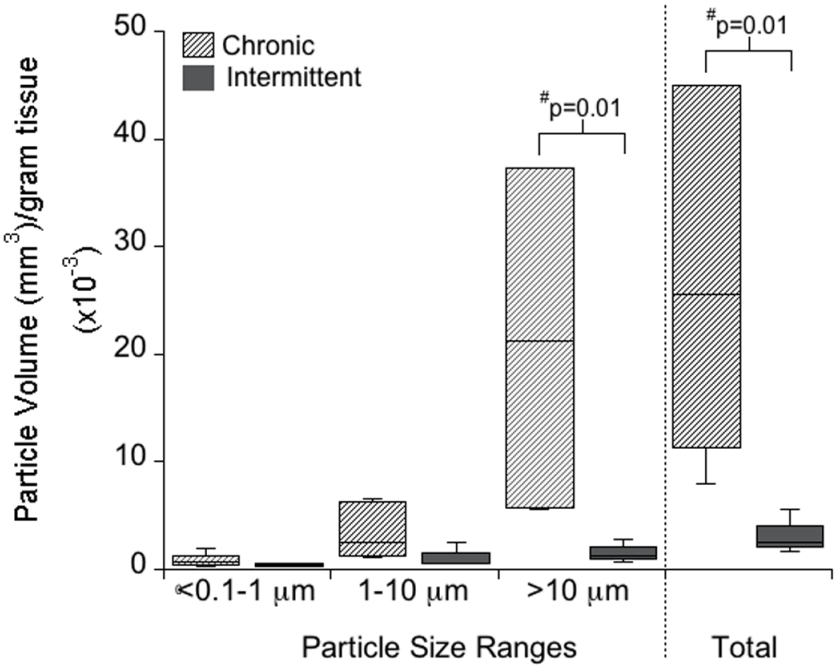

Figure 4-16. Differences were observed in the total particle volume based on impingement classification. For TDRs with chronic impingement, particle volume was increased for the >10 μm size range and the cumulative value of all three size ranges. Provided are boxed ranges of 25th to 75th percentile and whiskers showing the 10th and 90th percentile. Outliers are shown as open circles.

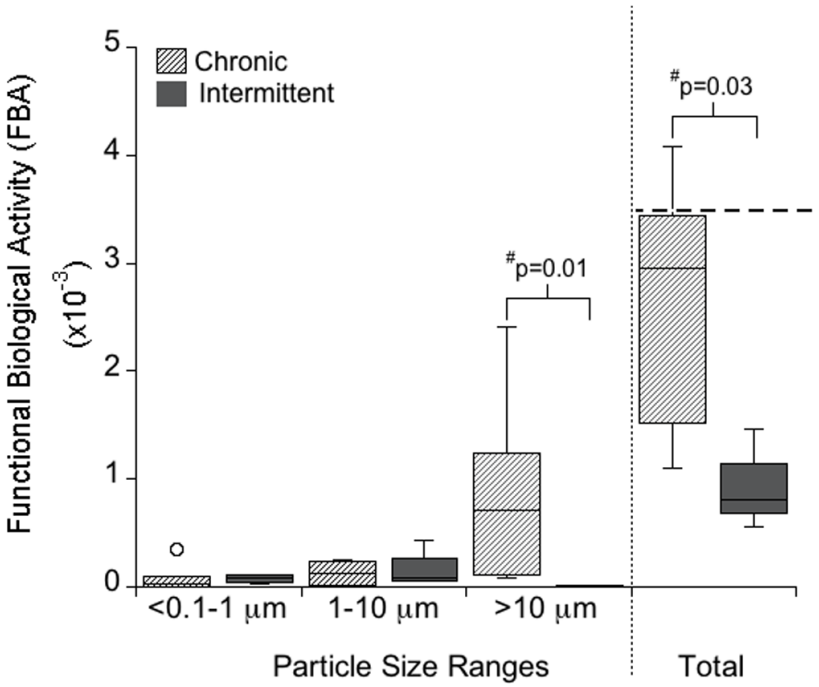

Figure 4-17. Differences were observed in the functional biological activity (FBA) based on impingement classification. FBA was increased for the >10 μm size range and the cumulative value of all three size ranges after normalizing SBA by particle volume (mm^3)/gram of tissue. Provided are boxed ranges of 25th to 75th percentile and whiskers showing the 10th and 90th percentile. Outliers are shown as open circles. The dotted line represents the FBA of polyethylene wear debris from the single TDR revised for osteolysis.

Correlations Between Regional TDR Damage or Oxidation and the Characteristics of Polyethylene Wear Debris

Although linear rim penetration was significantly increased in the chronic impingement group (p=0.03) (Figure 4-11), analysis of retrieved TDRs revealed varying amounts of regional penetration and oxidation (Table 4-4 and Table 4-5). However, when considering component and wear particle variables for all patients, the extent of linear rim penetration positively correlated with increasing particle size (ρ=0.68, p=0.02) and particle number (ρ=0.72, p=0.013) (Figure 4-18 and Figure 4-19). In addition, linear rim penetration positively correlated with increasing values of FBA (ρ=0.75, p=0.01) (Figure 4-20).

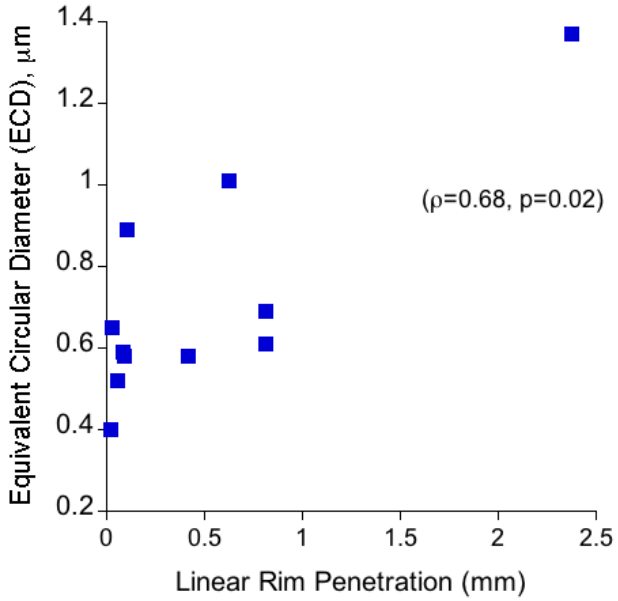

Figure 4-18. Positive correlations were observed between increasing linear rim penetration (mm) and mean equivalent circular diameter (µm) using Spearman rank correlation tests.

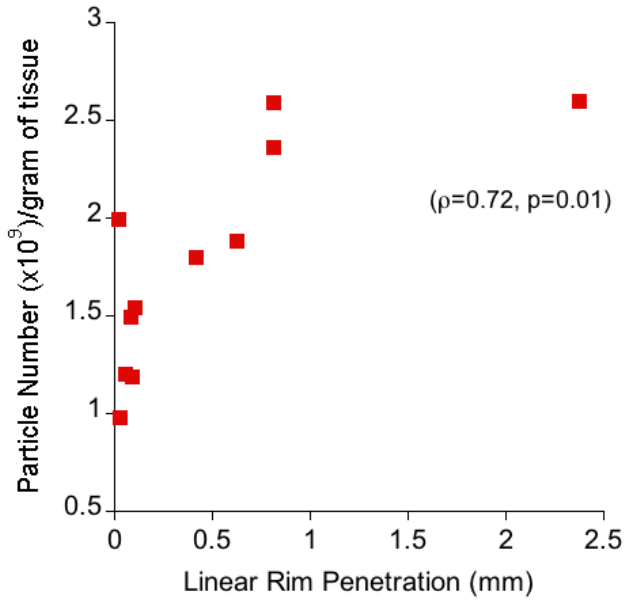

Figure 4-19. Positive correlations were observed between increasing linear rim penetration (mm) and polyethylene wear particle number (x10^9/gram tissue) using Spearman rank correlation tests.

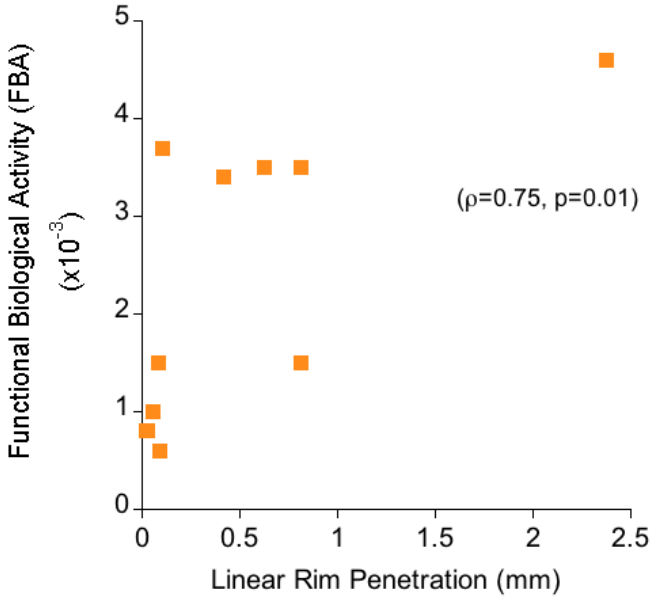

Figure 4-20. Positive correlations were observed between increasing linear rim penetration (mm) and functional biological activity (FBA) using Spearman rank correlation tests.

Discussion

Based on clinical experience with polyethylene bearings in THA and TKA studies, it is known that polyethylene wear particles play a critical role in the inflammatory responses that contribute to the development of osteolysis and, ultimately, the need for revision surgery [54, 67-71]. However, in TDRs, where osteolysis is rarely observed, the inflammatory role of polyethylene is uncertain, in part because the characteristics of TDR wear particles *in vivo* have not been clearly defined [13]. Therefore, the current study was performed using scanning electron microscopy to determine following: (1) the concentration, size and shape of polyethylene wear particles between 0.05-2.00 μm in periprosthetic tissues from retrieved TDRs, (2) to identify correlations between the characteristics of TDR wear debris and visible damage to the polyethylene core.

The current chapter contains the following limitations: (i) The TDR wear particles were obtained from polyethylene that was gamma-irradiated in air, a historical sterilization method that is no longer employed for spine and orthopedic implants. Nevertheless, the particle data reported here provide a crucial, heretofore unavailable, reference point for future studies of conventional gamma inert-sterilized polyethylenes that are currently used for contemporary total disc arthroplasty. (ii) In the comparison of TDR impingement groups, a limited number of tissues were available for the analysis of polyethylene wear debris. However, when comparing data for all 48 TDRs against the subset of 11 TDR implants with available periprosthetic tissues, no differences were observed between measurements of oxidation or penetration [53]. Thus, the conclusions regarding TDR polyethylene wear particle characteristics are drawn from a subset of components that is representative of the larger published TDR cohort. (iii) For the comparison of TDR impingement groups, the post-hoc statistical power was less than 0.80 for detecting differences in mean values of particle size and number based on impingement classification. Nevertheless, the results emphasize the utility of using biological activity to illustrate the collective differences in particle size, shape and number characteristics from TDR failure modes. (iv) Finally, a 0.05 μm polycarbonate filter was chosen based on the ESEM study by Scott et al. (2001) [59] showing that only a small percentage (2.8%) of THA particles were smaller than the 0.05 μm pore size [59]. Thus, it is unlikely that the method of sample preparation contributes to an under- or overestimate of the concentration, size or shape of wear particles present in the current TDR and THA revision tissues. In addition, the

volume contribution of these potentially excluded particles is negligible to the total volume [59], and the biological activity of particles <0.1 μm as a distinct size range is still under investigation [24, 72-74].

Collectively, these data represent the largest characterization of submicron- as well as micron-sized polyethylene wear debris from revised lumbar TDRs. The assumption that polyethylene wear debris generation from TDRs implant would be minimal is not supported by the current findings. TDR revision tissues contained over a billion wear particles/gram, which represents a substantial load within the spinal tissue. This first implementation of the biological activity model to particles isolated from periprosthetic tissues also highlights the differences in wear particle characteristics due to impingement. Specifically, this study shows that increased rim penetration associated with chronic impingement exacerbates the production of biologically relevant polyethylene wear debris. Given that retrieved TDRs more frequently exhibited signs of chronic rim impingement, this finding may represent a negative consequence of this unintended wear mode. Thus, the results of this study serve as an important benchmark both in terms of understanding the clinical significance of polyethylene wear particles in the spine, and for the future development of test methods to simulate TDR rim impingement *in vitro*.

Studies discussing the characteristics of polyethylene wear particles in the lumbar spine are, for the most part, limited to a single *in vitro* study of Charité TDRs by Serhan et al., (2006) [22]. In theirs and the current study, particles visualized by ESEM ranged from submicron to >10 μm in size; however, their mean reported

particle size of 5 μm is an order of magnitude larger than the overall mean particle size, 0.72 μm, in the current study. Additionally, TDR components tested *in vitro* were not loaded in a manner that would induce rim impingement. Overall, the sizes of particles from TDRs with intermittent and chronic impingement were similar to previous studies of particles isolated from hip and knee tissues, respectively [75, 76]. However, while the range of particle sizes observed for TDRs with intermittent (0.40-0.65 μm) and chronic impingement (0.58-1.37 μm) appeared to be influenced by differences in conformity and wear patterns, mean values of particle size, shape or number were not significantly different [77-79]. Importantly, separation of particles according to biologically relevant size ranges revealed differences, specifically that particles from the chronic impingement group were larger and more numerous in the >10 μm and 1-10 μm size ranges, respectively. Thus, the use of mean particle characteristics alone is less sensitive in distinguishing differences associated with multiple modes of component wear.

Others and we have recently published on prevalent wear mechanisms affecting mobile-bearing TDRs, which include adhesive/abrasive wear of the highly conforming dome region and predominantly fatigue wear at isolated points of rim contact. [12, 20, 30] In a radiographic study of 66 ProDisc mobile-bearing TDRs, Kafer et al. (2008) identified posterior component impingement with an incidence of 11-15% depending on lumbar level and/or extension angle [21]. However, unlike the current findings, their study could not directly evaluate whether TDR impingement increased the production of wear debris because implants were still

functioning *in vivo*. The correlations between increasing linear rim penetration with increasing particle size and number are also supported by hip and knee retrieval studies. In both THA and TKA, contact resulting from impingement contributes to localized cracking, fragmentation, an increase in wear and an overall altered distribution of forces [37, 52, 80, 81] Similarly for TDRs, Rundell et al., (2010) showed that peak contact stress significantly correlated with rim penetration rate (mm/year) at the interface of the superior footplate and the central polyethylene core based on a validated computational model of mobile-bearing TDRs in the lumbar spine [31]. In their model, the propensity for TDRs to develop chronic impingement was made worse by increased disc height distraction and after anterior placement of the endplate.

Since the biological activity model was initially published in 2001, it has been implemented in simulator studies to investigate the effect of surface roughness [62, 82], complexity of wear paths [83-87], polymer crosslinking [82, 86-89], and/or type of material [90, 91] on particle generation. Based on differences in the biomaterials and/or testing parameter(s) used *in vitro*, published values of specific biological activity (SBA) range from 0.08 to 0.94 [57, 88, 92]. In the current study, the SBA of wear particles from revised TDRs also exhibited substantial variability, ranging from 0.05 to 0.34. In general, differences in SBA are affected by both the ranked biological activity scalar and particle volume fraction of each size range. For the intermittent group, the decreased mean particle size in the >10 μm range contributed to its lower volume fraction, and concurrently increased the volume

fraction of both the <0.1-1 μm and 1-10 μm size ranges. In contrast, for TDRs with chronic impingement, the decreased volume fraction of <0.1-1 and 1-10 micron-sized wear particles resulted in reduced values of SBA. To eliminate the volume fraction bias, functional biological activity (FBA), SBA normalized by the total particle volume (mm^3)/gram of tissue, was implemented to account for the contribution of particle number and size to particle volume. For the chronic group, FBA was increased for the >10 μm size range and the combined value of all three particle size ranges, which can be attributed to an increased number of particles in the 1-10 μm size range and a larger mean equivalent circular diameter for particles in the >10 μm size range. For the single case of osteolysis, the increased values of both SBA and FBA are due to an equal magnitude of dome and rim penetration, which generated both a large volume fraction of biologically relevant particles and a large total volume of wear debris.

At present, the biological activity model does not include the contributions of pro-inflammatory factors *in vivo* (e.g. adsorption of endotoxin/protein [93-98] and/or the extent of polyethylene wear particle oxidation [99-101]), and further investigation of the inflammatory cytokine responses to wear debris in the spine is warranted. Nevertheless, these results lend support to the use of biological activity calculations, combined with characteristics of particle size and number from individual size ranges, to better illustrate differences in TDR clinical failure modes. Moreover, the effect of impingement on functional biological activity highlights the importance of developing test methods that reproduce a comprehensive range of

TDR wear modes *in vitro.* In the remaining chapter, the biological activity of wear particles are determined for three cohorts of polyethylenes currently used in THA.

Acknowledgements:

This study was funded in part by NIH R01 AR47904, R01 AR056264, and the Food and Drug Administration's Critical Path Initiative. Special thanks to Jonathan Peck and Genevieve Hill from the FDA for their assistance and support, and to Ryan Siskey and Dr. Steven Kurtz at Exponent for their role in writing the grant that made this project possible. Special thanks to Dr. Nancy Pleshko and Arash Hanifi at Temple University and Dan MacDonald at Drexel University for their assistance with FTIR measurements. Last, but not least, to the collaborators at Maastricht Hospital in the Netherlands, who include but are not limited to Dr. André van Ooij and Ilona Punt, for their contributions to the total disc repository.

References

1. Eck, J.C., S.C. Humphreys, and S.D. Hodges, *Adjacent-segment degeneration after lumbar fusion: a review of clinical, biomechanical, and radiologic studies.* Am J Orthop, 1999. 28(6): p. 336-40.
2. Etebar, S. and D.W. Cahill, *Risk factors for adjacent-segment failure following lumbar fixation with rigid instrumentation for degenerative instability.* Journal of Neurosurgery, 1999. 90(4): p. 163-169.
3. Blumenthal, S., et al., *A prospective, randomized, multicenter Food and Drug Administration investigational device exemptions study of lumbar total disc replacement with the CHARITE artificial disc versus lumbar fusion: part I: evaluation of clinical outcomes.* Spine (Phila Pa 1976), 2005. 30(14): p. 1565-75; discussion E387-91.
4. Geisler, F.H., *The CHARITE Artificial Disc: design history, FDA IDE study results, and surgical technique.* Clin Neurosurg, 2006. 53: p. 223-8.
5. Link, H.D., *History, design and biomechanics of the LINK SB Charite artificial disc.* Eur Spine J, 2002. 11 Suppl 2: p. S98-S105.

6. David, T., *Long-term results of one-level lumbar arthroplasty: minimum 10-year follow-up of the CHARITE artificial disc in 106 patients.* Spine (Phila Pa 1976), 2007. 32(6): p. 661-6.
7. Guyer, R.D., et al., *Prospective, randomized, multicenter Food and Drug Administration investigational device exemption study of lumbar total disc replacement with the CHARITE artificial disc versus lumbar fusion: five-year follow-up.* Spine J, 2009. 9(5): p. 374-86.
8. Lemaire, J.P., et al., *Clinical and radiological outcomes with the Charite artificial disc: a 10-year minimum follow-up.* J Spinal Disord Tech, 2005. 18(4): p. 353-9.
9. Putzier, M., et al., *Charite total disc replacement--clinical and radiographical results after an average follow-up of 17 years.* Eur Spine J, 2006. 15(2): p. 183-95.
10. van den Eerenbeemt, K.D., et al., *Total disc replacement surgery for symptomatic degenerative lumbar disc disease: a systematic review of the literature. .* Eur Spine J 2010. 19: p. 1262-80.
11. Yajun, W., et al., *A meta-analysis of artificial total disc replacement versus fusion for lumbar degenerative disc disease.* Eur Spine J, 2010. 19(8): p. 1250-61.
12. Kurtz, S.M., et al., *Polyethylene wear and rim fracture in total disc arthroplasty.* Spine Journal: Official Journal of the North American Spine Society, 2007. 7(1): p. 12-21.
13. Punt, I.M., et al., *Periprosthetic tissue reactions observed at revision of total intervertebral disc arthroplasty.* Biomaterials, 2009. 30(11): p. 2079-84.
14. Agarwal, S., *Osteolysis: Science, incidence, and diagnosis.* Curr Orthop, 2004. 18(3): p. 220-231.
15. Amstutz, H.C., et al., *Mechanism and clinical significance of wear debris-induced osteolysis.* Clin Orthop Relat Res, 1992(276): p. 7-18.
16. Purdue, P.E., et al., *The central role of wear debris in periprosthetic osteolysis.* Hss J, 2006. 2(2): p. 102-13.
17. Revell, P.A., N. al-Saffar, and A. Kobayashi, *Biological reaction to debris in relation to joint prostheses.* Proc Inst Mech Eng [H], 1997. 211(2): p. 187-97.
18. Willert, H.G., H. Bertram, and G.H. Buchhorn, *Osteolysis in alloarthroplasty of the hip. The role of ultra-high molecular weight polyethylene wear particles.* Clinical Orthopaedics & Related Research, 1990(258): p. 95-107.
19. Devin, C.J., T.G. Myers, and J.D. Kang, *Chronic failure of a lumbar total disc replacement with osteolysis. Report of a case with nineteen-year follow-up.* J Bone Joint Surg Am, 2008. 90(10): p. 2230-4.
20. van Ooij, A., et al., *Polyethylene wear debris and long-term clinical failure of the Charite disc prosthesis: a study of 4 patients.[erratum appears in Spine. 2007 Apr 20;32(9):1052].* Spine, 2007. 32(2): p. 223-9.
21. Kafer, W., et al., *Posterior component impingement after lumbar total disc replacement: a radiographic analysis of 66 ProDisc-L prostheses in 56 patients.* Spine (Phila Pa 1976), 2008. 33(22): p. 2444-9.

22. Serhan, H.A., et al., *In vitro wear assessment of the Charite Artificial Disc according to ASTM recommendations.* Spine, 2006. 31(17): p. 1900-10.
23. Hirakawa, K., et al., *Characterization and comparison of wear debris from failed total hip implants of different types.* J Bone Joint Surg Am, 1996. 78(8): p. 1235-43.
24. Howling, G.I., et al., *Quantitative characterization of polyethylene debris isolated from periprosthetic tissue in early failure knee implants and early and late failure Charnley hip implants.* J Biomed Mater Res, 2001. 58(4): p. 415-20.
25. Mochida, Y., et al., *Debris from failed ceramic-on-ceramic and ceramic-on-polyethylene hip prostheses.* Clinical Orthopaedics & Related Research, 2001(389): p. 113-25.
26. Schmalzried, T.P. and J.J. Callaghan, *Wear in total hip and knee replacements.* J Bone Joint Surg Am, 1999. 81(1): p. 115-36.
27. Willert, H.G., *Reactions of the articular capsule to wear products of artificial joint prostheses.* Journal of Biomedical Materials Research, 1977. 11(2): p. 157-64.
28. McAfee, P.C., et al., *Revisability of the CHARITE artificial disc replacement: analysis of 688 patients enrolled in the U.S. IDE study of the CHARITE Artificial Disc.* Spine (Phila Pa 1976), 2006. 31(11): p. 1217-26.
29. Murtagh, R.D., et al., *Normal and abnormal imaging findings in lumbar total disk replacement: devices and complications.* Radiographics, 2009. 29(1): p. 105-18.
30. Goreham-Voss, C.M., et al., *Preferential superior surface motion in wear simulations of the Charité total disc replacement.* Eur Spine J, 2010.
31. Rundell, S.A., et al., *Derivation of clinically relevant boundary conditions suitable for evaluation of chronic impingement of lumbar total disc replacement: Application to standard development.* ASTM, 2010.
32. Shkolnikov, Y.P., et al., *Wear pattern observations from TDR retrievals using autoregistration of voxel data.* J Biomed Mater Res B Appl Biomater, 2010. 94(2): p. 312-7.
33. Kurtz, S.M., et al., *What is the correlation of in vivo wear and damage patterns with in vitro TDR motion response?* Spine (Phila Pa 1976), 2008. 33(5): p. 481-9.
34. Casey, D., et al., *PFC knee replacement: osteolytic failures from extreme polyethylene degradation.* Clinical Orthopaedics & Related Research, 2007. 464: p. 157-63.
35. Brown, T.D. and J.J. Callaghan, *Impingement in Total Hip Replacement: Mechanisms and Consequences.* Curr Orthop, 2008. 22(6): p. 376-391.
36. Favre, P., et al., *Influence of component positioning on impingement in conventional total shoulder arthroplasty.* Clin Biomech (Bristol, Avon), 2008. 23(2): p. 175-83.
37. Haas, B.D., *Tibial post impingement in posterior-stabilized total knee arthroplasty.* Orthopedics, 2006. 29(9 Suppl): p. S83-5.

38. Hamai, S., et al., *Evaluation of impingement of the anterior tibial post during gait in a posteriorly-stabilised total knee replacement.* J Bone Joint Surg Br, 2008. 90(9): p. 1180-5.
39. Holley, K.G., et al., *Impingement of acetabular cups in a hip simulator: comparison of highly cross-linked and conventional polyethylene.* J Arthroplasty, 2005. 20(7 Suppl 3): p. 77-86.
40. Labek, G., et al., *High failure rate of the Duraloc Constrained Inlay.* Acta Orthop, 2009. 80(5): p. 545-7.
41. Malik, A., A. Maheshwari, and L.D. Dorr, *Impingement with total hip replacement.* J Bone Joint Surg Am, 2007. 89(8): p. 1832-42.
42. Powers, C.C., et al., *Five Duraloc Locking Ring Failures.* J Arthroplasty, 2010.
43. Malik, A., L.D. Dorr, and W.T. Long, *Impingement as a mechanism of dissociation of a metasul metal-on-metal liner.* J Arthroplasty, 2009. 24(2): p. 323 e13-6.
44. Onda, K., et al., *Cup-neck impingement due to the malposition of the implant as a possible mechanism for metallosis in metal-on-metal total hip arthroplasty.* Orthopedics, 2008. 31(4): p. 396.
45. Lee, Y.K., et al., *Alumina-on-alumina total hip arthroplasty: a concise follow-up, at a minimum of ten years, of a previous report.* J Bone Joint Surg Am, 2010. 92(8): p. 1715-9.
46. Matar, W.Y., et al., *Revision Hip Arthroplasty for Ceramic-on-Ceramic Squeaking Hips Does Not Compromise the Results.* Journal of Arthroplasty, 2010.
47. Murali, R., et al., *Osteolysis in third-generation alumina ceramic-on-ceramic hip bearings with severe impingement and titanium metallosis.* J Arthroplasty, 2008. 23(8): p. 1240 e13-9.
48. Hwang, D.S., Y.M. Kim, and C.H. Lee, *Alumina femoral head fracture in uncemented total hip arthroplasty with a ceramic sandwich cup.* J Arthroplasty, 2007. 22(3): p. 468-71.
49. Restrepo, C., et al., *Natural history of squeaking after total hip arthroplasty.* Clin Orthop Relat Res, 2010. 468(9): p. 2340-5.
50. Popescu, D., et al., *Fracture of a ceramic liner in a total hip arthroplasty with a sandwich cup.* Arch Orthop Trauma Surg, 2008. 128(8): p. 783-5.
51. Furmanski, J., et al., *Clinical fracture of cross-linked UHMWPE acetabular liners.* Biomaterials, 2009. 30(29): p. 5572-82.
52. Duffy, G.P., et al., *Fracture of a cross-linked polyethylene liner due to impingement.* J Arthroplasty, 2009. 24(1): p. 158 e15-9.
53. Kurtz, S.M., et al., *The natural history of polyethylene oxidation in total disc replacement.* Spine (Phila Pa 1976), 2009. 34(22): p. 2369-77.
54. Margevicius, K.J., et al., *Isolation and characterization of debris in membranes around total joint prostheses.* J Bone Joint Surg Am, 1994. 76(11): p. 1664-75.
55. Slouf, M., et al., *Isolation, characterization and quantification of polyethylene wear debris from periprosthetic tissues around total joint replacements.* Wear, 2007. 262: p. 1171-1181.

56. *F 1877-05e Standard Practice for Characterization of Particles*, in *ASTM International*. 2005.
57. Fisher, J., et al., *A novel method for the prediction of functional biological activity of polyethylene wear debris.* Proceedings of the Institution of Mechanical Engineers. Part H - Journal of Engineering in Medicine, 2001. 215(2): p. 127-32.
58. Matthews, J.B., et al., *Comparison of the response of primary human peripheral blood mononuclear phagocytes from di!erent donors to challenge with model polyethylene particles of known size and dose.* Biomaterials, 2000. 21: p. 2033-2044.
59. Scott, M., K. Widding, and S. Jani, *Do current wear particle isolation procedures underestimate the number of particles generated by prosthetic bearing components.* Wear, 2001. 251: p. 1213-1217.
60. Galvin, A.L., et al., *Wear and biological activity of highly crosslinked polyethylene in the hip under low serum protein concentrations.* Proceedings of the Institution of Mechanical Engineers, 2007. Part H - Journal of Engineering in Medicine. 221(1): p. 1-10.
61. Scott, M., et al., *Particle Analysis for the Determination of UHMWPE Wear.* Journal of Biomedical Materials Research: Applied Biomaterials, 2005. 73B: p. 325-337.
62. Bowsher, J.G., et al., *"Severe" wear challenge to 36 mm mechanically enhanced highly crosslinked polyethylene hip liners.* Journal of Biomedical Materials Research, 2008. Part B, Applied Biomaterials. 86(1): p. 253-63.
63. Lapcikova, M., et al., *Nanometer size wear debris generated from ultrahigh molecular weight polyethylene in vivo.* Wear, 2009. 266: p. 349-355.
64. *F 2102-06e1 Standard Guide for Evaluating the Extent of Oxidation in Ultra-High-Molecular-Weight Polyethylene Fabricated Forms Intended for Surgical Implants*, in *ASTM International*. 2006.
65. Costa, L., et al., *Oxidation and oxidation potential in contemporary packaging for polyethylene total joint replacement components.* J Biomed Mater Res B Appl Biomater, 2006. 78(1): p. 20-6.
66. Lacoste, J. and D.J. Carlsson, *A critical comparison of methods for hydroperoxide measurement in oxidized polyolefins.* Polym Degr Stab, 1991. 32: p. 377-86.
67. Campbell, P., et al., *Isolation of predominantly submicron-sized UHMWPE wear particles from periprosthetic tissues.* J Biomed Mater Res, 1995. 29(1): p. 127-31.
68. Green, T.R., et al., *Polyethylene particles of a 'critical size' are necessary for the induction of cytokines by macrophages in vitro.* Biomaterials, 1998. 19(24): p. 2297-302.
69. Maloney, W.J., et al., *Isolation and characterization of wear particles generated in patients who have had failure of a hip arthroplasty without cement.* J Bone Joint Surg Am, 1995. 77(9): p. 1301-10.

70. Revell, P.A., *The combined role of wear particles, macrophages and lymphocytes in the loosening of total joint prostheses.* J R Soc Interface, 2008. 5(28): p. 1263-78.
71. Shanbhag, A.S., et al., *Composition and morphology of wear debris in failed uncemented total hip replacement.* J Bone Joint Surg Br, 1994. 76(1): p. 60-7.
72. Tipper, J.L. *The Biological Response to Nanometre-Sized Particles*. in *4th UHMWPE International Meeting*. 2009. Torino, Italy.
73. Gallo, J., M. Slouf, and S.B. Goodman, *The relationship of polyethylene wear to particle size, distribution, and number: A possible factor explaining the risk of osteolysis after hip arthroplasty.* J Biomed Mater Res B Appl Biomater, 2010. 94(1): p. 171-7.
74. Revell, P.A., *The biological effects of nanoparticles.* Nanotechnology Perceptions, 2006. 2: p. 283-298.
75. Campbell, P., et al., *Wear and morphology of ultra-high molecular weight polyethylene wear particles from total hip replacements.* Proc Inst Mech Eng H, 1996. 210(3): p. 167-74.
76. Shanbhag, A.S., et al., *Quantitative analysis of ultrahigh molecular weight polyethylene (UHMWPE) wear debris associated with total knee replacements.* J Biomed Mater Res, 2000. 53(1): p. 100-10.
77. Schmalzried, T., et al., *Shapes and Dimensional Characteristics of Polyethylene Wear Particles Generated In Vivo by Total Knee Replacements Compared to Total Hip Replacements.* J Biomed Mater Res, Part B, 1997. 38: p. 203-210.
78. Kobayashi, A., et al., *The size and shape of particulate polyethylene wear debris in total joint replacements.* Proceedings of the Institution of Mechanical Engineers. Part H - Journal of Engineering in Medicine, 1997. 211(1): p. 11-5.
79. Kobayashi, A., et al., *Number of polyethylene particles and osteolysis in total joint replacements. A quantitative study using a tissue-digestion method.* Journal of Bone & Joint Surgery - British Volume, 1997. 79(5): p. 844-8.
80. Birman, M.V., et al., *Cracking and impingement in ultra-high-molecular-weight polyethylene acetabular liners.* J Arthroplasty, 2005. 20(7 Suppl 3): p. 87-92.
81. Verborgt, O. and J. Victor, *Post impingement in posterior stabilised total knee arthroplasty.* Acta Orthop Belg, 2004. 70(1): p. 46-50.
82. Galvin, A.L., et al., *Nanometre size wear debris generated from crosslinked and non-crosslinked ultra high molecular weight polyethylene in artificial joints.* Wear, 2005. 259: p. 977-83.
83. Ge, S., et al., *Wear behavior and wear debris distribution of UHMWPE against Si3N4 ball in bi-directional sliding.* Wear, 2008. 264: p. 571-8.
84. Fisher, J., et al., *Wear-simulation analysis of rotating-platform mobile-bearing knees.* Orthopedics, 2006. 29(9 Suppl): p. S36-41.
85. Tipper, J., et al., *Isolation and characterization of UHMWPE wear particles down to ten nanometers in size from in vitro hip and knee joint simulators.* Journal of Biomedical Materials Research, 2006. 78A: p. 473-480.
86. McEwen, H.M.J., et al., *The influence of design, materials and kinematics on the in vitro wear of total knee replacements.* Journal of Biomechanics, 2005. 38(2): p. 357-65.

87. Utzschneider, S., et al., *Influence of design and bearing material on polyethylene wear particle generation in total knee replacement.* Acta Biomater, 2009. 5(7): p. 2495-502.
88. Endo, M., et al., *Comparison of wear, wear debris and functional biological activity of moderately crosslinked and non-crosslinked polyethylenes in hip prostheses.* Proc IME HJ Eng Med, 2002. 216(2): p. 111-22.
89. Williams, P.A., et al., *Highly Crosslinked Polyethylenes in Hip Replacements: Improved Wear Performance of Paradox?* STLE Tribology Transactions, 2007. 50(2): p. 227-290.
90. Ingram, J., et al., *Comparison of the biological activity of grade GUR 1120 and GUR 415HP UHMWPE wear debris.* Biomed Mater Eng, 2002. 12(2): p. 177-88.
91. Tipper, J.L., et al., *Estimation of the osteolytic potential of noncrosslinked and crosslinked polyethylenes and ceramic total hip prostheses. .* Journal of American Society for Testing Materials International, 2006. 3: p. 1-17.
92. Fisher, J., et al. *Predictions of the biological activity of polyethylene wear debris generated under different conditions in vitro*. in *Orthopaedic Research Society*. 2000. Orlando, Florida.
93. Xing, Z., et al., *Accumulation of LPS by Polyethylene Particles Decreases Bone Attachment to Implants.* Journal of Orthopaedic Research, 2006. 24: p. 959-966.
94. Bi, Y., et al., *Adherent endotoxin on orthopedic wear particles stimulates cytokine production and osteoclast differentiation.* Journal of Bone & Mineral Research, 2001. 16(11): p. 2082-91.
95. Wilkins, R., M. Tucci, and H. Benghuzzi, *Evaluation of endotoxin binding to uhmwpe and inflammatory mediator production by macrophages.* Biomed Sci Instrum, 2008. 44: p. 459-64.
96. Greenfield, E.M., et al., *Does endotoxin contribute to aseptic loosening of orthopedic implants?* J Biomed Mater Res B Appl Biomater, 2005. 72(1): p. 179-85.
97. Elfick, A.P., et al., *Opsonization of polyethylene wear particles regulates macrophage and osteoblast responses in vitro.* J Biomed Mater Res B Appl Biomater, 2004. 71(2): p. 244-51.
98. Cho, D.R., et al., *The role of adsorbed endotoxin in particle-induced stimulation of cytokine release.* J Orthop Res, 2002. 20(4): p. 704-13.
99. Rocha, M.F., et al., *Macrophage Response to UHMWPE Submitted to Accelerated Ageing in Hydrogen Peroxide.* Open Biomed Eng J, 2010. 4: p. 107-12.
100. Maitra, R., et al., *Immunogenecity of modified alkane polymers is mediated through TLR1/2 activation.* PLoS One, 2008. 3(6): p. e2438.
101. Brach del Prever, E.M., et al., *The biological reaction to polyethylene wear debris can be related with oxidation of the UHMWPE cups.* Chir Organi Mov, 2003. 88(3): p. 291-303.

5. Osteolytic Potential of Wear Debris from Revised Conventional and Highly Crosslinked Polyethylene Hip Implant Components[5]

Abstract

Despite the widespread implementation of highly crosslinked polyethylene (HXLPE) liners to reduce the clinical incidence of osteolysis, it is not known if the substantially improved wear resistance will outweigh the inflammatory potential of HXLPE wear debris generated *in vivo*. To address these unanswered questions with regard to wear debris in THA, a detailed analysis of the differences in size, shape, number and biological activity of polyethylene wear particles was performed. Pseudocapsular tissues were obtained from the primary revision surgery of four gamma inert-sterilized conventional polyethylene liners (CPE), five annealed HXLPE liners and five remelted HXLPE liners. Subsequently, tissues were digested using nitric acid and polyethylene wear particles (>0.05 μm) were evaluated using scanning electron microscopy to determine particle size, shape, number and biological activity. Tissues from both remelted and annealed HXLPE cohorts contained significantly smaller and rounder particles compared to the CPE cohort. Despite the increased percentage of submicron particles, the total number of particles was also lower for both HXLPE cohorts. The volume fraction distribution and specific biological activity per unit volume (SBA) were not significantly different between any of the cohorts. However, the decreased size and number of HXLPE

[5] Baxter RM, Kurtz SM, Steinbeck MJ. Decreased Functional Biological Activity of HXLPE Wear Debris *In Vivo.* CORR. 2011 *In Review.*

wear debris resulted in a significant decrease in the total particle volume (mm^3) per gram of tissue. Accordingly, when the SBA was normalized by the total particle volume, functional biological activity of the HXLPE wear debris was significantly decreased compared to the CPE cohort. Overall, these data show that despite the increased percentage of submicron wear particles, the osteolytic potential of wear debris generated by HXLPE liners *in vivo* is significantly reduced by the improvements in polyethylene wear resistance.

Introduction

Ultra-high molecular weight polyethylene (polyethylene) wear particle-induced osteolysis and, ultimately, implant loosening are recognized as major factors limiting the longevity of total joint replacement components [1-3]. To improve implant wear resistance and decrease the incidence of osteolysis, highly crosslinked polyethylenes (HXLPE) were introduced as an alternative to conventional, gamma inert-sterilized polyethylene (CPE)[4-7]. The manufacturing specifics of first-generation HXLPE liners were initially provided in the introduction, but are again provided below for their relevance to the work performed in the current chapter. The first generation of HXLPE components were created by an initial phase of gamma-irradiation in an inert environment followed by an annealing or remelting phase performed above or below the crystalline transition temperature, respectively [5, 8, 9]. To date, both approaches have yielded improved clinical outcomes with regard to the reduction of osteolysis at early-term (≤5 year) [10-15] and mid-term (5-10 year) follow-up [16-21]. However, the manufacture of annealed polyethylene results in the formation of residual free radicals with the potential to cause oxidation and component destabilization *in vivo* [22-25]; whereas remelted polyethylene eliminates the entrapment of free radicals within the polymer but at the expense of reduced mechanical properties [26-29]. Moreover, the observation of comparable surface damage for both CPE and newer HXLPE components [30] raises questions regarding the generation of biologically relevant wear debris [31, 32]. Collectively, these issues may be detrimental to the long-term

clinical performance of HXLPE components currently used in total hip arthroplasty (THA).

Despite the introduction of HXLPE liners more than 10 years ago, the characterization of HXLPE wear debris is predominantly limited to wear simulations of THA [33-40] or TKA [41, 42] bearing designs *in vitro*. While these studies have unfailingly shown a reduction in the wear volume of HXLPE as compared with CPE components, there is less agreement regarding a similar reduction in the number of HXLPE particles [34, 40, 43]. Furthermore, the clinical implications of *in vitro* studies showing a reduction in polyethylene wear particle size with increased crosslinking dose are unknown [34, 39, 44, 45].

Early *in vitro* studies demonstrated that exposure to polyethylene wear debris within a critical, biologically-relevant size range (0.1-1 μm) resulted in enhanced macrophage activation and pro-inflammatory cytokine expression [46-48]. More recently, HXLPE and CPE wear debris were isolated from a hip simulator and added to macrophages *in vitro*. At the highest particle concentration based on surface area ratio, the macrophage expression of tumor necrosis factor-α, a potent pro-inflammatory cytokine, was increased by 50% in response to HXLPE wear debris (mean size, 0.111 μm) compared to CPE wear debris (mean size, 0.196 μm) [45]. These *in vitro* data highlight the importance of understanding whether the substantially improved wear resistance will outweigh the inflammatory potential of HXLPE wear debris generated *in vivo*. To address this important unanswered issue, differences in size, shape, number and biological activity of polyethylene wear

particles were evaluated for tissues obtained during primary THA revision surgery of CPE versus remelted or annealed HXLPE liners. The current chapter was performed to test two hypotheses. Based on the results of an *in vivo* study comparing CPE and HXLPE used in TKA, the first hypothesis was that polyethylene wear particle size, shape and number would also be reduced for HXLPE components used in THA. The second hypothesis was that the functional biological activity of HXLPE wear debris generated *in vivo* would be reduced compared to particles from the CPE cohort.

Methods

Patient Selection

Pseudocapsular tissue samples were collected from fourteen patients undergoing primary revision arthroplasty of uncemented, metal-on-polyethylene hip components. Informed consent was obtained prior to tissue collection, and all procedures were performed in accordance with Institutional Review Board guidelines of the participating institutes. For the gamma inert-sterilized conventional polyethylene cohort (CPE, n=4), liners were revised after an average of 6.4 years (range 2.3-9.3 years) for polyethylene wear, loosening and osteolysis (Table 1). For the annealed highly crosslinked polyethylene (HXLPE) cohort (n=5), liners were revised after an average of 4.2 years (range 2.0-5.2 years) for loosening or malposition (Table 2). For the remelted HXLPE cohort (n=5), liners were revised after an average of 3.3 years (ranges 1.7-6.6 years) for loosening or malposition

(Table 3). Implantation time was not significantly different between cohorts (p=0.333, Kruskal-Wallis).

Table 5-1. Summary of clinical information for patients from the CPE cohort (n=4)

RI/Explant #	Implant Model	Revision Reason	Implantation Time (years)	Gender	Age at Revision (years)	Radiographic Osteolysis? (Y/N)
RIH346/645	Howmedica Omnifit	Loose (Fem.)	2.3	F	78	Y
RIH280/591	Biomet Ringloc	PE wear, instability	5.1	F	63	N
RIH400/692	Biomet Ringloc	Loose (Acet. & Fem.)	8.8	F	66	Y
RIH286/595	Zimmer Trilogy	Loose (Fem.)	9.3	F	66	Y

Abbreviations: fem, femoral; acet, acetabular; PE, polyethylene

Table 5-2. Summary of clinical information for patients from the remelted HXLPE cohort (n=5)

RI/Explant #	Implant Model	Revision Reason	Implantation Time (years)	Gender	Age at Revision (y)	Radiographic Osteolysis? (Y/N)
H658/878	Zimmer Trilogy	Loose (Fem.)	1.7	F	56	N
H107/451	Zimmer Trilogy	Loose (Acet. & Fem.)	1.7	F	66	N
H254/570	Zimmer Trilogy	Malposition	2.9	F	58	N
H656/876	Zimmer Trilogy	Loose (Fem.)	3.6	M	59	N
H007/766	Zimmer Trilogy	Dislocation	6.6	F	67	N

Abbreviations: fem, femoral; acet, acetabular. Sorted by increasing implantation time.

Table 5-3. Summary of clinical information for patients from the annealed HXLPE cohort (n=5)

RI/Explant #	Implant Model	Revision Reason	Implantation Time (years)	Gender	Age at Revision (years)	Radiographic Osteolysis? (Y/N)
H199/520	Stryker Trident	Loose (Fem.)	2.0	M	55	N
H413/702	Stryker Trident	Loose (Acet.)	2.7	F	57	N
H194/515	Stryker Trident	Loose (Acet.)	5.2	F	57	N
H460/736	Stryker Trident	Malposition	5.2	F	71	N
H450/729	Stryker Trident	Loose (Fem.)	5.9	M	63	N

Abbreviations: fem, femoral; acet, acetabular. Sorted by increasing implantation time.

Wear Particle Isolation

At the time of surgery, tissue samples were collected and processed into cassettes embedded in paraffin. Wear particle isolation was performed according to the methods outlined in Chapter 4.

Wear Particle Analysis

Image analysis of ESEM micrographs was initially performed using a gray-scale level threshold in Adobe Photoshop (San Jose, CA). After analysis of the histogram, the threshold (grayscale value) corresponding to the right side of the main peak was chosen for all images. Subsequently, using a scale bar from each micrograph, the individual particle areas and dimensions were determined using a custom macro in NIH ImageJ (National Institutes of Health, USA). The resulting areas and dimensions were used to characterize particle number, size (equivalent circular diameter, ECD) (Equation 1) and shape (aspect ratio, AR (Equation 2); roundness, R (Equation 3); form factor, FF (Equation 4)) based on guidelines for wear particle analysis outlined in ASTM F1877 [49]. To determine particle number per gram of tissue, the number of imaged particles was scaled by the total filter area and by the initial tissue weight (Equation 5).

To characterize particle biological activity, the current study utilized equations originally developed by Fisher, et al. (2001), which were based on a model of cytokine secretion from cultured macrophages in response to varying

doses of particle size and volume [50, 51]. The biological activity function, B(r), which separately ranks the biological relevance of particles in <0.1-1, 1-10 and >10 μm size ranges, was assumed to be the same as previously published (Figure 4-3) [50]. *In vitro* scalars were determined by normalizing all three size ranges by the response observed for particles from the <1 μm size range. Results indicated that the biological response initiated by particles in the lowest size range was 5-fold larger than for particles in the 1-10 μm size range and 25-fold larger than for particles the >10 μm size range.

To determine particle volume in the current study, V_P (Equation 6), calculations were based on the work of Scott, et al. (2005) [52]. Subsequently, the volume of particles within each size range (expressed as a fraction of the total volume) was used to determine the volume fraction distribution, V(r) for the <1, 1-10 and >10 μm size ranges [50]. Previous studies that used gravimetric filter weights to determine V(r) had the advantage of much larger quantities of wear debris and a controlled environment from which to collect the particulates. In addition, the gravimetric method assumes a constant particle thickness and uses values of weight and polyethylene density to determine volume, which ignores the potential influence of individual particles. For the current study, gravimetric values were considered to be inaccurate given the small initial tissue weights.

To determine the specific biological activity per unit volume, (SBA) (Equation 7), the dot-product of $B(r)$ and $V(r)$ was evaluated over each range of particle size. The lowest predicted value of specific biological activity, 0.04, would be obtained if

particle volumes were all in the >10 μm size range; whereas, the highest value, 1, would be obtained if particle volumes were all in the <0.1-1 μm size range. Intermediate values would be achieved as the distribution of volume percentage was shared between all three particle size ranges. provides examples showing the possible range of SBA.

Finally, to determine functional biological activity, FBA, SBA was scaled by the total particle volume (mm^3)/gram of tissue (Equation 8.). *In vitro* studies have previously determined FBA after normalizing by the volume of wear removed from the component. Such studies have the benefit of using a standardized number of cycles; whereas, for retrieval implants the level of patient activity is variable even after normalizing by implantation time. In addition, retrieved components often have some level of iatrogenic damage caused during revision surgery, which is potentially confounding when making determinations of total volume loss from the bearing surface. Other similarities and differences in the determination of particle biological activity are shown in Table 4-2 and Table 4-3.

Western Blot Protocol

The original model of particle biological activity was determined based on macrophage secretion of TNF-α in response to varying particle sizes and volumes [50]. To validate the outputs of the biological activity model, Western Blot analysis was performed on the revised tissue samples to determine patient-specific levels of TNF-α. To extract proteins from tissue samples collected at the time of revision surgery, samples stored in Optimal Cutting Temperature (OCT) medium were

removed from -80°C and placed in liquid nitrogen for 30 seconds. Using a surgical hammer, tissue samples were removed from the frozen OCT blocks by blunt dissection and added, along with 2 ml of Extraction Buffer (EB) to the pulverizing chamber of a Cryogenic Spex Mill (Spex Sample Prep, 6870). The lower enclosure of the Spex Mill was also filled with liquid nitrogen, allowing the temperature-sensitive samples to be pulverized to facilitate protein extraction. At the end of the Spex Mill grinding cycles, powdered samples were placed in an additional 2 ml of EB in a falcon tube, which was stored at -20°C for 1 hour to facilitate protein extraction before moving to -80°C overnight. From each sample, 2 ml aliquots containing EB and proteins were placed in an eppendorf tube and centrifuged for 10 minutes at 12,000 g. The upper layer was removed with a pipette and placed in a new eppendorf tube, and the tissue precipitate was discarded. Centrifugation steps were performed a total of three times. To determine the initial protein content in each sample, an 8-point standard curve was determined using a SPECTRAFluor Plus 96-well plate reader (XFLUOR4 V 4.51, Serial # 94335) at an absorbance wavelength of 590 nm. Based on the slope and y-intercept of the Bovine Serum Albumin (BSA) standard curve, the amount of protein (μg) was standardized across all study samples by adjusting volume (μl). The protein volume and 5 μl of loading dye were used to determine the volume of mammalian protein extraction reagent (MPER) based on a total volume of 30 μl (Appendix III).

Protein Separation and Transfer

In each well, 30 μl of protein + dye + MPER solutions were loaded into the stacking gels after boiling for 7 minutes. A molecular weight ladder marker was loaded in the final well to identify the molecular weight locations of proteins on the final membrane. Top-down separation of proteins by molecular weight was performed by applying an electric current between the anode and cathode at a voltage of 100V for 1 hour. The running phase was performed at room temperature in a buffer containing dH_20 (900 ml) and 10X Tris-Glycine + SDS (TGS) (100 ml). After verifying that the dye was below lowest molecular weight marker, the separating phase was terminated. Subsequently, gels were placed against nitrocellulose membranes activated in methanol, which were held between two sets of filter papers. The horizontal transfer of proteins from the gel to the membrane was performed by again applying an electric current between the anode and the cathode at a voltage of 100 V for 1 hour. The transfer phase was performed on ice at -4°C in a buffer containing dH_20 (700 ml), methanol (200 ml) and 10X Tris-Glycine (TG) (100 ml).

Primary and Secondary Antibodies for Tumor Necrosis Factor-α

After the transfer was complete, membranes were blocked for 1 hour with TBST (10X Tris-Buffered Saline (TBS) (100 ml), dH_20 (900 ml) and 20% Tween (10 ml)) containing 2% blocking reagent (GE Lifesciences, Amersham ECL Prime Blocking Reagent, Product code: RPN418) at room temperature. Membranes then were incubated overnight in rabbit polyclonal TNF-α antibody (Abcam Ab-9739, 1:2500

in TBST containing 2% blocking reagent) in hermetically sealed pouches at 4°C on an oscillating table. Subsequently, samples were washed with TBST for three 5-minute intervals to remove residual primary antibody. Membranes were then incubated for 1 hour in goat polyclonal secondary antibody to rabbit IgG (Abcam, Ab-97200, 1:1000 in TBST containing 2% blocking reagent). Subsequently, samples were washed with TBST for three 5-minute intervals to remove residual secondary antibody.

Enhanced Luminol-Based Chemiluminescent Western Blot Detection

Antibody-labeled proteins were detected using an enhanced luminol-based chemiluminescent (ECL) western blot detection kit (GE Lifesciences, Amersham ECL™ Advance, Product code: RPN2135). 500 μl of ECL Advance Solution A and B were mixed in an eppendorf tube and applied to the surface of the membrane. After approximately 1 minute, the membrane was detected using a Fujifilm LAS-1000 detection system (Fujifilm, Sweden). Finally, bands were quantitatively analyzed using a customized macro in ImagePro Plus, which determined the average pixel density of a standardized rectangular area.

Primary and Secondary Antibodies for Glyceraldehyde 3-phosphate dehydrogenase

To normalize TNF-α results for individual patient tissues, stripping buffer was applied to the membrane for 45 minutes at 37C, blocked for 1 hour in TBST containing 2% blocking reagent and incubated overnight in rabbit polyclonal Glyceraldehyde 3-phosphate dehydrogenase (GAPDH, control) primary antibody

(Abcam, Ab-9385, 1:2500 in TBST containing 2% blocking reagent) at 4°C on an oscillating table. Subsequently, samples were washed with TBST for three 5-minute intervals to remove residual primary antibody. Membranes were then incubated for 1 hour in goat polyclonal secondary antibody to rabbit IgG (Abcam, Ab-97200, 1:1000 in TBST containing 2% blocking reagent). Subsequently, samples were washed with TBST for three 5-minute intervals to remove residual secondary antibody. After detection, density results for each TNF-α band were normalized by corresponding GAPDH bands.

Statistical Analysis

For each polyethylene cohort, the size, shape, number and biological activity of polyethylene wear debris were determined after isolation from periprosthetic tissues. To determine whether particle characteristics varied by polyethylene cohort, differences were evaluated by Kruskal-Wallis ANOVA. Strictly where indicated, differences in particle characteristics were evaluated by the Wilcoxon Mann-Whitney test for each polyethylene cohort (CPE versus remelted or annealed HXLPE). Based on the previous analysis of wear particle biological activity from revised total disc replacement components in chapter 4, the sample sizes in the current chapter were sufficiently powered (>90%) to detect a significant difference in the predicated values of functional biological activity. Statistical analysis was performed using JMP 8.0 (SAS Institute Inc, Cary, NC).

Results

Differences in Particle Size, Shape and Number between Conventional and Highly Crosslinked Polyethylene Implant Components

Major differences were observed in the size, shape and number of particles between the CPE cohort and both the annealed and remelted HXLPE cohorts. Comparison of size distributions revealed an increased equivalent circular diameter (ECD) for the CPE cohort compared to the remelted and annealed HXLPE cohort tissues ($p<0.001$, Power=1)(Figure 5-1). Specifically, the mean ECD of particles from the CPE cohort was 26% larger than the remelted and 28% larger than the annealed HXLPE cohort (Table 5-4). For particle shape, >90% of particles were granular or ellipsoidal for all three groups (Figure 5-2). For the HXLPE cohorts, a composite showing the range of particle shapes is provided to assist in the interpretation of particle shape results (Figure 5-3). Comparing aspect ratio distributions, the ratio of length to breadth, particles from the CPE cohort showed a 7% increase ($p<0.001$, Power=1) (Figure 5-4). Similarly, roundness, a measure of circularity based on length, was decreased by 6% for particles from the CPE cohort as compared to both HXLPE cohorts ($p<0.001$, Power=1) (Figure 5-5). The biggest difference in particle morphology was observed in the form factor distribution, a measure of circularity based on perimeter. Specifically, form factor of particles from the CPE cohort was decreased by 17% and 20% compared to the annealed and remelted HXLPE groups, respectively ($p<0.001$, Power=1) (Figure 5-6). Despite these differences, the percentage of fibrils was not significantly different between cohorts, and represented <10% of the total debris (Table 5-4).

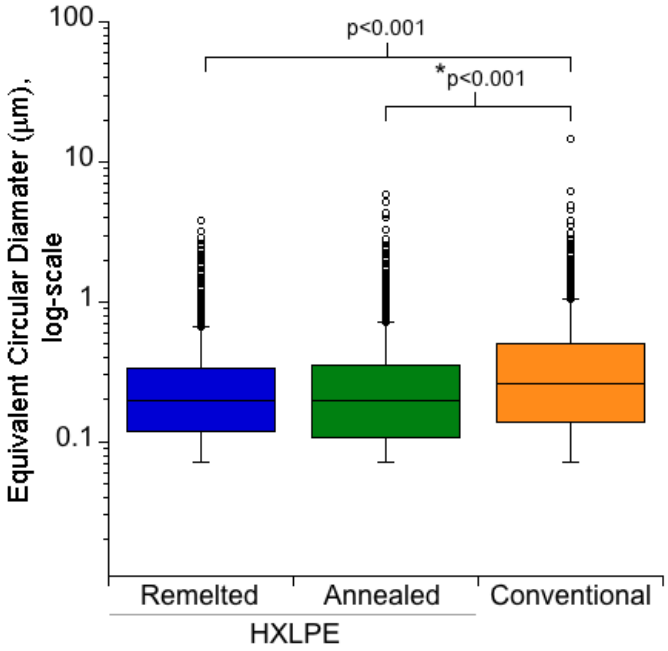

Figure 5-1 Equivalent circular diameter was decreased for both HXLPE cohorts compared to the CPE cohort. For all three polyethylene groups, predominantly submicron-sized particles were observed. The y-axis is shown as a log-scale for easier interpretation of the range of particle sizes. Provided are medians with a boxed range of 25th to 75th percentiles and whiskers showing the 10th and 90th percentiles. Outliers are shown as open circles.

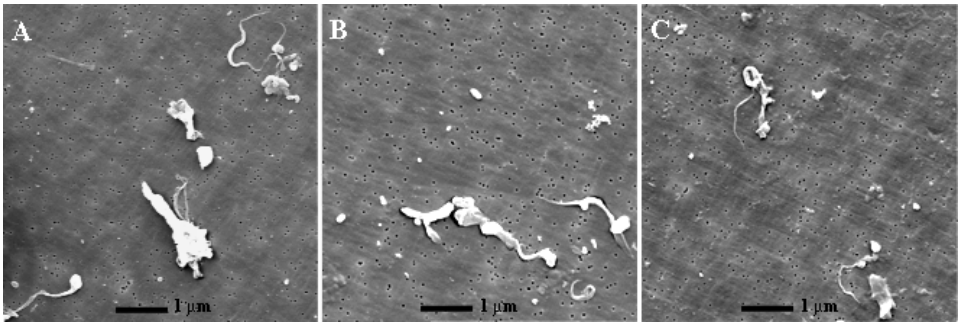

Figure 5-2. Representative images of polyethylene wear debris from (A) CPE, (B) Remelted HXLPE and (C) Annealed HXLPE cohorts

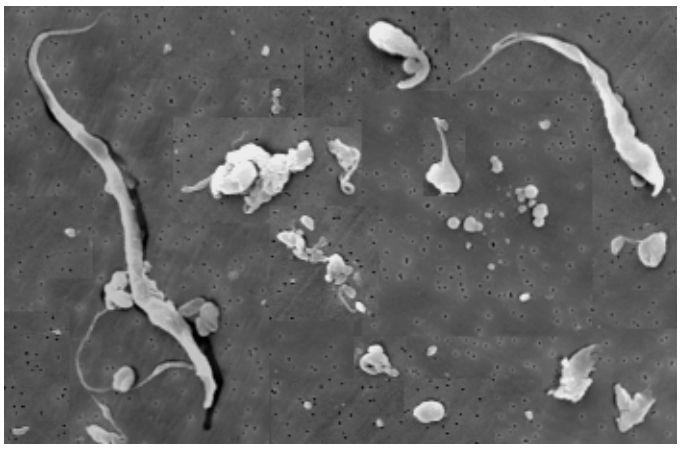

Figure 5-3. Composite showing the range of HXLPE wear particle shapes. Note: Particles were not observed with the spatial frequency that is represented by the composite image. The frequency of particle shapes can be observed in the aspect ratio distribution (showing ratio of length to breadth) in Figure 5-4.

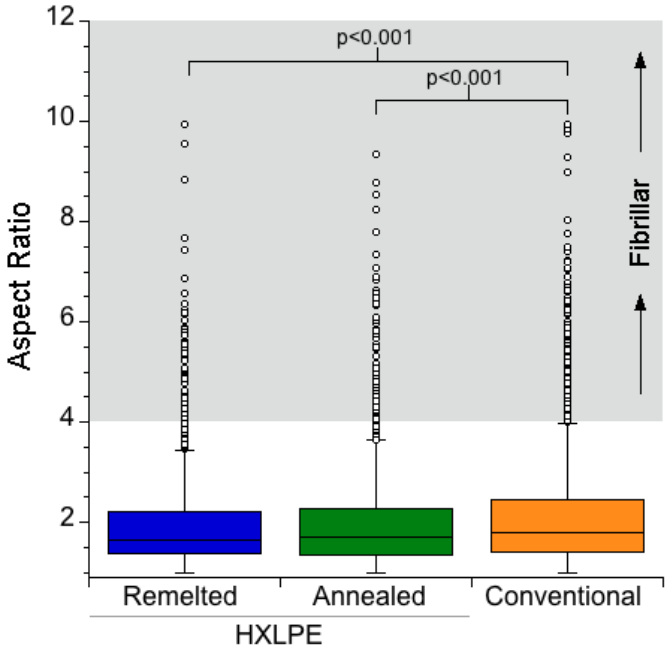

Figure 5-4. Aspect ratio was decreased for particles from both HXLPE cohorts compared to the CPE cohort. Fibrillar particles with an aspect ratios ranging from 4 to 10 were observed in all three polyethylene cohorts. Provided are medians with a boxed range of 25th to 75th percentiles and whiskers showing the 10th and 90th percentiles. Outliers are shown as open circles.

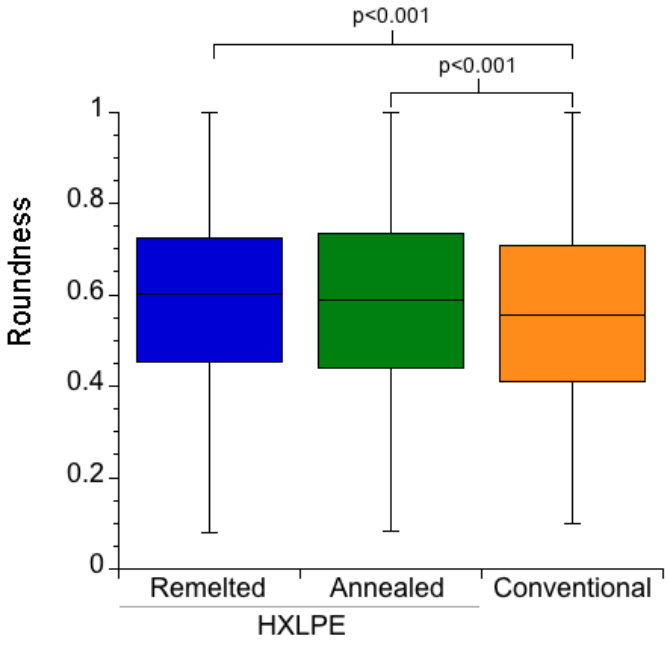

Figure 5-5. Roundness was increased for particles from both HXLPE cohorts compared to the CPE cohort. On a scale of 0-1, increased values of roundness suggest that the particle diameter is more consistent with the area of a circular particle. Provided are medians with a boxed range of 25th to 75th percentiles and whiskers showing the 10th and 90th percentiles.

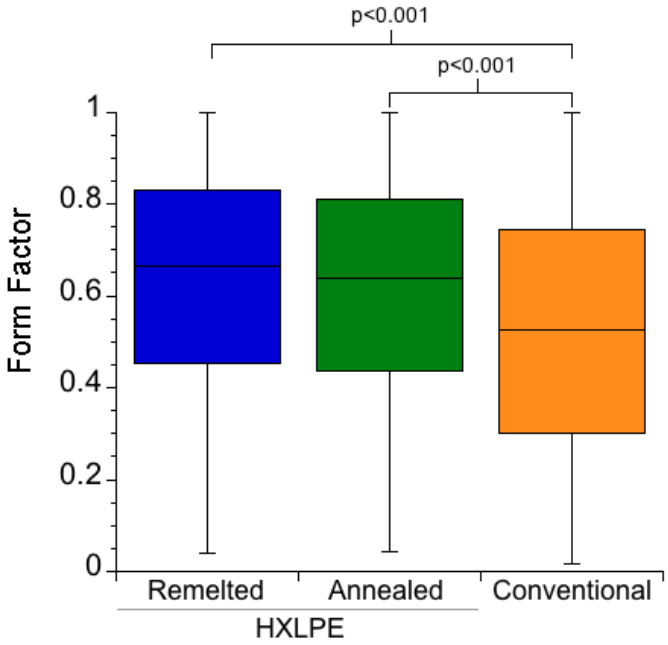

Figure 5-6. Form factor was increased for particles from both HXLPE cohorts compared to the CPE cohort. On a scale of 0-1, increased values of form factor suggest that particle perimeter is more consistent with the area of a circular particle. Provided are medians with a boxed range of 25th to 75th percentiles and whiskers showing the 10th and 90th percentiles.

Table 5-4. Summary of wear particle characteristics

Parameter	Remelted HXLPE Mean ± 1 SD, (Median)	Annealed HXLPE Mean ± 1 SD, (Median)	Conventional Mean ± 1 SD, (Median)	*P* Value
ECD (μm)	0.32 ± 0.37, (0.20)	0.31 ± 0.39, (0.20)	0.43 ± 0.53, (0.26)	***P*<0.001**
AR (unitless)	2.00 ± 1.06, (1.66)	2.01 ± 1.07, (1.70)	2.15 ± 1.13, (1.80)	***P*<0.001**
R (unitless)	0.59 ± 0.19, (0.60)	0.58 ± 0.19, (0.59)	0.55 ± 0.19, (0.56)	***P*<0.001**
FF (unitless)	0.63 ± 0.25, (0.66)	0.61 ± 0.24, (0.64)	0.52 ± 0.26, (0.53)	***P*<0.001**
Fibril (*AR>4*) (%)	4.5 ± 1.7, (4.4)	4.6 ± 2.5, (4.3)	6.1 ± 2.9, (5.8)	*P*=0.396[#]
Total Estimated number/gram (x10^8)	1.23 ± 0.54, (1.09)	1.45 ± 0.45, (1.72)	5.14 ± 3.37, (3.78)	***P*=0.005**
Submicron number (%)	94.8 ± 0.7, (95.3)	94.8 ± 0.2, (94.6)	90.5 ± 3.6, (91.0)	***P*=0.016**
Total Estimated volume (mm^3)/gram ($x10^{-3}$)	0.36 ± 0.05, (0.35)	0.62 ± 0.60, (0.27)	6.47 ± 4.83, (5.73)	***P*=0.006**
Submicron volume (%)	13.4 ± 5.0, (11.5)	12.8 ± 6.2, (12.3)	8.3 ± 5.1, (9.5)	*P*=0.367[#]
SBA	0.31 ± 0.04, (0.29)	0.30 ± 0.05, (0.30)	0.26 ± 0.05, (0.28)	*P*=0.326[#]
FBA ($x10^{-3}$)	0.11 ± 0.03, (0.10)	0.17 ± 0.13, (0.08)	1.51 ± 0.93, (1.49)	***P*=0.014**

[#] Kruskal-Wallis ANOVA. Abbreviations: SD, standard deviation; ECD, equivalent circular diameter; AR, aspect ratio; R, roundness; FF, form factor; SBA, specific biological activity; FBA, functional biological activity.

After normalizing particle number per gram of tissue, the mean number of particles in the CPE cohort was 72% higher than the annealed and 76% higher than the remelted HXLPE cohorts (p=0.005, Power=0.923) (Figure 5-7). However, in both HXLPE cohorts, submicron particles represented ~95% of the total debris, which was significantly higher than the 90% found in CPE cohort tissues (p=0.016, Power=0.816) (Figure 5-8).

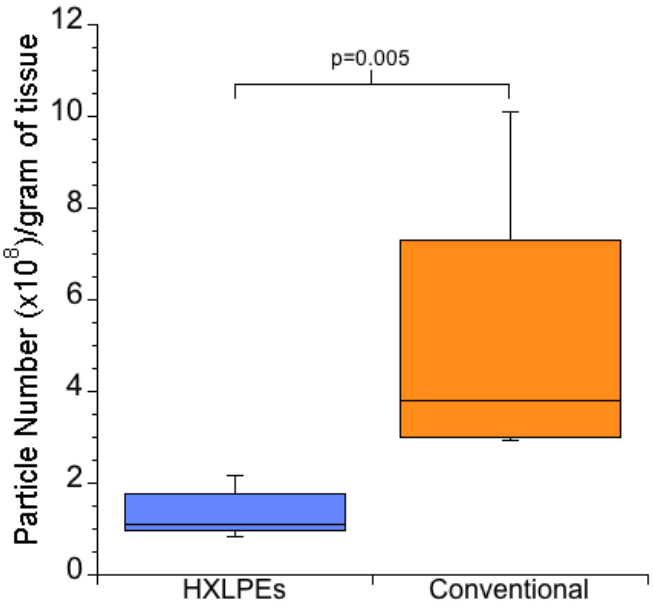

Figure 5-7. Total particle number (per gram of tissue) was significantly decreased for both HXLPE cohorts compared to the CPE cohort. The column labeled "HXLPEs" represents the combined data from remelted and annealed HXLPE cohorts. Provided are medians with a boxed range of 25th to 75th percentiles and whiskers showing the 10th and 90th percentiles.

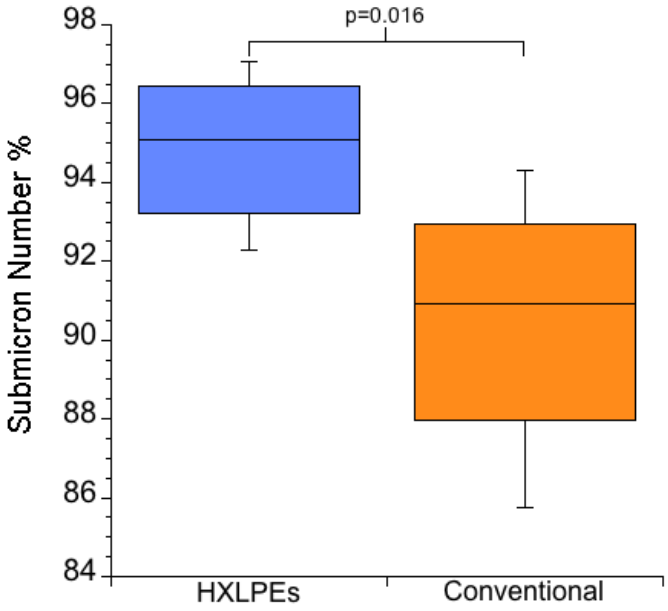

Figure 5-8. The number percentage of submicron particles was significantly increased for both HXLPE cohorts compared to the CPE cohort. The column labeled "HXLPEs" represents the combined data from remelted and annealed HXLPE cohorts. Provided are medians with a boxed range of 25th to 75th percentiles and whiskers showing the 10th and 90th percentiles.

Differences in Particle Volume and Biological Activity between Conventional and Highly Crosslinked Polyethylene Implant Components

To determine the specific biological activity per unit volume (SBA), particles were separated by size ranges that represent high (<0.1-1 μm), intermediate (1-10 μm) and low (>10 μm) biological relevance. Initially comparing the percentages of particle volume (mm^3) in each size range revealed no significant differences between cohorts (Table 5-4). The volume percentage in each size range was then normalized by a ranked biological activity scalar to determine particle SBA, which was also comparable between polyethylene cohorts (Table 5-4).

On the contrary, major differences were observed between polyethylene cohorts when total particle volume (mm^3) was normalized per gram of tissue. Specifically, the increased particle size (>25%) and number/gram (>70%) of CPE wear debris contributed to a >90% increase in particle volume (mm^3)/gram compared to the annealed and remelted HXLPE cohorts ($p=0.006$, Power=0.966) (Figure 5-9). Similarly, after normalizing SBA by the total particle volume (mm^3)/gram to obtain functional biological activity (FBA), significant increases were observed for particles from the CPE cohort compared to both HXLPE cohorts ($p=0.014$, Power=0.995) (Figure 5-10).

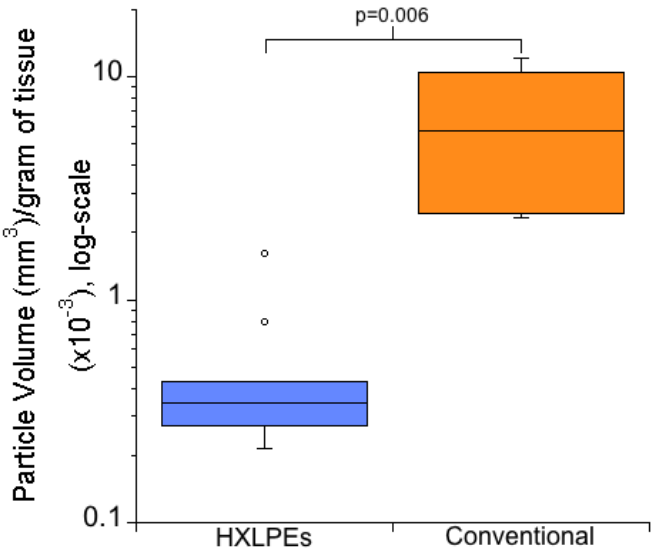

Figure 5-9. Particle volume (mm^3) per gram of tissue was significantly lower for both HXLPE cohorts compared to the CPE cohort. The y-axis is shown as a log-scale for easier interpretation of the entire range of particle volume data. The column labeled "HXLPEs" represents the combined data from remelted and annealed HXLPE cohorts. Provided are medians with a boxed range of 25th to 75th percentiles and whiskers showing the 10th and 90th percentiles. Outliers are shown as open circles.

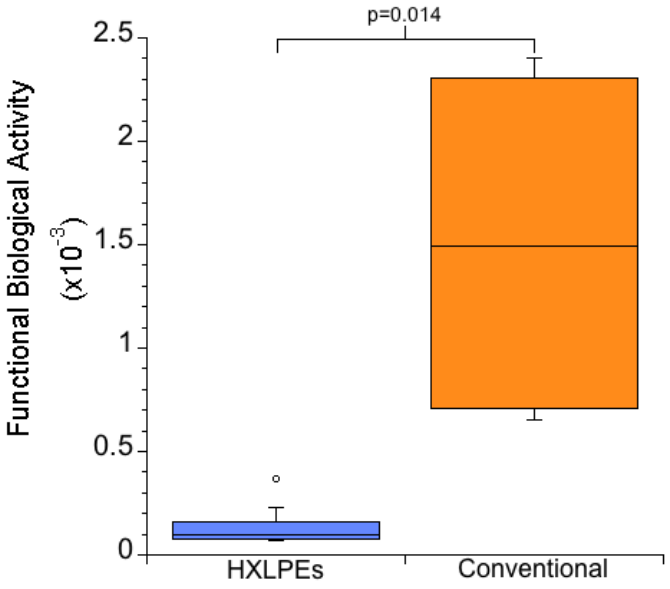

Figure 5-10. After normalizing specific biological activity by the total particle volume (mm3)/gram of tissue, functional biological activity was significantly lower for both HXLPE cohorts compared to the CPE cohort. The column labeled "HXLPEs" represents the combined data from remelted and annealed HXLPE cohorts. Provided are medians with a boxed range of 25th to 75th percentiles and whiskers showing the 10th and 90th percentiles. Outliers are shown as open circles.

Of note, the largest value of FBA for the HXLPE cohort was from an annealed HXLPE liner revised for malposition after implantation for 5.2 years (Figure 5-9). The increased particle volume generated by this abnormal wear condition was predominantly due to an increase in overall particle size.

Western Blot Analysis of Tumor Necrosis Factor-Alpha

Tumor necrosis factor (TNF)-α tissue levels were evaluated by Western blot for comparison to the *in vitro* model of particle biological activity response [50]. TNF-α bands were quantified by densitometry and normalized by GAPDH bands. Particle characteristics and biological activity were also collected to evaluate potential correlations with TNF-α levels in individual tissues. Between individual patient variables, a positive correlation was observed between increasing implantation time and increasing particle number/gram (ρ=0.821, p=0.023). Correlations were also observed between decreasing Specific Biological Activity and increasing particle size (ρ=-0.821, p=0.023) as well as increasing Functional Biological Activity (ρ=-0.893, p=0.007). For TNF-α levels, the small number of tissue samples and the variability between repeated measures limited the ability to determine statistically significant trends between particle characteristics or implantation time. Generally, TNF-α levels were decreased in tissue samples from the two patients with the longest implantation time.

Table 5-5. Summary of particle characteristics and biological activity

Sample Number	Sample ID	Implantation Time (years)	Particle Number ($x10^9$/gram)	Mean Particle Size (μm)	Specific Biological Activity	Functional Biological Activity
1 (C)	H209 (I)	15.6	3.25	0.42	0.25	1.58
2 (C)	H215 (I)	15.4	1.79	0.50	0.20	1.52
3 (C)	H286 (II)	8.6	0.29	0.34	0.27	2.21
4 (C)	H346 (II)	2.3	1.01	0.51	0.18	2.40
5 (C)	H199 (III)	2	0.10	0.31	0.30	0.08
6 (C)	H311 (III)	1.7	0.11	0.37	0.32	0.12
7 (C)	H194 (III)	5.4	0.97	0.27	0.33	0.07
I, gamma air-sterilized polyethylene; II, gamma inert-sterilized polyethylene; III, annealed highly crosslinked polyethylene						

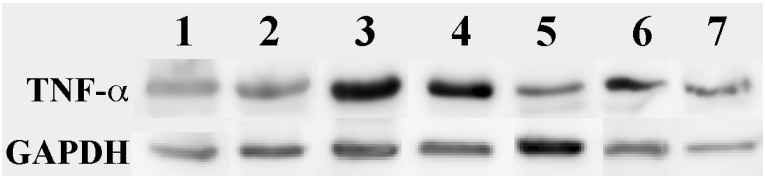

Figure 5-11. Representative TNF-α and GAPDH bands showing protein levels for individual patient tissues.

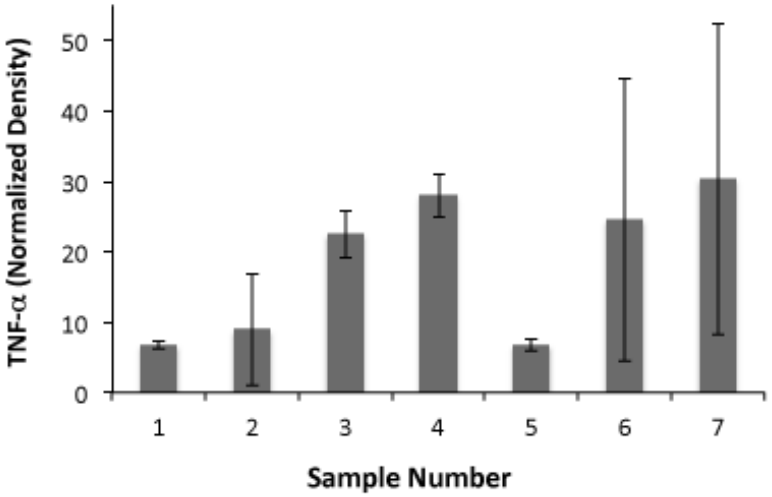

Figure 5-12. TNF-α normalized density values for individual patient tissues showing the mean and standard deviation obtained from repeated measures.

Discussion

Despite the widespread implementation of highly crosslinked polyethylene (HXLPE) liners to reduce the clinical incidence of osteolysis, it is unknown if the substantially improved wear resistance will outweigh the inflammatory potential of HXLPE wear debris generated *in vivo*. To address this important unanswered issue, differences in size, shape, number and biological activity of polyethylene wear particles were determined for tissues obtained during primary THA revision surgery of CPE versus remelted or annealed HXLPE liners.

The current chapter contains the following limitations: (i) The analysis of wear debris from pseudocapsular tissues may represent a conservative estimate of the total number of particles and/or inflammatory cytokines in the environment surrounding the joint. However, selecting the same tissue region for all three polyethylene cohorts does not introduce additional bias in the current comparison of wear particle characteristics. (ii) The lower size limit of wear debris was determined using polycarbonate membranes with a pore size of 0.05 μm. Similar to the interpretation from Chapter 4, this pore size is only expected to exclude a small percentage (~2.8%) of particles whose biological activity is still under investigation *in vitro* [53-56].

Similar to a prior study of HXLPE in TKA by Iwakiri et al., (2008), the current study showed that both remelted and annealed first-generation HXLPE liners used in THA generated significantly fewer, smaller, and rounder particles than CPE liners [57]. To the author's knowledge, the study by Iwakiri et al., (2008) was the only other study comparing HXLPE and CPE wear debris isolated from tissues obtained at the time of revision surgery, albeit from TKA instead of the current comparison of particles from THA. In addition, the current study determined wear particle volume, which was reduced for both HXLPE cohorts, and resulted in a significant decrease in functional biological activity compared to the CPE cohort. Other investigations of HXLPE wear debris *in vivo* are limited to two case studies of THA liners, both of which were revised after the development of severe wear conditions [31, 32]. In the first case study, re-revision of a cemented THA was performed after 4 years

following the collapse of a hydroxyapetite (HA) impaction graft. Scanning electron microscopy (SEM) analysis showed a mean particle size of 0.66 μm, which was >2-fold larger than in the current study (0.31 μm). This size difference may be attributed to their methodological exclusion of <0.2 μm particles, the effect of HA granules embedded in the acetabular liner and/or the effect of using tissue samples from re-revision THA. In addition, their summary of particle shape showing a maximum aspect ratio of 2.4 was considerably different than the current findings, which identified aspect ratios as large as 10 in both HXLPE cohorts. In particular, for the study by Minoda et al., (2008), it was anticipated that the particle aspect ratio would be larger than 2.4 given the observation of HA granules embedded in the acetabular liner. In the second study, revision of a cemented THA was performed after 2 years due to osteolysis and impingement of the acetabular rim. Polarized light and SEM analysis of periprosthetic tissue sections indicated that particle size ranged from 1-5 μm, but a full particle characterization was not performed [41].

In agreement with the current findings, *in vitro* studies evaluating differences in wear debris from CPE and HXLPE liners have shown decreased HXLPE particle size and a concomitant increase in the percentage of submicron particles for these liners [34, 38, 58]. Overall, the mean HXLPE particle size in the current study, 0.31 μm, falls within the ranges reported for the articulation of HXLPE against smooth (0.08 to 0.26 μm) [35, 38, 43, 45] and artificially roughened counterfaces (0.39-0.50 μm) [40, 59].

Similar to *in vitro* characterizations of particle shape, particle morphology was predominantly granular or ellipsoidal, with fibrils occurring at a frequency of ~5% in both HXLPE cohorts [40, 45]. In a separate *in vitro* study, the incidence of fibrils (aspect ratio >4) decreased with increasing crosslinking dose; whereas, a difference in the percentage of fibrils was not detected between polyethylene cohorts [34]. In a unifying publication of wear, Wang et al., (2001) described the formation of fibrillar extensions on the bearing surface along the predominant direction of wear [60]. Thus, fibrillar debris observed in this study may represent the liberation of these surface extensions after high levels of cross-shear and multidirectional loading *in vivo*. These findings are concerning given studies showing increased gene expression of IL-1β and TNF-α in response to fibrils in a murine model of osteolysis [61, 62].

In vitro studies have consistently reported a decrease in component wear of HXLPE liners compared to CPE [35, 38, 59]. However, the current results showing a reduced number of HXLPE particles lacks a clear consensus *in vitro*, with studies reporting decreased, similar and increased particle numbers for HXLPE liners compared to CPE [34, 40, 43]. The current findings for particle number more consistently agree with *in vitro* studies showing an increased percentage of submicron particles generated from HXLPE liners compared to CPE liners [33, 38, 58].

For particle volume distribution, the current particle data most closely agree with a recent study investigating the biological activity of wear debris generated

from HXLPE and CPE liners *in vitro* [63]. In their study and in the current chapter, neither the distribution of particle volume nor the relative biological activity per unit volume of wear debris (specific biological activity, SBA) were significantly different between polyethylene cohorts. Others have also observed similar values of SBA after testing HXLPE and CPE liners against artificially roughened counterfaces [40, 58] Mean values of SBA in the current study, 0.31 for both HXLPE cohorts, were again within the range of values (0.86 and 0.08) previously reported for articulation of HXLPE against smooth and artificially roughened counterfaces, respectively [40, 63].

In the current study and others, increases in the level of crosslinking resulted in a significant reduction in the total volume of HXLPE wear debris [40, 63]. Thus, despite an increased percentage of submicron particles in both HXLPE cohorts, this assessment of wear debris from pseudocapsular hip tissues ultimately revealed a significant decrease in functional biological activity (FBA) for both HXLPE cohorts.

TNF-α tissue levels were evaluated by Western blot for comparison to the *in vitro* model of particle biological activity response [50]. For the current polyethylene cohorts, functional biological activity proved to be useful in distinguishing differences in wear particles generated *in vivo*. However, for the Western Blot analysis, the number of patient samples and the large amount of patient variability were limiting to the determination of statistically significant trends between TNF-α and wear particle characteristics or implantation time. Nevertheless, for the samples with the longest implantation, quantification of the

bands consistently revealed a lower amount of TNF-α despite the largest particle number/gram of tissue. Despite its pivotal role in early stages of inflammation, recent work by Shanbhag et al., (2007) has also identified a decreased involvement of TNF-α in well-established osteolytic responses [64]. A potential explanation for this finding is the effect of progressive tissue necrosis after cell apoptosis, which would diminish the baseline inflammatory potential of the affected tissue region [65]. For the two tissue samples obtained from revision surgery of gamma inert-sterilized polyethylene components, TNF-α levels were consistently higher, which is more consistent with results previously obtained *in vitro*. Additional studies will be necessary to expand the number of patient tissues and to pursue alternate cytokines with an increased relevance to both early and late stages of wear particle-induced inflammatory responses *in vivo*.

Overall, the current data provide a direct confirmation that the osteolytic potential of HXLPE wear debris *in vivo* is outweighed by a significant improvement in wear resistance. The lack of agreement previously shown between gravimetric wear and particle number *in vitro* [44] highlights the importance of evaluating the characteristics and biological activity of wear debris from THA revision tissues.

Acknowledgements

Special thanks to Christine Macolino and Carol Diallo for their instructional guidance related to the Western Blot analyses performed at Thomas Jefferson University. In addition, thanks to Dee Breger and Dr. Edward Basgall of the

Centralized Research Facility at Drexel University for their training and for answering all of my ESEM questions.

References

1. Willert, H.G., H. Bertram, and G.H. Buchhorn, *Osteolysis in alloarthroplasty of the hip. The role of ultra-high molecular weight polyethylene wear particles.* Clinical Orthopaedics & Related Research, 1990(258): p. 95-107.
2. Purdue, P.E., et al., *The central role of wear debris in periprosthetic osteolysis.* Hss J, 2006. 2(2): p. 102-13.
3. Goodman, S.B., *Wear particles, periprosthetic osteolysis and the immune system.* Biomaterials, 2007. 28(34): p. 5044-8.
4. Harris, W.H. and O.K. Muratoglu, *A review of current cross-linked polyethylenes used in total joint arthroplasty.* Clinical Orthopaedics & Related Research, 2005(430): p. 46-52.
5. Kurtz, S.M., *The UHMWPE Biomaterials Handbook: Ultra-High Molecular Weight Polyethylene in Total Joint Replacement and Medical Devices*. 2nd Edition ed. 2009, Burlington, MA Academic Press.
6. McKellop, H., et al., *Development of an extremely wear-resistant ultra high molecular weight polyethylene for total hip replacements.* J Orthop Res, 1999. 17(2): p. 157-67.
7. Muratoglu, O.K., et al., *A novel method of cross-linking ultra-high-molecular-weight polyethylene to improve wear, reduce oxidation, and retain mechanical properties. Recipient of the 1999 HAP Paul Award.* J Arthroplasty, 2001. 2001: p. 149-160.
8. Oral, E. and O.K. Muratoglu, *Radiation cross-linking in ultra-high molecular weight polyethylene for orthopaedic applications.* Nucl Instrum Methods Phys Res B, 2007. 265(1): p. 18-22.
9. Gomez-Barrena, E., F. Medel, and J.A. Puertolas, *Polyethylene oxidation in total hip arthroplasty: evolution and new advances.* Open Orthop J, 2009. 3: p. 115-20.
10. Kurtz, S.M., et al., *Mechanical properties of retrieved highly cross-linked crossfire liners after short-term implantation.* J Arthroplasty, 2005. 20(7): p. 840-9.
11. Rajadhyaksha, A.D., et al., *Five-year comparative study of highly cross-linked (crossfire) and traditional polyethylene.* J Arthroplasty, 2009. 24(2): p. 161-7.
12. Digas, G., et al., *5-year experience of highly cross-linked polyethylene in cemented and uncemented sockets: two randomized studies using radiostereometric analysis.* Acta Orthopaedica, 2007. 78(6): p. 746-54.
13. D'Antonio, J.A., et al., *Five-year experience with Crossfire highly cross-linked polyethylene.* Clin Orthop Relat Res, 2005. 441: p. 143-50.

14. Olyslaegers, C., et al., *Wear in conventional and highly cross-linked polyethylene cups: a 5-year follow-up study.* Journal of Arthroplasty, 2008. 23(4): p. 489-94.
15. Geerdink, C.H., et al., *Crosslinked polyethylene compared to conventional polyethylene in total hip replacement: pre-clinical evaluation, in-vitro testing and prospective clinical follow-up study.* Acta Orthopaedica, 2006. 77(5): p. 719-25.
16. Engh, C.A., Jr., et al., *A randomized prospective evaluation of outcomes after total hip arthroplasty using cross-linked marathon and non-cross-linked Enduron polyethylene liners.* J Arthroplasty, 2006. 21(6 Suppl 2): p. 17-25.
17. Rohrl, S.M., et al., *Very low wear of non-remelted highly cross-linked polyethylene cups: an RSA study lasting up to 6 years.* Acta Orthopaedica, 2007. 78(6): p. 739-45.
18. Geerdink, C.H., et al., *Cross-linked compared with historical polyethylene in THA: an 8-year clinical study.* Clin Orthop Relat Res, 2009. 467(4): p. 979-84.
19. Kurtz, S.M., et al., *Mechanical properties, oxidation, and clinical performance of retrieved highly cross-linked Crossfire liners after intermediate-term implantation.* Journal of Arthroplasty, 2010. 25(4): p. 614-23 e1-2.
20. Kurtz, S.M., H.A. Gawel, and J. Patel, *History and Systematic Review of Wear and Osteolysis Outcomes for First-Generation Highly Crosslinked Polyethylene.* Clin Orthop Relat Res, 2011. Epub Mar 23.
21. Langlois, J. and M. Hamadouche, *New animal models of wear-particle osteolysis.* Int Orthop, 2011. 35(2): p. 245-51.
22. Costa, L., et al., *In vivo UHMWPE biodegradation of retrieved prosthesis.* Biomaterials, 1998. 19(15): p. 1371-1385.
23. Kurtz, S.M., et al., *2006 Otto Aufranc Award Paper: significance of in vivo degradation for polyethylene in total hip arthroplasty.* Clin Orthop Relat Res, 2006. 453: p. 47-57.
24. Maitra, R., et al., *Immunogenecity of modified alkane polymers is mediated through TLR1/2 activation.* PLoS One, 2008. 3(6): p. e2438.
25. Ferroni, D. and V. Quaglini, *Thermal stabilization of highly crosslinked UHMWPE: a comparative study between annealed and remelted resins.* J Appl Biomater Biomech, 2010. 8(2): p. 82-8.
26. Pruitt, L.A., *Deformation, yielding, fracture and fatigue behavior of conventional and highly cross-linked ultra high molecular weight polyethylene.* Biomaterials, 2005. 26(8): p. 905-15.
27. Oral, E., A.S. Malhi, and O.K. Muratoglu, *Mechanisms of decrease in fatigue crack propagation resistance in irradiated and melted UHMWPE.* Biomaterials, 2006. 27(6): p. 917-25.
28. Tower, S.S., et al., *Rim cracking of the cross-linked longevity polyethylene acetabular liner after total hip arthroplasty.* J Bone Joint Surg Am, 2007. 89(10): p. 2212-7.
29. Furmanski, J., et al., *Clinical fracture of cross-linked UHMWPE acetabular liners.* Biomaterials, 2009. 30(29): p. 5572-82.

30. Schroder, D.T., et al., *Retrieved highly crosslinked UHMWPE acetabular liners have similar wear damage as conventional UHMWPE.* Clin Orthop Relat Res, 2011. 469(2): p. 387-94.
31. Bradford, L., et al., *Early failure due to osteolysis associated with contemporary highly cross-linked ultra-high molecular weight polyethylene. A case report.* Journal of Bone & Joint Surgery - American Volume, 2004. 86-A(5): p. 1051-6.
32. Minoda, Y., et al., *Wear particle analysis of highly crosslinked polyethylene isolated from a failed total hip arthroplasty.* Journal of Biomedical Materials Research, 2008. Part B, Applied Biomaterials. 86B(2): p. 501-5.
33. Endo, M.M., et al., *Comparative wear and wear debris under three different counterface conditions of crosslinked and non-crosslinked ultra high molecular weight polyethylene.* Biomed Mater Eng, 2001. 11(1): p. 23-35.
34. Yamamoto, K., et al., *Microwear phenomena of ultrahigh molecular weight polyethylene cups and debris morphology related to gamma radiation dose in simulator study.* Journal of Biomedical Materials Research, 2001. 56(1): p. 65-73.
35. Saikko, V., O. Calonius, and J. Keranen, *Wear of conventional and cross-linked ultra-high-molecular-weight polyethylene acetabular cups against polished and roughened CoCr femoral heads in a biaxial hip simulator.* J Biomed Mater Res, 2002. 63(6): p. 848-53.
36. Cho, D.R., et al., *The role of adsorbed endotoxin in particle-induced stimulation of cytokine release.* J Orthop Res, 2002. 20(4): p. 704-13.
37. Oonishi, H., et al., *Assessment of wear in extensively irradiated UHMWPE cups in simulator studies.* J Biomed Mater Res A, 2004. 68(1): p. 52-60.
38. Affatato, S., et al., *Wear behaviour of cross-linked polyethylene assessed in vitro under severe conditions.* Biomaterials, 2005. 26: p. 8.
39. Williams, P.A., et al., *Highly Crosslinked Polyethylenes in Hip Replacements: Improved Wear Performance of Paradox?* STLE Tribology Transactions, 2007. 50(2): p. 227-290.
40. Bowsher, J.G., et al., *"Severe" wear challenge to 36 mm mechanically enhanced highly crosslinked polyethylene hip liners.* Journal of Biomedical Materials Research, 2008. Part B, Applied Biomaterials. 86(1): p. 253-63.
41. Burroughs, B.R., et al., *Comparison of conventional and highly crosslinked UHMWPE patellae evaluated by a new in vitro patellofemoral joint simulator.* J Biomed Mater Res B Appl Biomater, 2006. 79(2): p. 268-74.
42. Utzschneider, S., et al., *Influence of design and bearing material on polyethylene wear particle generation in total knee replacement.* Acta Biomater, 2009. 5(7): p. 2495-502.
43. Scott, M., et al., *Particle Analysis for the Determination of UHMWPE Wear.* Journal of Biomedical Materials Research: Applied Biomaterials, 2005. 73B: p. 325-337.
44. Ries, M.D., M.L. Scott, and S. Jani, *Relationship between gravimetric wear and particle generation in hip simulators: conventional compared with cross-linked polyethylene.* Journal of Bone & Joint Surgery - American Volume, 2001. 83-A Suppl 2 Pt 2: p. 116-22.

45. Illgen, R.L., 2nd, et al., *Highly crosslinked vs conventional polyethylene particles--an in vitro comparison of biologic activities.* Journal of Arthroplasty, 2008. 23(5): p. 721-31.
46. Sabokbar, A., et al., *Human arthroplasty derived macrophages differentiate into osteoclastic bone resorbing cells.* Ann Rheum Dis, 1997. 56(7): p. 414-20.
47. Green, T.R., et al., *Polyethylene particles of a 'critical size' are necessary for the induction of cytokines by macrophages in vitro.* Biomaterials, 1998. 19(24): p. 2297-302.
48. Green, T.R., et al., *Effect of size and dose on bone resorption activity of macrophages by in vitro clinically relevant ultra high molecular weight polyethylene particles.* J Biomed Mater Res, 2000. 53(5): p. 490-7.
49. *F 1877-05e Standard Practice for Characterization of Particles*, in *ASTM International*. 2005.
50. Fisher, J., et al., *A novel method for the prediction of functional biological activity of polyethylene wear debris.* Proceedings of the Institution of Mechanical Engineers. Part H - Journal of Engineering in Medicine, 2001. 215(2): p. 127-32.
51. Matthews, J.B., et al., *Comparison of the response of primary human peripheral blood mononuclear phagocytes from di!erent donors to challenge with model polyethylene particles of known size and dose.* Biomaterials, 2000. 21: p. 2033-2044.
52. Scott, M., K. Widding, and S. Jani, *Do current wear particle isolation procedures underestimate the number of particles generated by prosthetic bearing components.* Wear, 2001. 251: p. 1213-1217.
53. Tipper, J.L. *The Biological Response to Nanometre-Sized Particles*. in *4th UHMWPE International Meeting*. 2009. Torino, Italy.
54. Howling, G.I., et al., *Quantitative characterization of polyethylene debris isolated from periprosthetic tissue in early failure knee implants and early and late failure Charnley hip implants.* J Biomed Mater Res, 2001. 58(4): p. 415-20.
55. Gallo, J., M. Slouf, and S.B. Goodman, *The relationship of polyethylene wear to particle size, distribution, and number: A possible factor explaining the risk of osteolysis after hip arthroplasty.* J Biomed Mater Res B Appl Biomater, 2010. 94(1): p. 171-7.
56. Revell, P.A., *The biological effects of nanoparticles.* Nanotechnology Perceptions, 2006. 2: p. 283-298.
57. Iwakiri, K., et al., *In Vivo Comparison of Wear Particles Between Highly Crosslinked Polyethylene and Conventional Polyethylene in the Same Design of Total Knee Arthroplasties.* J Biomed Mater Res B Appl Biomater, 2009. 91: p. 799-804.
58. Endo, M., et al., *Comparison of wear, wear debris and functional biological activity of moderately crosslinked and non-crosslinked polyethylenes in hip prostheses.* Proc IME HJ Eng Med, 2002. 216(2): p. 111-22.
59. Saikko, V., O. Calonius, and J. Keranen, *Effect of counterface roughness on the wear of conventional and crosslinked ultrahigh molecular weight polyethylene*

studied with a multi-directional motion pin-on-disk device. J Biomed Mater Res, 2001. 57(4): p. 506-12.

60. Wang, Z., et al., *Modulation of nitric oxide on lymphokine-activated killer cells in patients with bladder cancer.* Chin Med Sci J, 2001. 16(4): p. 213.
61. Ren, W., et al., *Distinct gene expression of receptor activator of nuclear factor-kappaB and rank ligand in the inflammatory response to variant morphologies of UHMWPE particles.* Biomaterials, 2003. 24(26): p. 4819-26.
62. Yang, S., et al., *Diverse cellular and apoptotic responses to variant shapes of UHMWPE particles in a murine model of inflammation.* Biomaterials, 2002. 23: p. 3535-3543.
63. Galvin, A.L., et al., *Wear and biological activity of highly crosslinked polyethylene in the hip under low serum protein concentrations.* Proceedings of the Institution of Mechanical Engineers, 2007. Part H - Journal of Engineering in Medicine. 221(1): p. 1-10.
64. Shanbhag, A.S., et al., *Assessing osteolysis with use of high-throughput protein chips.* Journal of Bone & Joint Surgery - American Volume, 2007. 89(5): p. 1081-9.
65. Fang, H.W., et al., *The potential role of phagocytic capacity in the osteolytic process induced by polyethylene wear particles.* Journal of International Medical Research, 2006. 34(6): p. 655-64.

Conclusion

For highly crosslinked polyethylene THA components as well as mobile-bearing TDRs, osteolysis is rarely observed at the time of revision surgery performed after 5-10 years. Much of what is known about these devices was originally derived from *in vitro* wear simulations. However, the true complexity of *in vivo* implant wear is not fully reproduced by *in vitro* wear simulations, and computer models are only beginning to address the combined effects of multiple variables. The lack of agreement previously shown between gravimetric wear and particle number *in vitro* further highlights the importance of evaluating the characteristics and biological activity of wear debris from revision tissues.

The previous chapters discussed several unknown issues related to the effects of polyethylene wear on the performance of total joint replacement components in the hip and, briefly, in the spine. Specifically, the current dissertation addresses the following questions: (1) What is the comparative efficiency of established tissue digestion methods for polyethylene wear particle extraction? (2) What morphological changes and immune cells are present in tissues obtained at early revision surgery of loosened highly crosslinked polyethylene (HXLPE) components in the absence of radiographic osteolysis? (3) How do modes of implant wear affect the biological activity of polyethylene wear debris generated *in vivo*? (4) Can the reduced incidence of osteolysis around HXLPE components be attributed to a decrease in the biological activity of polyethylene wear debris generated *in vivo*?

The initial chapter evaluated a wide range of digestion conditions for polyethylene wear particle extraction, which have been shown to vary considerably within the published literature with little indication of their relative efficiency. In this comparison of tissue digestion methods, porcine and human hip tissues were exposed to basic, acidic or enzymatic agents, which revealed significantly increased digestion efficiency for 5*M* sodium hydroxide (NaOH), 5 and 15*M* potassium hydroxide (KOH), or 15.8*M* nitric acid (HNO_3). For reagents with the highest tissue digestion efficiency, compatibility was confirmed for GUR415 polyethylene powder, Ceridust 3715 HDPE particles using scanning electron microscopy. In addition, for concentrated nitric acid, compatibility was confirmed for the polycarbonate membrane used in subsequent steps of polyethylene particle filtration. In an earlier investigation, nitric acid was shown to have limited effect on metal wear debris after short intervals of exposure. Overall, these results provided a framework for thorough and efficient digestive methods for polyethylene wear debris extraction.

In chapter 2, attention was focused on tissues collected during revision surgery of gamma air-sterilized conventional polyethylene (CPE) and highly crosslinked polyethylene (HXLPE) implant components. For the CPE cohort, evaluation of the incidence (image %), degree (qualitative rank) and co-localization of histomorphologic changes and wear (overlapping full-field arrays in brightfield and polarized light) revealed predominantly histiocytes and giant cells associated with polyethylene wear debris, along with frequent focal regions of necrosis. For the HXLPE cohort, inflammation and associated wear debris were limited, but in tissues

from patients revised after implantation times of longer than 2 years a response was observed; whereas significant amounts of fibrocartilage/bone, potentially due to micromotion, were observed at earlier implantation times. Based on the infrequent observation of radiographic osteolysis in patients receiving HXLPE implant components, the tissue responses (moderate numbers of histiocytes, necrosis, fibrocartilage) observed in these nine patients with aseptic loosening may represent the contribution of factors other than polyethylene wear debris, particularly at the earliest time points.

In chapter 3, tissue samples from gamma air-sterilized CPE and HXLPE implant components were evaluated to examine potential correlations between polyethylene wear debris and immune cells after revision THA. Differences in the aggregate immune cell responses were also evaluated for separate tissue regions from each cohort. For the CPE cohort, correlations were observed between wear debris and the magnitude of individual patient macrophage and T cell responses and between the overall number of macrophages and T cells in revision tissues. In comparison, the HXLPE cohort showed a correlation between polyethylene wear debris and the magnitude of macrophage responses and between the overall number of macrophages and T cells. Although macrophages and T cells were present in both cohorts, the HXLPE cohort had lower numbers, which may be associated with shorter implantation times. The results from this chapter highlight the variability among individual tissue sections, anatomical regions and individual patients. For both cohorts, positive correlations between macrophages and

polyethylene wear debris as well as the concomitant presence of macrophages and T cells indicate a combined role of innate and adaptive immune cells in the inflammatory response to polyethylene wear debris. Moreover, these data show that although implant loosening is a complex process involving surgical, patient and implant-specific factors, the presence of polyethylene wear debris and inflammation in HXLPE revision tissues may contribute to the process of loosening at early- to mid-term implantation. Based on the current findings, the effect of HXLPE wear debris after long-term implantation remains of crucial interest.

In chapter 4, polyethylene wear debris was investigated for a cohort of mobile-bearing total disc replacements (TDRs) to determine the effect of multiple wear modes. Initially, it was anticipated that the generation of wear debris would be minimal based on previous studies of TDRs *in vitro*. On the contrary, the current results identified a significant number of particles ($>10^9$) per gram of tissue. Further, it was observed that the characteristics of polyethylene wear debris were negatively affected by unanticipated wear modes such as impingement, which manifested itself as a concentrated region of damage at the polyethylene rim. When considering all TDRs regardless of impingement groups, increasing rim penetration was correlated with both increasing particle size and number. For TDRs with mild rim damage, the specific biological activity (SBA) per unit particle volume was increased due to an increased volume percentage of 0.1-1 μm and 1-10 μm polyethylene wear debris. On the contrary, for TDRs with severe rim damage, the increased number of particles in the 1-10 μm range, and larger particles in the >10

μm size range contributed to an increase in the total volume (mm^3)/gram of tissue. Accordingly, when SBA was normalized by polyethylene particle volume (mm^3)/gram tissue, functional biological activity (FBA) of the chronic impingement group was increased. For the single TDR revised for osteolysis, equal percentages of rim and dome penetration contributed to the increase in both SBA and FBA for this case study. The results of this study suggest that chronic rim impingement increases the production of biologically relevant polyethylene particles from mobile-bearing lumbar TDR components. These data highlight the potential hazards of impingement in other total joint replacement components, and warrant the development of *in vitro* test methods to simulate this unintended wear mode.

In the final chapter, the characteristics and biological activity of polyethylene wear particles from two cohorts of HXLPE acetabular liners were compared to a gamma inert-sterilized THA control group for the first time *in vivo*. In addition, using the model of biological activity introduced in Chapter 4, data in the current chapter demonstrated that the inflammatory potential of wear debris from newer, first-generation HXLPE acetabular liners is outweighed by significant improvements in implant wear resistance. For the Western Blot analysis, it was not possible to correlate the patient-specific values of tumor necrosis factor (TNF)-α with wear particle characteristics or implantation time due to sample size considerations and inter-patient variability. Moreover, the observed differences in functional biological activity for polyethylene wear debris generated *in vivo* represented a previously missing link between *in vivo* and *in vitro* assessments of implant performance.

Moreover, the current data support the hypothesis that the reduced incidence of osteolysis around HXLPE components can be attributed to decreased biological activity of polyethylene wear debris generated *in vivo*.

The combined effect of multiple implant wear modes on polyethylene wear particle characteristics is a relatively unknown, except for case reports showing their association with clinical failure. Separately or in combination, these wear modes can act as an accelerant to the wear process leading to the need for revision surgery at early time points. In the context of HXLPE components, this is clearly demonstrated in the THA case study by Bradford et al., (2004) showing liner revision due to osteolysis and impingement wear after only 2 years. While the HXLPE liners in the current study were not revised due to impingement, the annealed HXLPE liner revised for malposition after 5.2 years had both the largest wear particle volume (mm^3) and functional biological activity of either HXLPE cohort. Overall, for periprosthetic and pseudocapsular tissues that were currently available, these results lend themselves to a greater understanding of the significance of polyethylene wear debris *in vivo* in the context of the reasons for revision.

Future Directions

Based on paradigm shifts that have occurred in the field of orthopedics, the understanding of the clinical performance of total joint replacement has evolved considerably over the past six decades. Specifically, the shift toward improved wear

resistance has resulted in several changes to the sterilization and processing of polyethylene used in THR. The evolution of TJR component technology has traditionally been a slow process; however, within the last five years, several polyethylene bearing materials (i.e. – sequentially annealed highly crosslinked, vitamin E-stabilized) have been introduced clinically. To keep pace with advancements in both biological and biomaterial areas of study, potential future research topics are listed below.

I. With the advent of sequentially crosslinked/annealed or vitamin-E-stabilized acetabular liners, is of critical interest to understand the characteristics and biological activity of polyethylene wear particles generated in vitro and in vivo. Currently, for these second-generation HXLPE liners, the analysis of wear debris generated *in vivo* is critically limited by the lack of retrievals implanted for a range of 2-6 years.

II. For vitamin-E-stabilized components, the consequences of antioxidant elution from the bulk material are unknown. Recent data[6] suggests that the presence of low levels of antioxidant (either 0.3 or 3.0%) can confer a reduction in the inflammatory profile *in vitro* compared to virgin UHMWPE controls. At low concentrations, antioxidants can act as scavengers of free radicals; however, at sufficiently high concentrations, antioxidant levels may exceed the cellular toxicity threshold and

---

[6] S. Teramura, S. Russell, C.L. Bladen, J. Fisher, E. Ingham, N. Tomita, J.L. Tipper. Reduced biological response to wear particles from vitamin E enhanced UHMWPE. 2011; 93-B (Suppl. 1): 74.

induce tissue damage. Further studies are necessary to understand the effect(s) of Vitamin E and other antioxidant polymer additives *in vitro* and *in vivo*.

III. Ongoing research in Drexel's Implant Research Center has recently shown a role for oxidative stress responses in the development of osteolysis (not published). Generally, oxidative stress is the imbalance between the production of reactive oxygen species and the removal/detoxification of the intermediate products. Of critical interest is the identification of oxidative stress products (nitrotyrosine, 3-NT; 4-Hydroxynonenal, 4HNE) and/or enzymes (cyclooxygenase 2, COX-2; inducible nitric oxide synthase, iNOS) associated with early and late temporal changes at the bone-implant interface.

IV. For polyethylene implant components, the process of oxidation contributing to implant degradation is well documented. However, much less is known about the oxidation of individual particles generated from the bearing surface. A recent *in vitro* study[7] showed receptor binding and activation of toll-like receptor (TLR)-1 and TLR-2 pathways in macrophages exposed to oxidized wear debris. Specifically, oxidized wear debris uniquely possessed an increased affinity for TLR-2 binding sites. Future studies investigating the effects of oxidized versus unoxidized particles can provide a better mechanistic understanding of the biological response to polyethylene wear debris *in vivo*.

---

[7] R. Maitra, C.C. Clement, G.M. Crisi, N. Cobelli, L. Santambrogio. Immunogenecity of Modified Alkane Polymers is Mediated through TLR1/2 Activation. PloS ONE 2008;3(6):e2438.

Vita

Ryan Michael Baxter, M.S.

PhD (in process), Biomedical Engineering, Drexel University, 2011
MS, Biomedical Engineering, Drexel University, 2009
BS, Biomedical Engineering, Drexel University, 2006

Publications

VII. Baxter RM, Kurtz SM, Steinbeck MJ. Decreased Functional Biological Activity of HXLPE Wear Debris *In Vivo.* CORR. 2011 *In Review.*

VI. Baxter RM, MacDonald DW, Kurtz SM, Steinbeck MJ. Chronic Impingement of Lumbar Disc Arthroplasty Increases the Functional Biologic Activity of Polyethylene Wear Debris. JBJS. 2011 *In Review.*

V. Punt IM, Baxter RM, Kurtz SM, Steinbeck MJ. Submicron-sized UHMWPE wear particle analysis from revised SB Charité III total disc replacements. Acta Biomateriala. 2011 *In Press.*

IV. Baxter RM, Freeman TA, Kurtz SM, Steinbeck MJ. Do Tissues from THA Revision of HXLPE Liners Contain Wear Debris and Associated Inflammation? Clin Orthop Relat Res. Symposium: UHMWPE for Arthroplasty: From Powder to Debris. 2010 *Epub. Dec 7.*

III. Baxter RM, Ianuzzi A, Freeman TA, Kurtz SM, Steinbeck MJ. Distinct Immunohistomorphologic Changes in Periprosthetic Hip Tissues from Historical and Highly-crosslinked UHMWPE Implant Retrievals. J Biomed Mater Res A. 2010 Oct;95(1):68-78.

II. Baxter RM, Tipper JL, Parvizi J, Marcolongo M, Kurtz SM, Steinbeck MJ. Comparison of Periprosthetic Tissue Digestion Methods for Ultra-High Molecular Weight Polyethylene Wear Extraction. J Biomed Mater Res B Appl Biomater. 2009 Oct;91(1):409-18.

I. Choma TJ, Miranda J, Siskey RL, Baxter RM, Steinbeck MJ, Kurtz SM. Retrieval Analysis of a Prodisc-L Total Disc Replacement. J Spine Disorders/Techniques. 2009 Jun;22(4):290-96.

I. Appendix A - Polarized Light Input File

```
%polyprocess.m

%script to segment polyethylene from background

%read the fully polarized and brightfield images
iorig = imread('filename.jpg');
ibf = imread('filename.jpg');

%part1: polarized particle masking
%select the 'blue' channel
p1 = iorig(:,:,3);

%threshold the blue channel
%note: the .2 is image dependent, seems to work ok.
pth = im2bw(p1,.2);

%remove 'small objects' that are camera noise
%NOTE, 'nthresh' is camera/imaging dependent!
nthresh = 70;
apth = bwareaopen(pth,nthresh);

%build new RGB image for displaying only poly particles
for i=1:3, nap(:,:,i) = uint8(apth).*iorig(:,:,i);end

%display poly segmented image
%here is your chance to change nthresh accordingly
%imshow(nap); inactivate this line to get rid of the first image

%count poly pixels (area of poly)
inap = rgb2gray(nap);
ppix = sum(sum(apth));

%part2: brightfield masking
gibf = rgb2gray(ibf);

%threshold, note: must select value, 0.75 seems to work

%the ~ inverts the image to make tissue white
gibfth = ~im2bw(gibf,.8);

%count 'tissue' pixels
```

```
tpix = sum(sum(gibfth));

%easy to compute poly vs. tissue region ratio and display result
ratiopoly = ppix / tpix

%display poly and tissue maps
figure,imshow(apth*29 + gibfth*61,colorcube);

[L,num]= bwlabel(apth,8);

pnum=num

figure,imshow(L);
```

II. Appendix B – ImageJ ESEM macro

```
setAutoThreshold("Default");
//run("Threshold...");
setAutoThreshold("Default dark");
run("Set Scale...", "distance=“specify pixel num” known= “specify micron num” pixel=1 unit=micron");
run("Set Measurements...", "area mean standard modal min centroid center perimeter bounding fit shape feret's integrated median skewness kurtosis area_fraction stack redirect=None decimal=3");
run("Fill Holes");
run("Analyze Particles...", "size=0-Infinity circularity=0.00-1.00 show=Nothing display exclude summarize");
close();
```

III. Appendix C – Chapter Data

Chapter 2

Summary of Tissue Scoring for Histiocytes and Giant Cells

Patient	Histiocytes				Giant Cell			
Conventional	0	1+	2+	3+	0	1+	2+	3+
1 (C)	20	10	70	0	100	0	0	0
2 (C)	100	0	0	0	100	0	0	0
3 (C)	20	27	0	53	80	20	0	0
4 (C)	100	0	0	0	100	0	0	0
5 (C)	100	0	0	0	100	0	0	0
6 (C)	45	15	40	0	100	0	0	0
7 (C)	100	0	0	0	100	0	0	0
8 (C)	100	0	0	0	100	0	0	0
9 (C)	0	0	0	100	42	21	37	0
Conventional								
2 (PF)	0	0	10	90	45	45	10	0
3 (RA)	0	0	0	100	87	14	0	0
4 (PF)	0	0	42	58	58	42	0	0
6 (PF)	66	27	7	0	100	0	0	0
8 (PF)	0	16	42	42	95	5	0	0
8 (RA)	0	0	0	100	47	47	6	0
HXLPE								
1 (C)	100	0	0	0	100	0	0	0
2 (C)	100	0	0	0	100	0	0	0
3 (C)	83	17	0	0	100	0	0	0
4 (C)	100	0	0	0	100	0	0	0
5 (C)	100	0	0	0	100	0	0	0
6 (C)	100	0	0	0	100	0	0	0
7 (C)	45	22	33	0	100	0	0	0
8 (C)	100	0	0	0	100	0	0	0
9 (C)	100	0	0	0	100	0	0	0
HXLPE								
2 (PF)	50	30	20	0	100	0	0	0
4 (PF)	100	0	0	0	100	0	0	0
6 (PF)	85	10	5	0	100	0	0	0
7 (RA)	44	24	11	17	94	0	6	0

Chapter 5

Standard Curve

Concentration (x-axis)	Dilution (y-axis)
0.0986	0
0.1351	0.1
0.1843	0.2
0.2567	0.4
0.327	0.6
0.3882	0.8
0.4352	1
0.4806	1.2
0.1014	0
0.148	0.1
0.1861	0.2
0.2474	0.4
0.3153	0.6
0.3686	0.8
0.415	1
0.4638	1.2

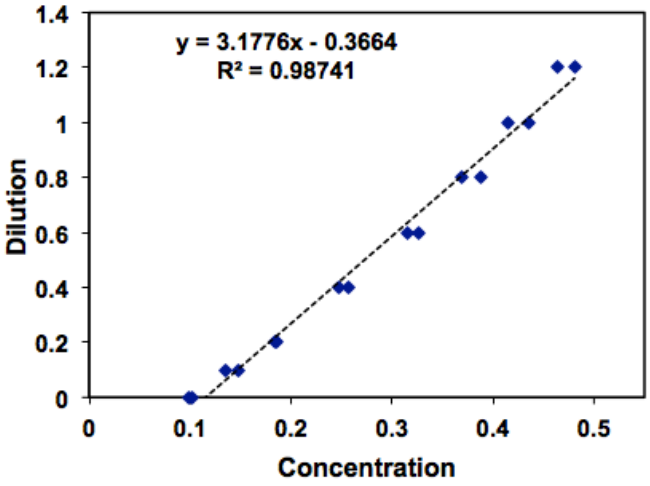

Protein, Mammalian Protein Extraction Reagent (MPER) and Dye Volumes

Sample #	Avg	Formula	µg/µL	40 µg	40 µg (x 2)	MPER	Dye	TOTAL
1	0.690	1.826	18.264	2.190	4.380	20.619	5	30
2	0.662	1.739	17.395	2.299	4.598	20.401	5	30
3	0.633	1.647	16.475	2.427	4.855	20.144	5	30
4	0.908	2.519	25.198	1.587	3.174	21.825	5	30
5	0.823	2.250	22.503	1.777	3.554	21.445	5	30
6	0.788	2.140	21.402	1.868	3.737	21.262	5	30
7	0.965	2.700	27.001	1.481	2.962	22.037	5	30
8	0.543	1.360	13.607	2.939	5.878	19.121	5	30

40 µg refers to the µl quantity required to standardize the amount of protein. After adding 5 µl of dye, MPER is determined by subtracting protein and dye volumes from a total of 30 µl.